Properties of the spherically symmetric polymer black holes

Wen-Cong Gan, Nilton O. Santos, Fu-Wen Shu, Anzhong Wang

Properties of the spherically symmetric polymer black holes

Wen-Cong Gan,[1,†] Nilton O. Santos,[2,‡] Fu-Wen Shu,[1,3,4,§] and Anzhong Wang[1,*]

[1]*GCAP-CASPER, Physics Department, Baylor University, Waco, Texas 76798-7316, USA*
[2]*Sorbonne Université, UPMC Université Paris 06, LERMA, UMRS8112 CNRS, Observatoire de Paris-Meudon, 5, Place Jules Janssen, F-92195 Meudon Cedex, France*
[3]*Department of Physics, Nanchang University, No. 999 Xue Fu Avenue, Nanchang 330031, China*
[4]*Center for Relativistic Astrophysics and High Energy Physics, Nanchang University, No. 999 Xue Fu Avenue, Nanchang 330031, China*

(Received 2 September 2020; accepted 24 November 2020; published 10 December 2020)

In this paper we systematically study a recently proposed model of spherically symmetric polymer black/white holes by Bodendorfer, Mele, and Münch (BMM), which generically possesses five free parameters. However, we find that, out of these five parameters, only three independent combinations of them are physical and uniquely determine the local and global properties of the spacetimes. After exploring the whole 3-dimensional (3D) parameter space, we show that the model has very rich physics, and depending on the choice of these parameters, various possibilities exist, including: (i) spacetimes that have the standard black/white hole structures, that is, spacetimes that are free of spacetime curvature singularities and possess two asymptotically flat regions, which are connected by a transition surface (throat) with a finite and nonzero geometric radius. The black/white hole masses measured by observers in the two asymptotically flat regions are all positive, and the surface gravity of the black (white) hole is positive (negative). In this case, there also exist possibilities in which the two horizons coincide, and the corresponding surface gravity vanishes identically. (ii) Spacetimes that have wormholelike structures, in which the two masses measured in the two asymptotically flat regions are all positive, but no horizons exist, neither a trapped (black hole) horizon nor an anti-trapped (white hole) horizon. (iii) Spacetimes that still possess curvature singularities, which can be either hidden inside trapped regions or naked. However, such spacetimes correspond to only some limit cases. In particular, the necessary (but not sufficient) condition is that at least one of the two "polymerization" parameters vanishes. These results are not in conflict to the Hawking-Penrose singularity theorems, as the effective energy-momentum tensor, purely geometric and resulted from the "polymerization" quantization, satisfies none of the three (weak, strong or dominant) energy conditions in any of the two asymptotically flat regions for any choice of the three independent free parameters, although they can hold at the throat and/or at the two horizons for some particular choices of them. In addition, it is true that quantum gravitational effects are mainly concentrated in the region near the throat, however, in this model even for solar mass black/white holes, such effects can be still very large at the black/white hole horizons, again depending on the choice of the parameters. Moreover, in principle the ratio of the two masses (for both of the black/white hole and wormhole spacetimes) can be arbitrarily large.

DOI: 10.1103/PhysRevD.102.124030

I. INTRODUCTION

There are few beacons on the road to the quantum theory of gravity. Among them singularities in classical general relativity (GR) are always the key one that any quantum theory of gravity needs to address properly. It is generally believed that spacetime singularities can be resolved once quantum gravity effects are taken into considerations. One of most successful and heuristic examples is the resolution of the big bang singularity in cosmology with the use of an effective tool developed by loop quantum cosmology (LQC) in the past few years (see, e.g., [1,2]).

Inspired by the remarkable achievements made in LQC, attempts to extend the approaches developed in LQC to black hole singularities, the ones inside black hole interiors, have recently attracted considerable attention in the loop quantum gravity (LQG) community, see, for example, [3–36] and references therein (See also [37–39] for a somehow different approach). Among these studies, most attention was paid to the Schwarzschild black hole. This is on one hand because it is the simplest black hole in GR, and on the other hand it is because the interior of the Schwarzschild

*Corresponding author.
Anzhong_Wang@baylor.edu
†Wen-cong_Gan1@baylor.edu
‡Nilton.Santos@obspm.fr
§shufuwen@ncu.edu.cn

black hole is isometric to the Kantowski-Sachs cosmological model. Actually, it is this similarity that stimulates ones to borrow similar techniques from LQC to deal with singularities in the Schwarzschild black hole. In fact, the Kantowski-Sachs spacetime can be written in the form,

$$ds^2 = -N_\tau^2 d\tau^2 + \frac{p_b^2}{|p_c|L_0^2}dx^2 + |p_c|d^2\Omega, \tag{1.1}$$

where $d^2\Omega \equiv d^2\theta + \sin^2\theta d^2\phi$, and L_0 is the length of the fiducial cell with $x \in (0, L_0)$. The quantities b, c, p_b and p_c represent the dynamical variables with the commutation relations,

$$\{c, p_c\} = 2G\gamma, \qquad \{b, p_b\} = G\gamma, \tag{1.2}$$

where b and c are the conjugate momenta of the canonical variables p_b and p_c, G denotes the Newtonian constant, and γ the Barbero-Immirzi parameter, arising in the passage from classical to quantum theory. Its value is generally fixed to be $\gamma \simeq 0.2375$ using black hole entropy considerations [40]. Choosing (classically) the lapse function N_τ as

$$N_\tau^{\rm cl} = \frac{\gamma\,\mathrm{sgn}(p_c)|p_c|^{1/2}}{b}, \tag{1.3}$$

the corresponding Hamiltonian is given by

$$H_{\rm cl} = -\frac{1}{2G\gamma}\left[2cp_c + \left(b + \frac{\gamma^2}{b}\right)p_b\right]. \tag{1.4}$$

A key procedure in constructing effective quantum geometry which solves the classical singularity is the so-called "polymerization" [41] in the LQG literature, which is characterized by two quantum parameters δ_b and δ_c for spherical spacetimes [42]. It is related to the fact that in LQG, there is minimal area gap Δ_{pl}, which is nonzero and given by $\Delta_{pl} \equiv 4\sqrt{3}\pi\gamma\ell_{\rm Pl}^2$, where $\ell_{\rm Pl}$ denotes the Planck length. The basic idea is that the effective quantum theory can be achieved by replacing the canonical variables (b, c) in the phase space with their regularized ones,

$$b \to \frac{\sin(\delta_b b)}{\delta_b}, \qquad c \to \frac{\sin(\delta_c c)}{\delta_c}, \tag{1.5}$$

where δ_b and δ_c are the so-called "polymerization scales," which control the onset of quantum effects. With the above replacement, the effective Hamiltonian is given by [22],

$$H_{\rm eff} = -\frac{1}{2G\gamma}\left[2\frac{\sin(\delta_c c)}{\delta_c}|p_c| + \left(\frac{\sin(\delta_b b)}{\delta_b} + \frac{\gamma^2\delta_b}{\sin(\delta_b b)}\right)p_b\right]. \tag{1.6}$$

Clearly, as δ_b and δ_c approach 0, the classical limit is recovered. When quantum effects are supposed to become relevant, the above replacement effectively cures the classical divergence, suggesting that the polymerization scales are at the Planck one.

However, due to the lack of the full theory of quantum gravity, a complete route map on the choice of δ_b and δ_c is still absent. In the literature there are many different choices. Generally speaking they can be divided into the following three broad classes:

(i) μ_0-scheme: In this approach, the two quantum parameters δ_b and δ_c are simply taken as constants. This is the case studied, for example, in [3–5,9,25,26].

(ii) *Generalized* μ_0-scheme: In this approach, the quantum parameters δ_b and δ_c are considered as the Dirac observables, i.e., they are phase space variables, but are constants along the effective trajectories of the system [14,17,21,22,32].

(iii) $\bar{\mu}$-scheme: In this approach, the two quantum parameters δ_b and δ_c are the phase space functions, and their functional dependence on the canonical variables depends on the specific ways to carry out the quantization, which have been explored in detail in [6,7,10,11,13,15,16,24].

Table I summarizes these studies. In some of these schemes, the fiducial structure may appear in the final results [3–5], while in other approaches, the quantum effects could be large even in the semiclassical region [6,10,14,16,17]. See [32,42–45] for the debates over these issues.

In addition, in classical Hamiltonian mechanics, a canonical transformation

$$(q_i, p_i) \to (Q_i, P_i), \tag{1.7}$$

is always allowed, and does not change the physics of the system, where $Q_i = Q_i(q_k, p_k; t)$, $P_i = P_i(q_k, p_k; t)$,

TABLE I. Three broad classes of the choices of the quantum parameters δ_b, δ_c. The parameters α and β are constants with the values $\alpha = 1$ or $\beta = 1$ or $\alpha\beta = 1$. r_0 is the Schwarzschild radius, L_0 is the fiducial length to be specified. γ is the Barbero-Immirzi parameter, $\Delta_{pl} = 4\sqrt{3}\pi\gamma l_{pl}^2$ is LQG area gap. $m = GM$, where M is the (classical) Schwarzschild black hole mass.

μ_0 scheme	*Generalized* μ_0 scheme		$\bar{\mu}$ scheme	
$\delta_b, \delta_c =$ Constant	$\delta_b = \alpha\frac{\sqrt{\Delta_{pl}}}{r_0}$, $\delta_c = \beta\frac{\sqrt{\Delta_{pl}}}{L_0}$	$\delta_b = (\frac{\sqrt{\Delta_{pl}}}{\sqrt{2\pi\gamma^2 m}})^{1/3}$, $\delta_c = \frac{1}{2}(\frac{\gamma\Delta_{pl}^2}{4\pi^2 m})^{1/3}$	$\delta_b = \frac{\sqrt{\Delta_{pl}}}{p_b}$, $\delta_c = \frac{\sqrt{\Delta_{pl}}}{p_c}$	$\delta_b = \frac{\sqrt{\Delta_{pl}}}{p_c}$, $\delta_c = \frac{\sqrt{p_c\Delta_{pl}}}{p_b}$
[3–5,9,25,26]	[14,17]	[21,22,32]	[7,10]	[6,7,10,11,13,15,16]

$q_i = (b, c)$, and $p_i = (p_b, p_c)$ [46]. However, the polymerization (1.5) depends on the choice of the canonical variables, and different canonical variables in general lead to different effective theories. It was exactly along this vein, Bodendorfer, Mele, and Münch (BMM) considered the following transformation [47,48],

$$v_1 \equiv \frac{1}{24}|p_c|^{3/2}, \qquad v_2 \equiv -\frac{1}{8}p_b^2, \tag{1.8}$$

for which the corresponding conjugate momenta are denoted by P_1 and P_2, respectively. Then, instead of Eq. (1.5), now the polymerizations are carried out via the replacements [47],

$$P_1 \to \frac{\sin(\lambda_1 P_1)}{\lambda_1}, \qquad P_2 \to \frac{\sin(\lambda_2 P_2)}{\lambda_2}, \tag{1.9}$$

where λ_1 and λ_2 play the same role as δ_b and δ_c. In this approach, the polymerization scales (λ_1, λ_2) are taken as constants, but as pointed out in [48], this choice of polymerization scales does not correspond to μ_0-scheme in terms of the variables (b, c), instead, when translated back to (b, c), they correspond to a specific $\bar{\mu}$-scheme.

It must be noted that the BMM model is based on a set of new canonical variables (v_i, P_i). Although the canonical transformation (1.7) is always allowed classically, the corresponding loop quantization has not been carried out yet in terms of these new variables. As a result, it is not clear what are relations of such effective theory [obtained by simply the replacement of Eq. (1.9)] to LQG. Therefore, to be distinguished with the effective theory obtained from LQG by taking only the leading order of quantum corrections into account, we refer such black holes as polymer black holes. Additional questions related to this issue can be found from [3,49].

With the above caveat in mind, in this paper, we shall systematically study the local and global properties of the model proposed in [47]. In particular, we find that, out of the five parameters appearing in the model, only three independent combinations of them are physically relevant, and uniquely determine the properties of the spacetimes. In this 3D phase space, there exist regions, in which the solutions can represent two asymptotically flat regions connected by a throat with a finite and nonzero geometric radius, and the masses read off in these two asymptotically flat regions are all positive. In such case, a black/white horizon exists or not also depending on the choice of the three free parameters. When they do exist, the surface gravity at the black (white) hole horizon can be positive (negative). When they do not exist, the spacetimes have wormhole structures. In all these solutions, spacetime curvature singularities are absent, which does not contradict to the Hawking-Penrose singularity theorems [50], as now the effective energy-momentum tensor does not satisfy any of the three energy conditions in the two asymptotically flat regions, despite the fact that the masses measured by observers in these two asymptotical regions are all positive. This is mainly due to the fact that the relativistic Komar energy density [51] is still positive in a large region of the spacetime. The violation of the three energy conditions in the asymptotically flat regions is a generic feature of the model, independent of the choice of the parameters of the solutions. Spacetime curvature singularities can occur, but the necessary (not sufficient) condition is at least one of the two "polymerization" parameters vanishes. In addition, although it is true that quantum gravitational effects are mainly concentrated in the region near the throat, in this model such effects still can be very large at the black/white hole horizons even for solar mass black/white holes, again depending on the choice of the free parameters. Moreover, in principle the ratio of the two masses (for both of the black/white hole and wormhole spacetimes) can be arbitrarily large.

It should be noted that, despite the fact that in this paper we consider only a particular model, we believe the main conclusions should hold for more general cases. In particular, the Schwarzschild solution is the unique vacuum solution of GR with a single parameter—the black hole mass, according to the Birkhoff theorem [52]. However, due to the polymerization process, two more free parameters, δ_b and δ_c (or in the present case, λ_1 and λ_2), are introduced. So, the resulted spacetimes should be characterized physically by only three free parameters, although the two polymerization parameters may be completely fixed, when the quantization is carried out explicitly, such as in the case considered in [21,22]. Clearly, in order for this to be consistent with the Birkhoff theorem, effective matter must be present, purely due to the quantum geometric effects. In addition, to be in harmony with the Hawking-Penrose singularity theorems [50], the effective energy-momentum tensor necessarily violates the weak/strong energy conditions.

The rest of the paper is organized as follows: In Sec. II, we first review the model built in [47] and then write the corresponding solutions in terms of only three independent combinations of the original five parameters, which are denoted by $\mathcal{D}, \mathcal{C}, x_0$, defined explicitly in Eq. (2.6). Then, we study the model in detail over the whole parameter space in Secs. III–V, respectively, for $\Delta > 0$, $\Delta = 0$, and $\Delta < 0$, as in each case the spacetimes have quite different properties, where Δ is defined by Eq. (2.10). The main results in each of these sections are summarized, respectively, in Tables II–IV. The paper is ended up in Sec. VI, in which we summarize our main conclusions. An appendix is also included, in which the general expressions of the energy density and pressures of the effective energy-momentum tensor are given explicitly.

TABLE II. The main properties of the solutions given by Eqs. (2.7)–(2.10) with $\Delta > 0$ in various cases, where bhH ≡ black hole horizon, whH ≡ white hole horizon, ECs ≡ energy conditions, SAF ≡ spacetime is asymptotical flat, SCS ≡ spacetime curvature singularity, and Sch.S ≡ Schwarzschild solution. In addition, "✓" means yes, "✗" means no, while "N/A" means not applicable.

	$\Delta > 0$							
	$\mathcal{D} > 0$				$\mathcal{D} < 0$			
Properties	$\mathcal{C} \neq 0$, $x_0 \neq 0$	$\mathcal{C} \neq 0$, $x_0 = 0$	$\mathcal{C} = 0$, $x_0 \neq 0$	$\mathcal{C} = x_0 = 0$ (Sch.S)	$\mathcal{C} \neq 0$, $x_0 \neq 0$	$\mathcal{C} \neq 0$, $x_0 = 0$	$\mathcal{C} = 0$, $x_0 \neq 0$	$\mathcal{C} = x_0 = 0$ (Sch.S)
bhH exists?	✓	✓	✓	✓	✗	✗	✗	✗
ECs at bhH	Eq. (3.2)	✓	Eq. (3.56)	✓	N/A	N/A	N/A	N/A
whH exists?	✓	✗	✓	✗	✗	✗	✗	✗
ECs at whH	Eq. (3.2)	N/A	Eq. (3.56)	N/A	N/A	N/A	N/A	N/A
Throat exists?	✓	✓	✗	✗	✓	✓	✗	✗
ECs at throat	Eq. (3.10)	$\mathcal{C} = 2\mathcal{D}$	N/A	N/A	✗	✗	N/A	N/A
ECs at $x = \infty$	✗	✗	✗	✓	✗	✗	✗	✓
Mass at $x = \infty$	$\mathcal{D}$	$\mathcal{D}$	$\mathcal{D}$	$\mathcal{D}$	$\mathcal{D}$	$\mathcal{D}$	$\mathcal{D}$	$\mathcal{D}$
ECs at $x = -\infty$	✗	N/A ($x \geq 0$)	✗	N/A ($x \geq 0$)	✗	N/A ($x \geq 0$)	✗	N/A ($x \geq 0$)
Mass at $x = -\infty$	$\frac{\mathcal{D}\mathcal{C}^2}{x_0^2}$	SAF at $x = 0$	SCS	SCS at $x = 0$	$\frac{\mathcal{D}\mathcal{C}^2}{x_0^2}$	SAF at $x = 0$	SCS	SCS at $x = 0$

TABLE III. The main properties of the solutions given by Eqs. (2.7)–(2.10) with $\Delta = 0$, for which we have $x_H^{\pm} = 0$, and the white and black hole horizons always coincide. Here bhH ≡ black hole horizon, whH ≡ white hole horizon, ECs ≡ energy conditions, SAF ≡ spacetime is asymptotical flat, and SCS ≡ spacetime curvature singularity. In addition, "✓" means yes, "✗" means no, while "N/A" means not applicable.

	$\Delta = 0$					
	$\mathcal{D} > 0$		$\mathcal{D} = 0$		$\mathcal{D} < 0$	
Properties	$\mathcal{C} \neq 0$	$\mathcal{C} = 0$	$\mathcal{C} \neq 0$	$\mathcal{C} = 0$	$\mathcal{C} \neq 0$	$\mathcal{C} = 0$
bhH/whH exists?	✓	✓	✓	(Minkowski)	✗	✗
ECs at bhH/whH	✓	✓	✗	N/A	N/A	N/A
Throat exists?	✓	✗	✓	N/A	✓	✗
ECs at throat	Eq. (4.9)	N/A	✗	N/A	✗	N/A
ECs at $x = \infty$	✗	✗	✗	N/A	✗	✗
Mass at $x = \infty$	$\mathcal{D}$	$\mathcal{D}$	0	0	$\mathcal{D}$	$\mathcal{D}$
ECs at $x = -\infty$	✗	✗	N/A ($x \geq 0$)	N/A	✗	✗
Mass at $x = -\infty$	$\frac{\mathcal{C}^2}{\mathcal{D}}$	SCS ($b(-\infty) = 0$)	SAF ($x = 0$)	N/A	$\frac{\mathcal{C}^2}{\mathcal{D}}$	SCS ($b(-\infty) = 0$)

TABLE IV. The main properties of the solutions given by Eqs. (2.7)–(2.10) with $\Delta < 0$, for which no horizons exist in all these solutions. Here bhH ≡ black hole horizon, whH ≡ white hole horizon, ECs ≡ energy conditions, SAF ≡ spacetime is asymptotical flat, and SCS ≡ spacetime curvature singularity. In addition, "✓" means yes, "✗" means no, while "N/A" means not applicable.

	$\Delta < 0$					
	$\mathcal{D} > 0$		$\mathcal{D} = 0$		$\mathcal{D} < 0$	
Properties	$\mathcal{C}x_0 \neq 0$	$\mathcal{C} = 0, x_0 \neq 0$	$x_0\mathcal{C} \neq 0$	$\mathcal{C} = 0, x_0 \neq 0$	$\mathcal{C}x_0 \neq 0$,	$\mathcal{C} = 0, x_0 \neq 0$
bhH/whH exists?	✗	✗	✗	✗	✗	✗
Throat exists?	✓	✗	✓	✗	✓	✗
ECs at throat	Eq. (5.5)	N/A	✗	N/A	✗	N/A
ECs at $x = \infty$	✗	✗	✗	✗	✗	✗
Mass at $x = \infty$	$\mathcal{D}$	$\mathcal{D}$	$-x_0^2$	$-x_0^2$ (SAF)	$\mathcal{D}$	$\mathcal{D}$
ECs at $x = -\infty$	✗	✗	✗	✗	✗	✗
Mass at $x = -\infty$	$\frac{\mathcal{D}\mathcal{C}^2}{x_0^2}$	SCS	$-\frac{\mathcal{C}^4}{x_0^2}$	SCS	$\frac{\mathcal{D}\mathcal{C}^2}{x_0^2}$	SCS

Before proceeding further, we would like to point out that some solutions of the current model were lately studied in [53], including their perturbations and the associated quasinormal modes of massless scalar field perturbations, electromagnetic perturbations, and axial gravitational perturbations. In particular, the authors found that the corresponding quasinormal frequencies of perturbations with different spins share the same qualitative tendency with respect to the change of the quantum parameters involved in this model. For more details, we refer readers to [53].

II. SPHERICALLY SYMMETRIC POLYMER BLACK HOLES

Studying spherically symmetric spacetimes inside black holes, Bodendorfer, Mele, and Münch recently obtained the following spherically symmetric black hole solutions [47],

$$d\bar{s}^2 = -\frac{\bar{a}(x)}{L_0^2}d\bar{t}^2 + \frac{\mathcal{L}_0^2}{\bar{a}(x)}dx^2 + \bar{b}^2(x)d\Omega^2, \tag{2.1}$$

where $\mathcal{L}_0 = \sqrt{n}$, $x \in (-\infty, \infty)$, and

$$\begin{aligned}\bar{a}(x) = {} & n\left(\frac{\lambda_2}{\sqrt{n}}\right)^4\left(1+\frac{nx^2}{\lambda_2^2}\right)\left(1-\frac{3CD}{2\lambda_2\sqrt{1+\frac{nx^2}{\lambda_2^2}}}\right)\\ & \times\left[\frac{\lambda_2^6}{16C^2\lambda_1^2n^3}\left(\frac{\sqrt{n}x}{\lambda_2}+\sqrt{1+\frac{nx^2}{\lambda_2^2}}\right)^6+1\right]^{-2/3}\\ & \times\left(\frac{1}{3C^2D\lambda_1^2}\right)^{2/3}\left(\frac{\sqrt{n}x}{\lambda_2}+\sqrt{1+\frac{nx^2}{\lambda_2^2}}\right)^2,\\ \bar{b}(x) = {} & \frac{\sqrt{n}(3C^2D\lambda_1^2)^{1/3}}{\lambda_2}\\ & \times\frac{[\frac{\lambda_2^6}{16C^2\lambda_1^2n^3}(\frac{\sqrt{n}x}{\lambda_2}+\sqrt{1+\frac{nx^2}{\lambda_2^2}})^6+1]^{1/3}}{\frac{\sqrt{n}x}{\lambda_2}+\sqrt{1+\frac{nx^2}{\lambda_2^2}}},\end{aligned} \tag{2.2}$$

where $\lambda_1, \lambda_2, n, C$, and D are real constants with $n > 0$.

As shown in [47], there are two independent Dirac observables, F_Q and $\bar{F}_Q$, which are constants along the trajectories of the effective dynamics, and their on-shell values are given by,

$$\begin{aligned}F_Q &= \left(\frac{3D}{2}\right)^{4/3}\left(\frac{C}{\sqrt{n}}\right),\\ \bar{F}_Q &= \frac{3CD\sqrt{n}}{\lambda_2^2}(3DC^2\lambda_1^2)^{1/3}.\end{aligned} \tag{2.3}$$

It can be shown that both of them are invariant under a fiducial cell rescaling. As a result, the integration constants C and D are independent. In fact, at the limits, $x \to \pm\infty$, we have

$$\bar{a}(x) \propto \begin{cases} 1-\frac{F_Q}{\bar{F}_Q}, & x \to \infty,\\ 1-\frac{\bar{F}_Q}{F_Q}, & x \to -\infty.\end{cases} \tag{2.4}$$

Thus, they are essentially related to the black and white hole masses via the relations,

$$\begin{aligned}\bar{M}_{\rm BH} &= \frac{1}{2}F_Q = \left(\frac{3D}{2}\right)^{4/3}\left(\frac{C}{2\sqrt{n}}\right),\\ \bar{M}_{WH} &= \frac{1}{2}\bar{F}_Q = \frac{3CD\sqrt{n}}{2\lambda_2^2}(3DC^2\lambda_1^2)^{1/3}.\end{aligned} \tag{2.5}$$

Introducing the quantities,

$$\mathcal{D} \equiv \frac{3CD}{2\sqrt{n}}, \qquad \mathcal{C} \equiv (16C^2\lambda_1^2)^{1/6}, \qquad x_0 \equiv \frac{\lambda_2}{\sqrt{n}}, \tag{2.6}$$

we find that the metric (2.1) takes the form,

$$\begin{aligned}d\bar{s}^2 &= \left(\frac{3D}{16}\right)^{2/3}ds^2\\ &\equiv \left(\frac{3D}{16}\right)^{2/3}\left(-a(x)dt^2+\frac{dx^2}{a(x)}+b^2(x)d\Omega^2\right),\end{aligned} \tag{2.7}$$

with $t \equiv (\sqrt{n}/L_0)(16/3D)^{2/3}\bar{t}$, and

$$a(x) = \frac{(x^2-\Delta)XY^2}{(X+\mathcal{D})Z^2}, \qquad b(x) = \frac{Z}{Y}, \tag{2.8}$$

where

$$\begin{aligned}&X \equiv \sqrt{x^2+x_0^2}, \qquad Y \equiv x+X,\\ &Z \equiv (Y^6+\mathcal{C}^6)^{1/3},\end{aligned} \tag{2.9}$$

and

$$\Delta \equiv \mathcal{D}^2 - x_0^2 = \frac{9C^2D^2-4\lambda_2^2}{4n}. \tag{2.10}$$

Since ds^2 is related to $d\bar{s}^2$ only by a conformal constant factor $(3D/16)^{2/3}$,[1] without loss of generality, we shall consider only the spacetimes described by ds^2. Then, we can see that only three independent combinations of the five parameters $\lambda_1, \lambda_2, n, C$, and D appear in the metric coefficients, as defined by Eq. (2.6).

It is remarkable to note that in GR, due to the Birkhoff theorem [52], the black hole mass is the only free parameter. However, in LQG, due to the polymerizations

[1]Under this rescaling, the Ricci and Kretschmann scalars are scaling, respectively, as $R = (3D/16)^{2/3}\bar{R}$ and $K = (3D/16)^{4/3}\bar{K}$.

(1.9), two new parameters λ_1 and λ_2 are introduced, so now the solutions generically depend on three free parameters. When setting $\lambda_1 = \lambda_2 = 0$ (or $\mathcal{C} = x_0 = 0$), the above solutions reduce precisely to the Schwarzschild solution with $\mathcal{D}$ as the black hole mass.

One of our goals in this paper is to understand their physical and geometrical meanings. To this goal, let us first note the following:

(i) Since $x \in (-\infty, \infty)$, from Eq. (2.9) we find that

$$X \geq x_0, \qquad Y > 0, \qquad Z > \mathcal{C}^2. \tag{2.11}$$

(ii) In [47,48] it was assumed that

$$\mathcal{D} > 0, \qquad \Delta > 0, \tag{2.12}$$

so that two metric horizons always exist at $x_H^{\pm} \equiv \pm\sqrt{\Delta}$, and the asymptotic limits of Eq. (2.4) are always true (See also [53]).

(iii) The solutions were initially derived only in the region $-x_H^- < x < x_H^+$, in which the spacetime is homogeneous, and the Killing vector $\xi \equiv \partial_t$ is spacelike. The horizon at $x = x_H^+$ is referred to as the black hole horizon, while the one at $x = x_H^-$ is referred to as the white hole horizon, although in between them, no spacetime singularities exist at all [21,22]. However, following the standard process of extensions, one can easily extend the solutions beyond these horizons to the regions $|x| > \sqrt{\Delta}$. In the extended regions $x < x_H^-$ and $x > x_H^+$, the metrics will take the same form as that given by Eqs. (2.7)–(2.9), but now the Killing vector ∂_t becomes timelike.

In this paper, we shall not impose the conditions (2.12), except that we still assume that C and D are real. In particular, since C, D, n, λ_1, and λ_2 are arbitrary constants, in principle, they can take any real values. However, since $ds^2 = (3D/16)^{2/3} d\bar{s}^2$, we shall assume that $D = 0$ holds only in the limiting sense. In addition, the two constants λ_1 and λ_2 originate from the polymerization (1.9), so we also assume that $\lambda_1\lambda_2 \neq 0$, and consider the case $\lambda_1\lambda_2 = 0$ only as some limit cases, as to be explained explicitly below. Recall that we also assumed $n > 0$ in order to have the metric be real.

Then, the geometric radius $b(x)$ and the ranges of x all depend on the choices of the two parameters x_0 and $\mathcal{C}$, which are shown explicitly in Fig. 1. In particular, when $\mathcal{C}x_0 \neq 0$, we find that $x \in (-\infty, \infty)$, and a minimal point (the throat) of $b(x)$ always exists, with $b(\pm\infty) = \infty$, as shown by the upper panel of Fig. 1. When $\mathcal{C} \neq 0$, $x_0 = 0$, the range of x is restricted to $x \in (0, \infty)$ with $b(0) = \infty$ and $b(\infty) = \infty$. In this case, a minimum (throat) of $b(x)$ also exists, as shown explicitly in the middle panel of Fig. 1]. When $\mathcal{C} = 0$, $x_0 \neq 0$, the range of x is $x \in (-\infty, \infty)$, but now $b(x)$ is a monotonically increasing function of x with $b(-\infty) = 0$ and $b(\infty) = \infty$, and a throat does not exists [cf. the bottom panel of Fig. 1].

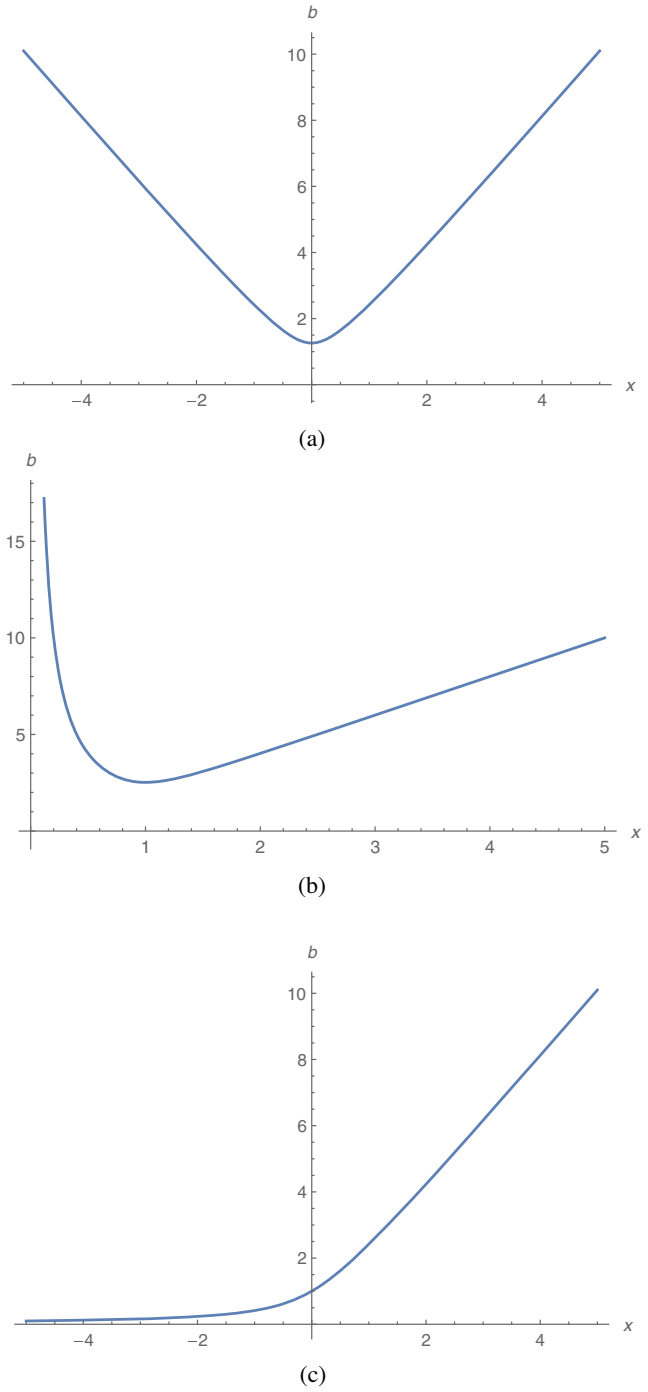

FIG. 1. The geometric radius $b(x)$ vs x. (a) Upper panel: $\mathcal{C}x_0 \neq 0$. When plotting this curve, we had set $x_0 = 1$, $\mathcal{C} = 1$. (b) Middle panel: $\mathcal{C} \neq 0$, $x_0 = 0$. When plotting this curve, we had set $\mathcal{C} = 2$. (c) Bottom panel: $\mathcal{C} = 0$, $x_0 \neq 0$. When plotting this curve, we had set $x_0 = 1$.

In this paper, we shall study the main properties of these spherical polymer black hole solutions. In particular, we shall pay particular attention to the locations of the throat and horizons, and the asymptotic behaviors of the spacetimes.

To these purposes, let us first notice that the effective energy-momentum tensor $T_{\mu\nu}$, defined as $T_{\mu\nu} \equiv \kappa^{-1} G_{\mu\nu}$, can be cast in the form,

$$T_{\mu\nu} = \rho u_\mu u_\nu + p_r v_\mu v_\nu + p_\theta(\theta_\mu\theta_\nu + \phi_\mu\phi_\nu), \tag{2.13}$$

where

$$\begin{aligned} &u^+_\mu = -a^{1/2}(x)\delta^t_\mu, \qquad v^+_\mu = a^{-1/2}(x)\delta^x_\mu, \\ &\theta_\mu = b^{1/2}(x)\delta^\theta_\mu, \qquad \phi_\mu = b^{1/2}(x)\sin\theta\delta^\phi_\mu, \quad (a > 0), \end{aligned} \tag{2.14}$$

and

$$\begin{aligned} \kappa\rho^+ &= -\frac{1}{b^2}[b(x)(2ab'' + a'b') + ab'^2 - 1], \\ \kappa p^+_r &= \frac{1}{b^2}[ba'b' + ab'^2 - 1], \\ \kappa p_\theta &= \frac{1}{2b}[ba'' + 2ab'' + 2a'b'], \quad (a > 0), \end{aligned} \tag{2.15}$$

with $\kappa \equiv 8\pi G/c^4$, $a' \equiv da(x)/dx$, and so on.

It should be noted that in writing down Eqs. (2.14) and (2.15) we had assumed that $a(x) > 0$, as already indicated in these equations, so the coordinate t is timelike. However, if a (black/white) horizon exists, across this horizon $a(x)$ becomes negative, and the two coordinates t and x exchange their roles. Then, in the region $a(x) < 0$, the effective energy-momentum tensor can be still cast in the form (2.13), but now with

$$\begin{aligned} u^-_\mu &= |a|^{-1/2}\delta^x_\mu, \qquad v^-_\mu = -|a|^{1/2}\delta^t_\mu, \\ \kappa\rho^- &= -\frac{1}{b^2}[ba'b' + ab'^2 - 1], \quad (a < 0), \\ \kappa p^-_r &= \frac{1}{b^2}[b(x)(2ab'' + a'b') + ab'^2 - 1], \end{aligned} \tag{2.16}$$

while θ_μ, ϕ_μ, and p_θ are still given by Eqs. (2.14) and (2.15).

It should be also noted that, although the effective energy-momentum tensor in both of the regions $a > 0$ and $a < 0$ is written in the same form given by Eq. (2.13), the physical interpretations of the quantities $\rho^\pm$ and $p^\pm_r$ are different. In particular, the energy density ρ^+ in the region $a > 0$ is measured by the observers who are moving along dt-direction, while their x, θ and ϕ coordinates are fixed. The quantity p^+_r is the principal pressure along the dx-direction measured by these observers. On the other hand, the energy density ρ^- in the region $a < 0$ is measured by the observers who are moving along dx-direction, while their t, θ, and ϕ coordinates are fixed. In addition, the quantity p^-_r now is the principal pressure along the dt-direction. Thus, in general such defined $\rho^\pm$ and $p^\pm_r$ are not continuous across the horizons. One way to avoid such discontinuities is to adopt the Eddington-Finkelstein coordinates, and then define a new set of observers, with respect to whom the energy density and principal pressure along the radial direction are continuous across these horizons. However, since in this paper we are mainly concerned with the energy conditions of "the effective (quantum) matter",[2] the current considerations are sufficient.

In addition, although this effective energy-momentum tensor is purely due to the polymerization (1.9), and is not related to any real matter fields, it does provide important information on how the spacetime singularity is avoided, and the deviation of the spacetimes from the classical one, as in GR the geometry is uniquely determined by the Schwarzschild spacetime, in which the spacetime is vacuum, and a spacetime curvature singularity is always present at the center of the black hole. In fact, this kind of singularities inevitably occurs in GR, as longer as the corresponding matter fields satisfy some energy conditions, as follows directly from the Hawking-Penrose singularity theorems [50].

The commonly used three energy conditions are *the weak, dominant, and strong energy conditions* [50]. For $T_{\mu\nu}$ given by Eq. (2.13), they can be expressed as follows: The weak energy condition (WEC) is satisfied, when

$$(i)\ \rho \geq 0, \qquad (ii)\ \rho + p_r \geq 0, \qquad (iii)\ \rho + p_\theta \geq 0, \tag{2.17}$$

while the dominant energy condition (DEC) is satisfied, provided that

$$(i)\,\rho \geq 0, \qquad (ii)\ -\rho \leq p_r \leq \rho, \qquad (iii)\ -\rho \leq p_\theta \leq \rho. \tag{2.18}$$

The strong energy condition (SEC) requires,

$$\begin{aligned} &(i)\ \rho + p_r \geq 0, \qquad (ii)\ \rho + p_\theta \geq 0, \\ &(iii)\ \rho + p_r + 2p_\theta \geq 0. \end{aligned} \tag{2.19}$$

Moreover, without causing any confusions, in the rest of this paper we shall absorb κ into ρ, p_r and p_θ, i.e.,

[2]As mentioned above, the BMM model has not been obtained from quantizations of gravity yet, but rather obtained by simply applying the "polymerization" (1.9) to the corresponding classical Hamiltonian. So, it is not clear whether these effects are indeed due to quantizations of gravity or not. In the rest of this paper, whenever we mention "quantum gravitational effects" or "quantum geometric effects" of this model, we always understand them as "polymerization effects" without any further explanations. In the same sense, the expression "quantum black holes" of this model really means polymer black holes.

$$\kappa(\rho, p_r, p_\theta) \to (\rho, p_r, p_\theta). \tag{2.20}$$

To study these solutions in more details, let us consider the cases $\Delta > 0$, $\Delta = 0$ and $\Delta < 0$, separately, in the following three sections.

III. SPACETIMES WITH $\Delta > 0$

From Eq. (2.10) we find that this case corresponds to

$$|\lambda_2| < \frac{3}{2}|CD|. \tag{3.1}$$

However, depending on the choice of the integration constants C and D, there are still the possibilities, $\mathcal{D} > 0$, and $\mathcal{D} < 0$, provided that $\Delta = \mathcal{D}^2 - x_0^2 > 0$. In each of these cases, the physics of the corresponding solutions is quite different, so in the following let us consider them case by case.

A. $\mathcal{D} > 0$

In this case, we have $CD > 0$, and $\Delta = \mathcal{D}^2 - x_0^2 > 0$ implies,

$$\beta \equiv \frac{\mathcal{D}}{|x_0|} > 1. \tag{3.2}$$

Then, we find that there are two asymptotically flat regions, corresponding to $x \to \pm\infty$, respectively. They are connected by a throat located at

$$b_m \equiv 2^{1/3}\mathcal{C}, \qquad x_m = \frac{1}{2\mathcal{C}}(\mathcal{C}^2 - x_0^2), \tag{3.3}$$

where $b_m \equiv b(x = x_m)$ and $b'(x = x_m) = 0$ [cf. Fig. 1(a)]. It is interesting to note that x_m can be positive, zero or negative, depending on the choice of the two parameters $\mathcal{C}$ and x_0 (or λ_1, λ_2, n and C).

On the other hand, in the current case the white and black hole horizons always exist, and are located, respectively, at

$$x_H^{\pm} = \pm\sqrt{\mathcal{D}^2 - x_0^2}. \tag{3.4}$$

Clearly, there exist the possibilities in which $|x_m| \le x_H^+$, or $|x_m| > x_H^+$. When $|x_m| \le x_H^+$, the throat is located in the region between the black and white hole horizons, in which we have $a(x) \le 0$, so the corresponding energy density and radial principal pressure in the region containing the throat are given by ρ^- and p_r^-. When $|x_m| > x_H^+$, the throat is located in the region where $a(x) > 0$, so the corresponding energy density and radial principal pressure at the throat are given by ρ^+ and p_r^+, respectively.

1. $x_H^- \le x_m \le x_H^+$

In this case, we find that $|x_m| \le x_H^+$ implies

$$(i)\ \alpha = 1, \quad \text{or} \tag{3.5}$$

$$(ii)\ \beta \ge 1 + \frac{(\alpha - 1)^2}{2\alpha}, \tag{3.6}$$

where $\alpha \equiv \mathcal{C}/|x_0| > 0$. Since now the throat is located inside the black hole horizon, in which we have $a(x) < 0$, we need to use Eq. (2.16) to calculate the effective energy density ρ and pressure p_r at the throat, and find that

$$\begin{aligned} \rho &= \frac{1}{2^{2/3}\mathcal{C}^2}, \\ p_r &= -\frac{\mathcal{C}(12\mathcal{D} - 5\mathcal{C}) - 5x_0^2}{2^{2/3}\mathcal{C}^2(x_0^2 + \mathcal{C}^2)}, \\ p_\theta &= \frac{(x_0^2 + \mathcal{C}^2)^3 - 4\mathcal{D}x_0^2\mathcal{C}^3}{2^{2/3}\mathcal{C}^2(x_0^2 + \mathcal{C}^2)^3}. \end{aligned} \tag{3.7}$$

Then, we find that at the throat WEC is satisfied for

$$(a)\ \beta \le 1 + \frac{(\alpha - 1)^2}{2\alpha}, \quad \text{or} \tag{3.8}$$

$$(b)\ \beta \le \frac{1}{2}\alpha. \tag{3.9}$$

Combining Eqs. (3.5)–(3.6) with Eqs. (3.8)–(3.9) and considering Eq. (3.2), we find that their common solutions are

$$\beta = 1 + \frac{(\alpha - 1)^2}{2\alpha}, \qquad \alpha \ne 1, \tag{3.10}$$

which leads to $x_m = x_H^+$.

On the other hand, SEC is also satisfied in the domain given by Eq. (3.10), while DEC requires

$$(a)\ 0 < \alpha < 2\beta, \qquad \beta \le \frac{\alpha^2 + 1}{2\alpha} \le \frac{3}{2}\beta, \quad \text{or} \tag{3.11}$$

$$(b)\ 2\beta \le \alpha < 3\beta, \qquad \beta \ge \frac{1 + \alpha^2}{3\alpha}. \tag{3.12}$$

Combining Eqs. (3.5)–(3.6) with Eqs. (3.11)–(3.12), we find that their common solution is also given by Eq. (3.10).

Therefore, at the throat none of the three energy conditions is satisfied, except for the case in which the throat coincides with the black hole horizon, $x_m = x_H^+$, which is a direct result of the condition Eq. (3.10). In Fig. 2, we show this case, from which one can see that the three energy conditions are satisfied indeed only at the throat. In Fig. 3, we show the case that does not satisfy the condition

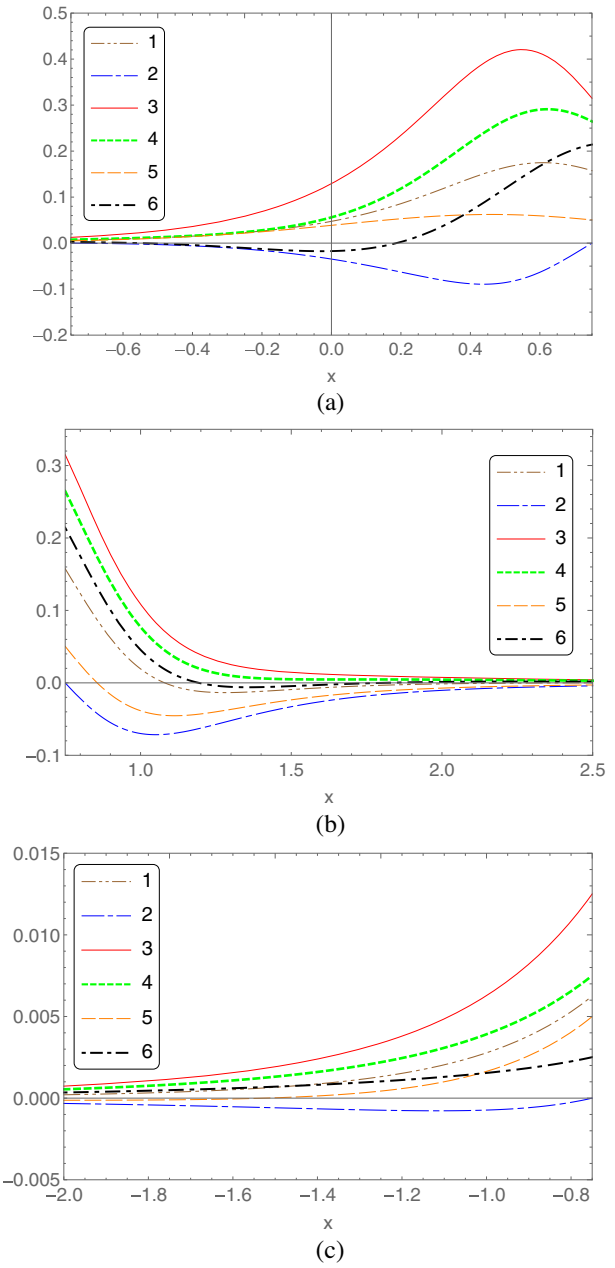

FIG. 2. Case $\Delta > 0, \mathcal{D} > 0, |x_m| < x_H^+, \beta = 1 + \frac{(\alpha-1)^2}{2\alpha}, \alpha \neq 1$: The physical quantities, ρ, $(\rho + p_r)$, $(\rho - p_r)$, $(\rho + p_\theta)$, $(\rho - p_\theta)$, and $(\rho + p_r + 2p_\theta)$, represented, respectively, by Curves 1–6, vs x: When plotting these curves, we had set $\alpha = 2$, $\beta = 5/4$, $x_0 = 1$, so that the condition (3.10) is satisfied, for which we have $x_m = x_H^+ = -x_H^- = 0.75$. Panel (a): the physical quantities in the region between the white and black horizons, $x_H^- \leq x \leq x_H^+$. Panel (b): the physical quantities in the region outside the black horizon, $x \geq x_H^+ = 0.75$. Panel (c): the physical quantities in the region outside the white horizon, $x \leq x_H^- = -0.75$.

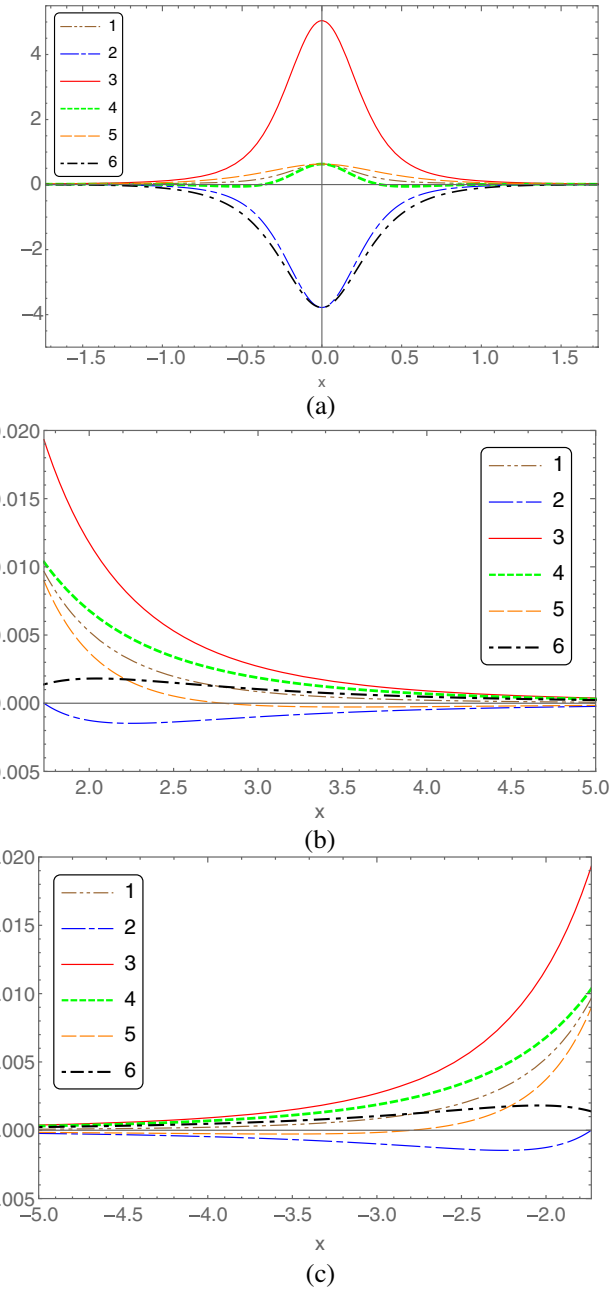

FIG. 3. Case $\Delta > 0, \mathcal{D} > 0, |x_m| < x_H^+, \beta \neq 1 + \frac{(\alpha-1)^2}{2\alpha}$: The physical quantities, ρ, $(\rho + p_r)$, $(\rho - p_r)$, $(\rho + p_\theta)$, $(\rho - p_\theta)$, and $(\rho + p_r + 2p_\theta)$, represented, respectively, by Curves 1–6, vs x: When plotting these curves, we had set $\alpha = 1$, $\beta = 2$, $x_0 = 1$, $x_H^\pm = \pm\sqrt{3}$, $x_m = 0$. None of the three energy conditions is satisfied at the throat, although all of them are satisfied at the two horizons $x = x_H^\pm$. Panel (a): the physical quantities in the region between the white and black horizons, $x_H^- \leq x \leq x_H^+$. Panel (b): the physical quantities in the region outside the black horizon, $x \geq x_H^+ = \sqrt{3}$. Panel (c): the physical quantities in the region outside the white horizon, $x \leq x_H^- = -\sqrt{3}$.

Eq. (3.10), from which one can see that none of the three energy conditions is satisfied at the throat ($x_m = 0$).

In addition, if we consider the limit to the black hole horizon from outside of it, then we have $\rho = \rho^+$ and $p_r = p_r^+$, and the energy density and pressures are given, respectively, by

$$\begin{aligned}\rho = -p_r = -\frac{Y^3}{XZ^8}[&(32\mathcal{D}^5\mathcal{C}^6 + 10\mathcal{D}x_0^{10} - 160\mathcal{D}^3x_0^8 + 672\mathcal{D}^5x_0^6 - 1024\mathcal{D}^7x_0^4 + 2\mathcal{D}x_0^4\mathcal{C}^6 + 512\mathcal{D}^9x_0^2 \\ &- 24\mathcal{D}^3x_0^2\mathcal{C}^6)\sqrt{\Delta} + 32\mathcal{D}^6\mathcal{C}^6 - x_0^{12} + 50\mathcal{D}^2x_0^{10} - 400\mathcal{D}^4x_0^8 + 1120\mathcal{D}^6x_0^6 - 1280\mathcal{D}^8x_0^4 + 10\mathcal{D}^2x_0^4\mathcal{C}^6 \\ &+ 512\mathcal{D}^{10}x_0^2 - 40\mathcal{D}^4x_0^2\mathcal{C}^6 + \mathcal{C}^{12}],\end{aligned} \tag{3.13}$$

$$\begin{aligned}p_\theta = \frac{Y^2}{2X^2Z^8}[&(128\mathcal{D}^7\mathcal{C}^6 + 2\mathcal{D}\mathcal{C}^{12} + 10\mathcal{D}x_0^{12} - 160\mathcal{D}^3x_0^{10} + 672\mathcal{D}^5x_0^8 - 1024\mathcal{D}^7x_0^6 - 12\mathcal{D}x_0^6\mathcal{C}^6 \\ &+ 512\mathcal{D}^9x_0^4 + 88\mathcal{D}^3x_0^4\mathcal{C}^6 - 192\mathcal{D}^5x_0^2\mathcal{C}^6)\sqrt{\Delta} + 128\mathcal{D}^8\mathcal{C}^6 + 2\mathcal{D}^2\mathcal{C}^{12} - x_0^{14} + 50\mathcal{D}^2x_0^{12} \\ &- 400\mathcal{D}^4x_0^{10} + 1120\mathcal{D}^6x_0^8 + 2x_0^8\mathcal{C}^6 - 1280\mathcal{D}^8x_0^6 - 40\mathcal{D}^2x_0^6\mathcal{C}^6 + 512\mathcal{D}^{10}x_0^4 + 168\mathcal{D}^4x_0^4\mathcal{C}^6 \\ &- 256\mathcal{D}^6x_0^2\mathcal{C}^6 - x_0^2\mathcal{C}^{12}].\end{aligned} \tag{3.14}$$

It can be shown that each of the three energy conditions is satisfied provided that $\beta > 1$, which is precisely the condition $\Delta > 0$, as shown in Eq. (3.2). In addition, the surface gravity of the black hole is given by,

$$\kappa_{\rm BH} \equiv \frac{1}{2}a'(x = \sqrt{\Delta}) = \frac{Y^2|x_0|^7}{2Z^5}[\sqrt{\beta^2 - 1}(32\beta^6 - 48\beta^4 + 18\beta^2 - 1 + \alpha^6) + 2\beta(16\beta^6 - 32\beta^4 + 19\beta^2 - 3)], \tag{3.15}$$

which is also always positive for $\beta > 1$.

At the white hole horizon ($x = -\sqrt{\Delta}$), taking the limit from the outside of it, so that $\rho = \rho^+$ and $p_r = p_r^+$, we find that

$$\begin{aligned}\rho = -p_r = -\frac{Y}{\mathcal{D}Z^8}([&128\mathcal{D}^7\mathcal{C}^6 + 2\mathcal{D}\mathcal{C}^{12} - 12\mathcal{D}x_0^{12} + 280\mathcal{D}^3x_0^{10} - 1792\mathcal{D}^5x_0^8 \\ &+ 4608\mathcal{D}^7x_0^6 - 2\mathcal{D}x_0^6\mathcal{C}^6 - 5120\mathcal{D}^9x_0^4 + 48\mathcal{D}^3x_0^4\mathcal{C}^6 + 2048\mathcal{D}^{11}x_0^2 - 160\mathcal{D}^5x_0^2\mathcal{C}^6]\sqrt{\Delta} - 128\mathcal{D}^8\mathcal{C}^6 \\ &- 2\mathcal{D}^2\mathcal{C}^{12} - x_0^{14} + 72\mathcal{D}^2x_0^{12} - 840\mathcal{D}^4x_0^{10} + 3584\mathcal{D}^6x_0^8 - 6912\mathcal{D}^8x_0^6 + 14\mathcal{D}^2x_0^6\mathcal{C}^6 + 6144\mathcal{D}^{10}x_0^4 \\ &- 112\mathcal{D}^4x_0^4\mathcal{C}^6 - 2048\mathcal{D}^{12}x_0^2 + 224\mathcal{D}^6x_0^2\mathcal{C}^6 + x_0^2\mathcal{C}^{12}), \\ p_\theta = \frac{Y^2}{2\mathcal{D}^2Z^8}([&128\mathcal{D}^7\mathcal{C}^6 + 2\mathcal{D}\mathcal{C}^{12} + 10\mathcal{D}x_0^{12} - 160\mathcal{D}^3x_0^{10} + 672\mathcal{D}^5x_0^8 - 1024\mathcal{D}^7x_0^6 - 12\mathcal{D}x_0^6\mathcal{C}^6 \\ &+ 512\mathcal{D}^9x_0^4 + 88\mathcal{D}^3x_0^4\mathcal{C}^6 - 192\mathcal{D}^5x_0^2\mathcal{C}^6]\sqrt{\Delta} - 128\mathcal{D}^8\mathcal{C}^6 - 2\mathcal{D}^2\mathcal{C}^{12} + x_0^{14} - 50\mathcal{D}^2x_0^{12} + 400\mathcal{D}^4x_0^{10} \\ &- 1120\mathcal{D}^6x_0^8 - 2x_0^8\mathcal{C}^6 + 1280\mathcal{D}^8x_0^6 + 40\mathcal{D}^2x_0^6\mathcal{C}^6 - 512\mathcal{D}^{10}x_0^4 - 168\mathcal{D}^4x_0^4\mathcal{C}^6 + 256\mathcal{D}^6x_0^2\mathcal{C}^6 + x_0^2\mathcal{C}^{12}).\end{aligned} \tag{3.16}$$

It can be shown that for $\beta > 1$, all the three energy conditions are satisfied at the white hole horizon. Moreover, at this white hole horizon, the surface gravity is given by,

$$\begin{aligned}\kappa_{WH} &\equiv \frac{1}{2}a'(x = -\sqrt{\Delta}) \\ &= -\frac{Y^2}{2Z^5} \times [(32\mathcal{D}^6 - x_0^6 + 18\mathcal{D}^2x_0^4 - 48\mathcal{D}^4x_0^2 + \mathcal{C}^6)\sqrt{\Delta} - 32\mathcal{D}^7 + 6\mathcal{D}x_0^6 - 38\mathcal{D}^3x_0^4 + 64\mathcal{D}^5x_0^2],\end{aligned} \tag{3.17}$$

which is always negative when the condition (3.2) holds.

In Figs. 2 and 3, we also show the physical quantities near the two horizons, and find that all the three energy conditions are indeed satisfied at these horizons, no matter whether Eq. (3.10) is satisfied or not. From these figures we can see that $\rho + p_r$ is the key quantity to determine the energy conditions. In particular, it is zero only at the two horizons and negative at other locations. Thus, the energy conditions are normally satisfied only at horizons. To show this more clearly, we plot $\rho + p_r$ vs x and the parameter $\mathcal{C}$ in Fig. 4, from which we can see that even with different choices of the free parameter, $\rho + p_r$ is non-negative only on the two horizons.

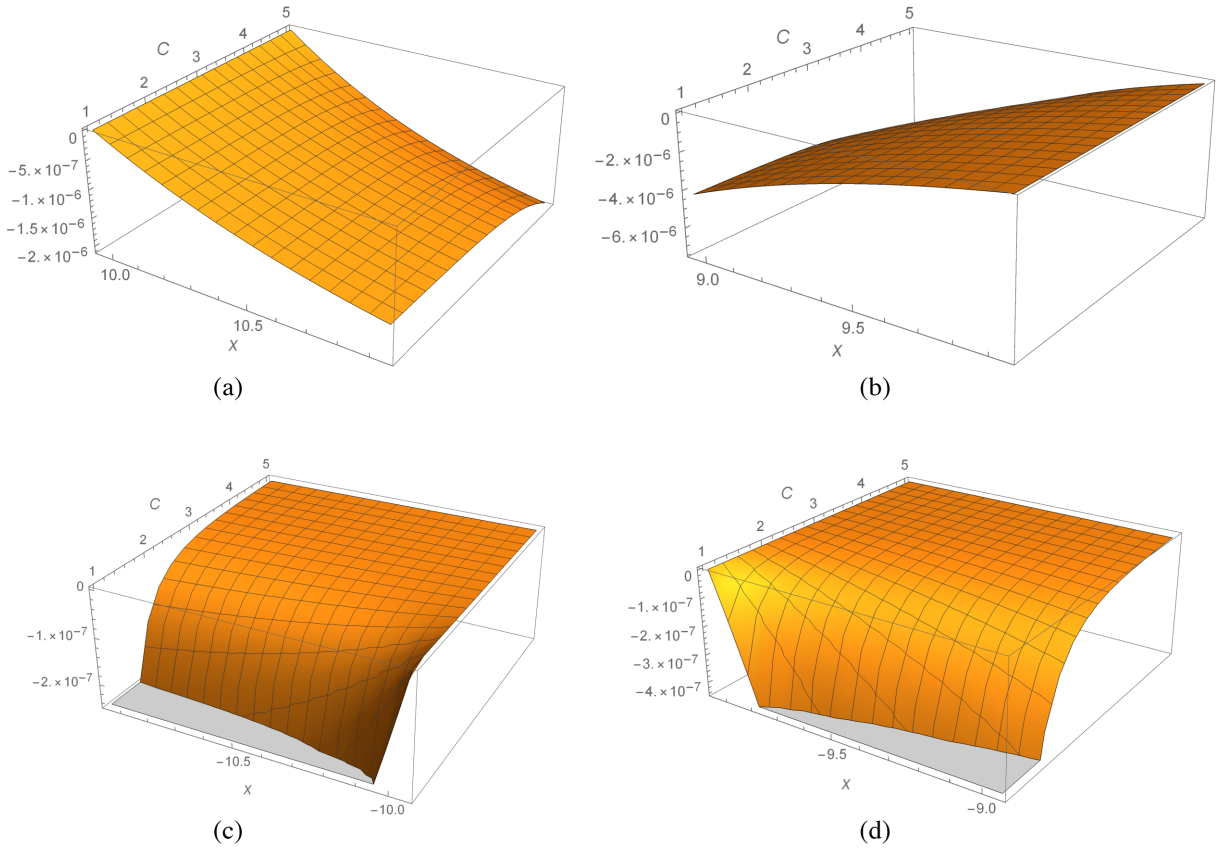

FIG. 4. The physical quantity $(\rho + p_r)$ vs the radial coordinate x and the parameter $\mathcal{C}$: (a) outside the black hole horizon; (b) inside the black hole horizon; (c) outside the white hole horizon; and (d) inside the white hole horizon. Graphs are plotted with $x_0 = 1, \mathcal{D} = 10$, for which the horizons are at $x_H^{\pm} \approx \pm 10$.

In addition, as $x \to \pm\infty$, we find that

$$\rho(x) = \begin{cases} \frac{\mathcal{D}x_0^2}{8x^5} + \mathcal{O}(\epsilon^6), & x \to \infty, \\ -\frac{\mathcal{D}x_0^6}{8x^5\mathcal{C}^4} + \mathcal{O}(\epsilon^6), & x \to -\infty, \end{cases}$$

$$p_r(x) = \begin{cases} -\frac{x_0^2}{4x^4} + \frac{\mathcal{D}x_0^2}{8x^5} + \mathcal{O}(\epsilon^6), & x \to \infty, \\ -\frac{x_0^6}{4x^4\mathcal{C}^4} - \frac{\mathcal{D}x_0^6}{8x^5\mathcal{C}^4} + \mathcal{O}(\epsilon^6), & x \to -\infty, \end{cases}$$

$$p_\theta(x) = \begin{cases} \frac{x_0^2}{4x^4} - \frac{\mathcal{D}x_0^2}{4x^5}, & x \to \infty, \\ \frac{x_0^6}{4x^4\mathcal{C}^4} + \frac{\mathcal{D}x_0^6}{4x^5\mathcal{C}^4} + \mathcal{O}(\epsilon^6), & x \to -\infty, \end{cases} \tag{3.18}$$

where $\epsilon \equiv 1/|x|$. Thus, in these two asymptotically flat regions, none of these three energy conditions holds. On the other hand, at these limits, we also have,

$$a(x) = \begin{cases} \frac{1}{4}\left(1 - \frac{2\mathcal{D}}{b}\right) + \mathcal{O}(\epsilon^2), & x \to \infty, \\ \frac{x_0^4}{4\mathcal{C}^4}\left(1 - \frac{(2\mathcal{D}\mathcal{C}^2/x_0^2)}{b}\right) + \mathcal{O}(\epsilon^2), & x \to -\infty, \end{cases}$$

$$b(x) \simeq \begin{cases} 2x, & x \to \infty, \\ -2(\mathcal{C}^2/x_0^2)x, & x \to -\infty, \end{cases} \tag{3.19}$$

from which we find that the masses of the black and white holes are given, respectively, by

$$M_{\rm BH} = \mathcal{D}, \qquad M_{WH} = \frac{\mathcal{D}\mathcal{C}^2}{x_0^2}. \tag{3.20}$$

To study the quantum gravitational effects further, let us turn to consider the Ricci scalar R and the relative difference $\Delta\mathcal{K}$ of the Kretschmann scalar, defined by

$$\Delta\mathcal{K} \equiv \frac{\mathcal{K} - \mathcal{K}^{GR}}{\mathcal{K}^{GR}}, \tag{3.21}$$

where $\mathcal{K}^{GR}$ denotes the Kretschmann scalar of the Schwarzschild solution, given by,

$$\mathcal{K}^{GR} \equiv R_{\alpha\beta\mu\nu}R^{\alpha\beta\mu\nu} = \begin{cases} \frac{48M_{\rm BH}^2}{b^6(x)}, & x > x_m, \\ \frac{48M_{WH}^2}{b^6(x)}, & x < x_m. \end{cases} \tag{3.22}$$

In GR, we have $R^{GR} = 0$, But due to the quantum geometric effects, clearly now we have $R \neq 0$. Therefore, both quantities, R and $\Delta\mathcal{K}$, will describe the deviations of the quantum black holes from the classical one. Before proceeding further, we would like to point out that Eqs. (3.21) and (3.22) are applicable when the two horizons

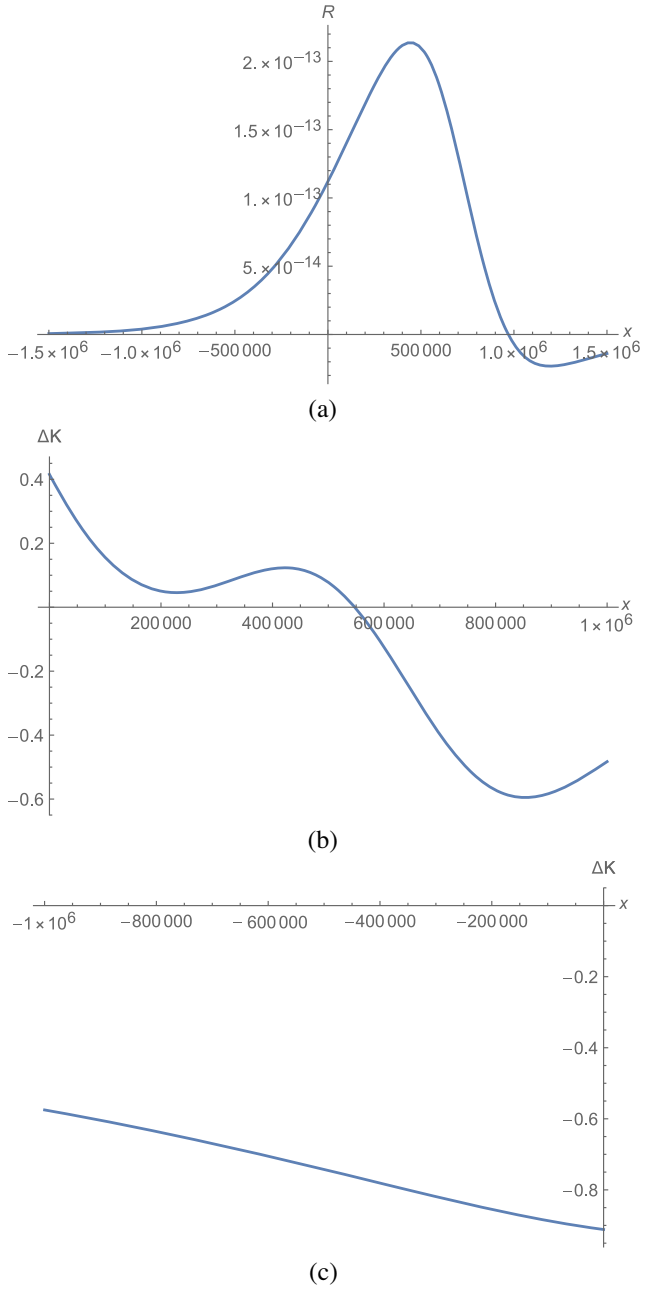

FIG. 5. Case $\Delta > 0, \mathcal{D} > 0, |x_m| \leq x_H^+, \beta = 1 + \frac{(\alpha-1)^2}{2\alpha}, \alpha \neq 1$: The quantities R and $\Delta\mathcal{K}$ vs x. Here we choose $\mathcal{C} = 2 \times 10^6, x_0 = 10^6, \mathcal{D} = \frac{5}{4} \times 10^6$, for which the horizons are located at $x_H^{\pm} = \pm 0.75 \times 10^6$, and the throat is at $x_m = x_H^+$, while the black and white hole masses are $M_{\rm BH} = \frac{5}{4} \times 10^6 M_{\rm Pl}$ and $M_{WH} = 5 \times 10^6 M_{\rm Pl}$, respectively.

and asymptotic regions exist. In some particular cases, this is not true, and a proper modification for $\Delta\mathcal{K}$ is needed, as to be shown below.

In addition, another important quantity is the scalar

$$C_{\mu\nu\alpha\beta}C^{\mu\nu\alpha\beta} = \mathcal{K}^2 + \frac{1}{3}R^2 - 2R_{\mu\nu}R^{\mu\nu}, \tag{3.23}$$

where $C_{\mu\nu\alpha\beta}$ denotes the Weyl tensor. However, for the sake of simplicity, in the following we shall consider only the quantities $\Delta\mathcal{K}$ and R, which are sufficient for our current purpose.

In Fig. 5, the quantities R and $\Delta\mathcal{K}$ are plotted in the region between the two horizons ($x_H^{\pm} = \pm 0.75 \times 10^6$), from which it can be seen that the deviation from GR are still large near these two horizons, although the curvature decays rapidly when away from them in both directions. In particular, for $M_{\rm BH} = 2 \times 10^6 M_{\rm Pl}$ and $M_{\rm WH} = 32 \times 10^6 M_{\rm Pl}$, near the horizons we find that $R(x_H^+) \lesssim 10^{-13}, R(x_H^-) \lesssim 10^{-14}$, and $|\Delta\mathcal{K}(x_H^+)| \lesssim 0.50$, $|\Delta\mathcal{K}(x_H^-)| \lesssim 0.65$, respectively. This is because now the throat coincides with the black hole horizon ($x_m = x_H^+ = 0.75 \times 10^6$), and to keep the throat open, the quantum effects at this point must be strong enough.

In Fig. 6, we plot R and $\Delta\mathcal{K}$ in the region that covers the throat ($x_m = 0$) as well as the two horizons ($x_H^{\pm} = \pm\sqrt{3} \times 10^{38}$). Thus, in the current case the throat is located far away from both of the two horizons. But, the deviations of the curvature near the two horizons are still large.

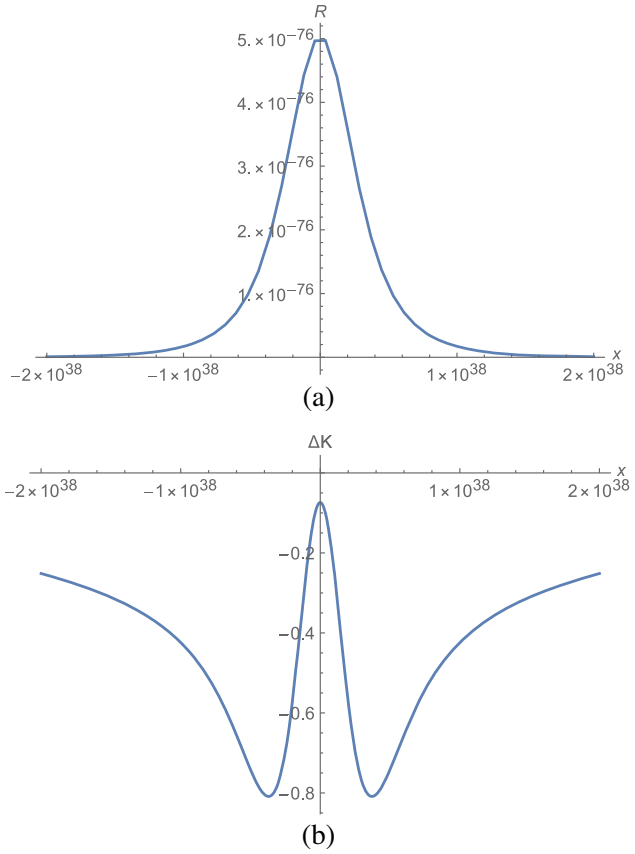

FIG. 6. Case $\Delta > 0, \mathcal{D} > 0, |x_m| < x_H^+, \beta \neq 1 + \frac{(\alpha-1)^2}{2\alpha}$: The quantities R and $\Delta\mathcal{K}$ vs x. Here we choose $\mathcal{C} = 10^{38}, x_0 = 10^{38}$, $\mathcal{D} = 2 \times 10^{38}$, for which the horizons are located at $x_H^{\pm} = \pm\sqrt{3} \times 10^{38}$, and the throat is at $x_m = 0$, while the black and white hole masses are $M_{\rm BH} = 2 \times 10^{38} M_{\rm Pl}$ and $M_{WH} = 2 \times 10^{38} M_{\rm Pl}$, respectively.

In particular, we find that $R(x_H^+) \lesssim 10^{-76}, R(x_H^-) \lesssim 10^{-76}$, and $|\Delta\mathcal{K}(x_H^+)| \lesssim 0.2$ and $|\Delta\mathcal{K}(x_H^-)| \lesssim 0.2$ for solar mass $M_{\rm BH} = 2 \times 10^{38} M_{\rm Pl}$ and $M_{WH} = 2 \times 10^{38} M_{\rm Pl}$. Therefore, in the current model the quantum gravitational effects can be still large near the horizons even for astrophysical black holes. More detailed analyses show that this is due to the fact that in the current case both x_0 and $\mathcal{C}$ are large ($x_0 = \mathcal{C} = 10^{38}$). Since large x_0 and $\mathcal{C}$ implies large λ_1 and λ_2, as one can see from the relations $\mathcal{C} \equiv (16C^2\lambda_1^2)^{1/6}$ and $x_0 \equiv \frac{\lambda_2}{\sqrt{n}}$. As mentioned above, the two parameters λ_1, λ_2 control quantum gravitational corrections. In particular, large λ_1 and λ_2 will lead to large quantum effects.

Therefore, to have negligible quantum gravitational effects, we must consider the cases where λ_1 and λ_2 are effectively small. In Fig. 7, we plot R and $\Delta\mathcal{K}$ in the region between the two horizons for $\mathcal{C} = 1, x_0 = 1, \mathcal{D} = 2 \times 10^6$,

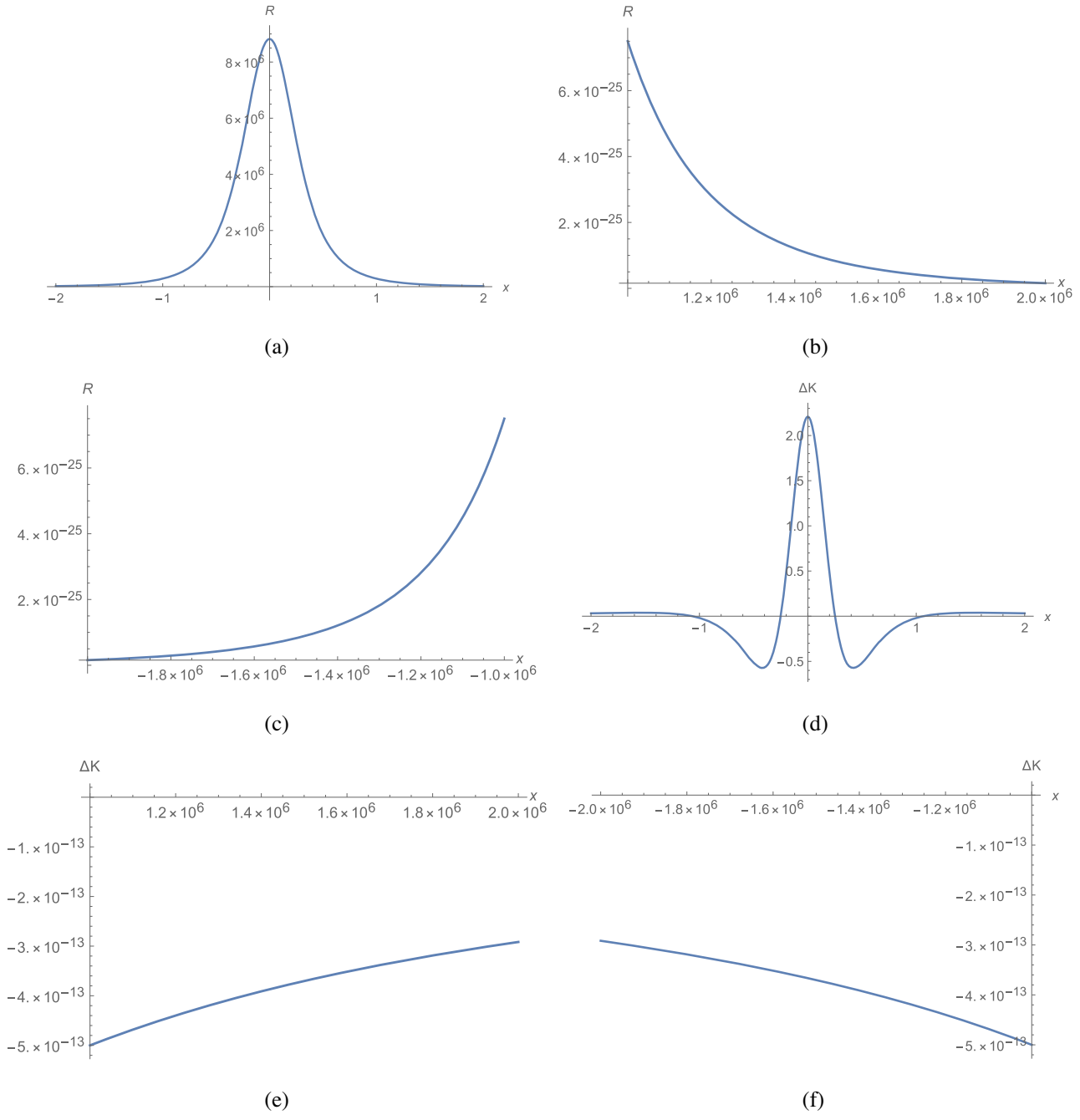

FIG. 7. Case $\Delta > 0, \mathcal{D} > 0, |x_m| \leq x_H^+, \beta \neq 1 + \frac{(\alpha-1)^2}{2\alpha}$: The quantities R and $\Delta\mathcal{K}$ vs x. Here we choose $\mathcal{C} = 1, x_0 = 1, \mathcal{D} = 2 \times 10^6$, for which the throat is at $x_m = 0$ and the black/white hole horizons are located at $x_H^{\pm} \approx \pm 2 \times 10^6$, respectively. The black and white hole masses are $M_{\rm BH} = M_{WH} = 2 \times 10^6 M_{\rm Pl}$.

for which the horizons are located at $x_H^{\pm} \approx \pm 2 \times 10^6$, and the throat is at $x_m = 0$, while the black and white hole masses are $M_{\rm BH} = M_{WH} = 2 \times 10^6 M_{\rm Pl}$. From this figure we can see that now the deviations from GR decays rapidly when away from the throat in both directions, and near the two horizons the quantum effects already become extremely small. In fact, near the two horizons now we find that $R(x_H^+) \lesssim 10^{-25}, R(x_H^-) \lesssim 10^{-25}$, and $|\Delta\mathcal{K}(x_H^+)| \lesssim 10^{-13}$ and $|\Delta\mathcal{K}(x_H^-)| \lesssim 10^{-13}$. Therefore, in the current case, the quantum gravitational effects are mainly concentrated in the neighborhood of the throat.

On the other hand, in Fig. 8 we plot R and $\Delta\mathcal{K}$ in the region between the two horizons for $\mathcal{C} = 10^{-6}, x_0 = 1, \mathcal{D} = 10^6$, for which the horizons are located at $x_H^{\pm} \approx \pm 10^6$, and the throat is at $x_m \approx -\frac{1}{2} \times 10^6$, while the black and white hole masses are $M_{\rm BH} = 10^6 M_{\rm Pl}$, $M_{WH} = 10^{-6} M_{\rm Pl}$, respectively. From this figure we can see that now the deviations from GR decays rapidly when away from the throat only in the black hole

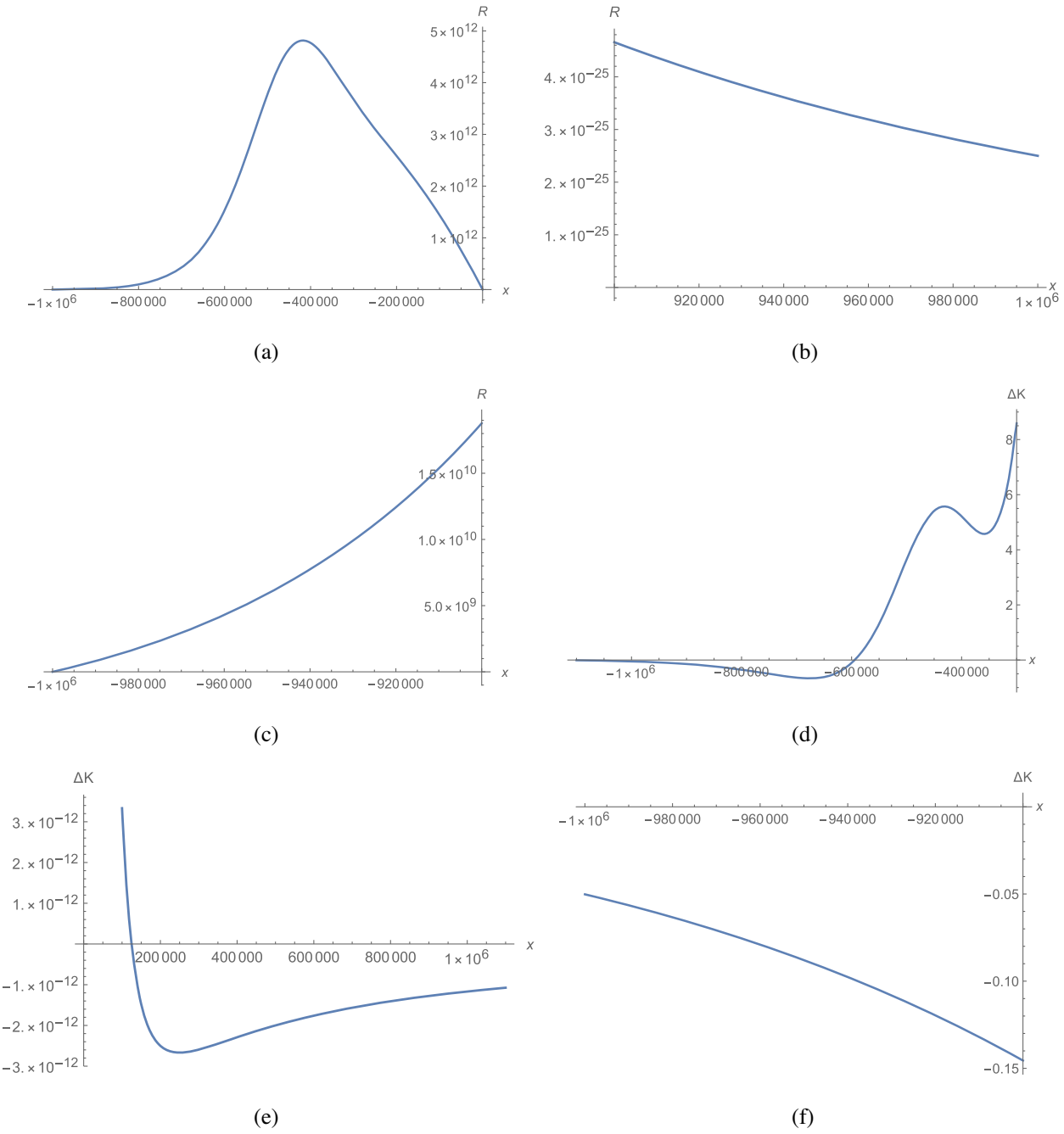

FIG. 8. Case $\Delta > 0, \mathcal{D} > 0, |x_m| \leq x_H^+, \beta \neq 1 + \frac{(\alpha-1)^2}{2\alpha}$: The quantities R and $\Delta\mathcal{K}$ vs x. Here we choose $\mathcal{C} = 10^{-6}, x_0 = 1, \mathcal{D} = 10^6$, for which the throat is at $x_m \approx -\frac{1}{2} \times 10^6$ and the black/white hole horizons are located at $x_H^{\pm} \approx \pm 10^6$, respectively. The black and white hole masses are $M_{\rm BH} = 10^6 M_{\rm Pl}$, $M_{WH} = 10^{-6} M_{\rm Pl}$.

direction, that is, only for $x > x_H^+$, and near the white hole horizon the quantum effects become very large again. In fact, near the two horizons now we find that $R(x_H^+) \lesssim 10^{-25}$, $R(x_H^-) \simeq 10^{10}$, and $|\Delta\mathcal{K}(x_H^+)| \lesssim 10^{-12}$ and $|\Delta\mathcal{K}(x_H^-)| \simeq 0.05$. Thus, in the current case the quantum gravitational effects are negligible only at the black hole horizon but still very large at the white hole horizon. This is due to the fact that the throat is now very close to the white hole horizon.

The above examples show clearly that, depending on the values of the three free parameters $\mathcal{C}, \mathcal{D}, x_0$ (or $\mathcal{D}, \lambda_1, \lambda_2$), quantum gravitational effects can be large, even for the cases in which the black/white hole masses are of order of solar masses. In particular, near the two horizons $x = x_H^\pm$, we find

$$R = \begin{cases} -\frac{x_0^6}{\mathcal{D}^2(2\mathcal{D}(\sqrt{\mathcal{D}^2-x_0^2}-\mathcal{D})+x_0^2)\mathcal{R}_H^+}, & x = x_H^+, \\ \frac{x_0^6}{\mathcal{D}^2(2\mathcal{D}(\mathcal{D}+\sqrt{\mathcal{D}^2-x_0^2})-x_0^2)\mathcal{R}_H^-}, & x = x_H^-, \end{cases} \tag{3.24}$$

where $\mathcal{R}_H^\pm \equiv ((\mathcal{D} \pm \sqrt{\mathcal{D}^2 - x_0^2})^6 + \mathcal{C}^6)^{2/3}$. Thus, for $\mathcal{D} \gg |x_0|$, we have

$$R \simeq \begin{cases} \frac{4x_0^2}{[(2\mathcal{D})^6+\mathcal{C}^6]^{2/3}}, & x = x_H^+, \\ \frac{x_0^6}{4\mathcal{D}^4\mathcal{C}^4}, & x = x_H^-. \end{cases} \tag{3.25}$$

Therefore, to have the effects negligibly small near the two horizons, we must require

$$\mathcal{C} \gtrsim |x_0|, \qquad \mathcal{D} \gg |x_0|. \tag{3.26}$$

On the other hand, as $x \to \pm\infty$, we find that

$$R \simeq \begin{cases} -\frac{x_0^2}{4x^4} + \frac{\mathcal{D}x_0^2}{2x^5} + \mathcal{O}(\epsilon^6), & x \to \infty, \\ -\frac{x_0^6}{4x^4\mathcal{C}^4} - \frac{\mathcal{D}x_0^6}{2x^5\mathcal{C}^4} + \mathcal{O}(\epsilon^6), & x \to -\infty, \end{cases} \tag{3.27}$$

and

$$\Delta\mathcal{K} \simeq \begin{cases} -\frac{4x_0^2}{3M_{\rm BH}x} + \mathcal{O}(\epsilon^2), & x \to \infty, \\ +\frac{4\mathcal{C}^2}{3M_{WH}x} + \mathcal{O}(\epsilon^2), & x \to -\infty, \end{cases} \tag{3.28}$$

where $M_{\rm BH}$ and M_{WH} are given by Eq. (3.20). Then, we have $|\Delta\mathcal{K}_+/\Delta\mathcal{K}_-| = 1 + \mathcal{O}(\epsilon^2)$, as $|x| \to \infty$. That is, whether $M_{WH} \gg M_{\rm BH}$ or not, $|\Delta\mathcal{K}_+|$ will always have the same asymptotic magnitude as $|\Delta\mathcal{K}_-|$, and both of them approach their GR limits as $\mathcal{O}(1/|x|)$.

Therefore, in the present case we find the following:

(i) The throat is always located in the region between the black and white hole horizons, $x_H^- \le x_m \le x_H^+$, and each of the three energy conditions, WEC, DEC, and SEC, is satisfied at the throat only in the case where the condition (3.10) holds. In this case the quantum gravitational effects are always large at the black hole horizon $x = x_H^+$. This is expected, as at the throat the quantum effects need to be strong, in order to keep the throat open, and when the condition (3.10) is satisfied, the black hole horizon always coincides with the throat, $x_m = x_H^+$.

(ii) Even the condition (3.10) does not hold, and the throat is far from both of the white and black hole horizons, that is, $|x_m| \ll |x_H^\pm|$, the quantum gravitational effects can be still large at the two horizons, including the cases in which both of the white and black hole masses are large, $M_{\rm BH}, M_{WH} \gg 10^6 M_{\rm Pl}$. Only in the case where the conditions (3.26) hold, can the effects become negligible at the two horizons.

(iii) In general, none of the three energy conditions is satisfied in the neighborhoods of the white and black hole horizons, $x = x_H^\pm$, except precisely at these two surfaces. However, the surface gravity at the black (white) hole horizon is always positive (negative), as now the condition $\rho + p_r + 2p_\theta > 0$ is still satisfied in the most part of the spacetime [51], as can be seen from Figs. 2 and 3. So, the trapped region ($x_H^- < x < x_H^+$) is still attractive to observers outside of it.

(iv) In the two asymptotically flat regions $x \to \pm\infty$, for which the geometrical radius becomes infinitely large, $b(\pm\infty) = \infty$, none of the three energy conditions is satisfied.

(v) The black and white hole masses read off from these two asymptotically flat regions are given by Eq. (3.20), which are always positive, no matter the condition (3.10) is satisfied or not. Again, this is because the relativistic Komar mass density $\rho + p_r + 2p_\theta$ is still positive in a large part of the spacetime. As a result, the total masses of the spacetime read off at the two asymptotically flat region are positive.

It should be noted that the absence of spacetime singularities in this case does not contradict to the Hawking-Penrose singularity theorems [50], as now none of the three energy conditions is satisfied in the two asymptotically flat regions, including the case in which the condition (3.10) holds, as shown in the above explicitly.

2. $|x_m| > x_H^+$

Now, let us turn to consider the case $|x_m| > x_H^+$, which implies that

$$\beta < 1 + \frac{(\alpha-1)^2}{2\alpha}. \tag{3.29}$$

In this case, since the throat is located in the region where $a(x) > 0$, then at the throat we have $\rho = \rho^+$ and $p_r = p_r^+$.

Hence, from Eq. (2.15) we find that the effective energy density ρ and pressures p_r and p_θ at the throat are given by

$$\rho = \frac{\mathcal{C}(12\mathcal{D}-5\mathcal{C})-5x_0^2}{2^{2/3}\mathcal{C}^2(x_0^2+\mathcal{C}^2)},$$
$$p_r = -\frac{1}{2^{2/3}\mathcal{C}^2},$$
$$p_\theta = \frac{(x_0^2+\mathcal{C}^2)^3-4\mathcal{D}x_0^2\mathcal{C}^3}{2^{2/3}\mathcal{C}^2(x_0^2+\mathcal{C}^2)^3}. \tag{3.30}$$

From these expressions, we find that in the 3D parameter space, WEC is satisfied when,

$$\beta \geq 1+\frac{(\alpha-1)^2}{2\alpha}, \quad \text{and} \quad \beta > \frac{1}{2}\alpha. \tag{3.31}$$

Clearly, these conditions contradict to the condition $|x_m| > x_H^+$, as it can be seen from Eq. (3.29). Therefore, in the current case WEC is always violated at the throat. In addition, for ρ, p_r and p_θ given by Eq. (3.30), we also find that neither DEC nor SEC is satisfied, after the conditions (3.29) are taken into account. Therefore, in the current case, *none of the three energy conditions is satisfied at the throat*.

On the other hand, following the analyses provided in the last subsection, it can be also shown that in the current case the following is true: (i) All the three energy conditions are not satisfied generically in the regions near the black hole and white hole horizons in the whole 3D phase space. But, the surface gravity at the black (white) hole horizon can be still positive (negative), as the relativistic Komar mass density can be still positive over a large region of the spacetime, so that its integration over the 3D spatial space can be positive, $\int_V(\rho+p_r+2p_\theta)dV > 0$. (ii) In the two asymptotically flat regions $x \to \pm\infty$, none of the three energy conditions is satisfied for any given values of $\mathcal{C}$, $\mathcal{D}$ and x_0, as longer as the condition (3.2) holds, which is resulted from the condition $\Delta > 0$. (iii) The black/white hole masses are also given by Eq. (3.20), which are all positive in the current case, too. (iv) The quantum effects are mainly concentrated near the throat. Since now the throat is always located either outside the black hole horizon ($x_m > x_H^+$) or outside the white hole horizon ($x_m < x_H^-$), the quantum effects can be large near the two horizons, even for the cases where the white/black hole masses are of order of solar masses.

It should be noted that the above analysis is not valid for the limit cases $x_0 \to 0$ and $\mathcal{C} \to 0$. So, in the following, let us consider these particular cases, separately.

3. $x_0 = 0$, $\mathcal{C} \neq 0$

If we assume that $\lambda_2 \neq 0$, from Eq. (2.6) we can see that this corresponds to the limit $\sqrt{n} \to \infty$. However, to keep $\mathcal{D} > 0$ and finite, we must require $D/\sqrt{n} \to$ finite and $CD > 0$. Then, we find that $\Delta = \mathcal{D}^2$, and from Eq. (2.9) we find $X = |x|$, and

$$Y = x + |x| = \begin{cases} 2x, & x \geq 0, \\ 0, & x < 0. \end{cases} \tag{3.32}$$

Hence, Eq. (2.8) implies $a(x) = 0$ and $b(x) = \infty$ for $x \leq 0$, that is, the metric becomes singular for $x \leq 0$. However, since $b(0) = \infty$, it is clear that now $x = 0$ already represents the spatial infinity. Therefore, in this case we only need to consider the region $x \in (0, \infty)$ [cf. Fig. 1(b)]. Then, we find that

$$X = x, \qquad Y = 2x, \qquad Z = 4(x^6+\hat{\mathcal{C}}^6)^{1/3}, \qquad (x \geq 0), \tag{3.33}$$

where $\hat{\mathcal{C}} \equiv \mathcal{C}/2$, and

$$a(x) = \frac{x^3(x-\mathcal{D})}{4(x^6+\hat{\mathcal{C}}^6)^{2/3}},$$
$$b(x) = \frac{2}{x}(x^6+\hat{\mathcal{C}}^6)^{1/3}. \tag{3.34}$$

Clearly, $a(x) = 0$ leads to two roots,

$$x_H^- = 0, \qquad x_H^+ = \mathcal{D}, \tag{3.35}$$

while the minimum of $b(x)$ now is located at $x_m \equiv \hat{\mathcal{C}}$, so we have

$$b(x) = \begin{cases} \infty, & x = 0, \\ 2^{4/3}\hat{\mathcal{C}}, & x = \hat{\mathcal{C}}, \\ \infty, & x = \infty. \end{cases} \tag{3.36}$$

It is interesting to note that the outer (black hole) horizon located at $x = x_H^+$ can be smaller than the throat $x = x_m$, that is, $\hat{\mathcal{C}} > \mathcal{D}$. In addition, the spacetime becomes anti-trapped at $x_H^- = 0$. Since $b(x=0) = \infty$, this antitrapped point now also corresponds to the spatial infinity at the other side (the white hole side) of the throat.

To study the solutions further, in the following let us consider the cases $\mathcal{D} \geq \hat{\mathcal{C}}$ and $\mathcal{D} < \hat{\mathcal{C}}$, separately.

(Case III.3.1) $\mathcal{D} \geq \hat{\mathcal{C}}$: In this case the throat locates always inside the black hole horizon, so in the region $x < x_H^+$ we always have $a(x) < 0$, and the corresponding effective energy density and pressures are given by

$$\rho(x) = \frac{\mathcal{C}^6[64\mathcal{D}x^6 + \mathcal{C}^6(2x-\mathcal{D})]x}{2^{13}(x^6+\hat{\mathcal{C}}^6)^{8/3}},$$
$$p_r(x) = -\frac{\mathcal{C}^6(\mathcal{D}\mathcal{C}^6 - 640x^7 + 704\mathcal{D}x^6)x}{2^{13}(x^6+\hat{\mathcal{C}}^6)^{8/3}},$$
$$p_\theta(x) = \frac{\mathcal{C}^6[64\mathcal{D}x^6 + \mathcal{C}^6(2x-\mathcal{D})]x}{2^{13}(x^6+\hat{\mathcal{C}}^6)^{8/3}}. \tag{3.37}$$

In particular, at the throat $(x = \hat{\mathcal{C}})$, we have

$$\rho = p_\theta = \frac{1}{2^{2/3}\mathcal{C}^2}, \qquad p_r = \frac{5\mathcal{C}-12\mathcal{D}}{2^{2/3}\mathcal{C}^3}, \tag{3.38}$$

from which we find that the WEC, SEC, and DEC are satisfied in the domain,

$$2\mathcal{D} \le \mathcal{C} \le 3\mathcal{D}. \tag{3.39}$$

Combining Eq. (3.39) with $\mathcal{C}/2 \le \mathcal{D}$, we have $\mathcal{C}/2 = \mathcal{D}$, which implies that the effective energy-momentum tensor satisfies all the three energy conditions at the throat only when the location of the throat and location of the black hole horizon coincide.

In Fig. 9 we plot the physical quantities $\rho, \rho \pm p_r, \rho \pm p_\theta$ and $\rho + p_r + 2 \pm p_\theta$ in the neighborhood of the throat.

In addition, as $x \to 0$ (or $b(x) \to \infty$), we find that

$$\rho = p_\theta = -\frac{8\mathcal{D}x}{\mathcal{C}^4} + \frac{16x^2}{\mathcal{C}^4} + \mathcal{O}(x^3),$$
$$p_r = -\frac{8\mathcal{D}x}{\mathcal{C}^4} + \mathcal{O}(x^3), \tag{3.40}$$

from which we find that the WEC, SEC, and DEC are satisfied only at $x = 0$.

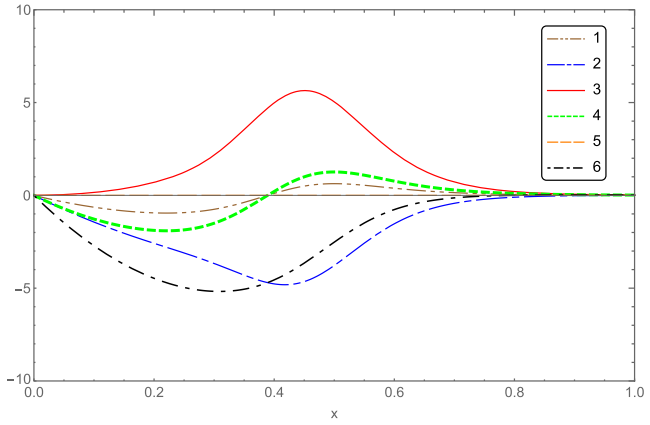

FIG. 9. Case $\Delta > 0, \mathcal{D} > 0, x_0 = 0, \mathcal{C} \neq 0$: The physical quantities, ρ, $(\rho + p_r)$, $(\rho - p_r)$, $(\rho + p_\theta)$, $(\rho - p_\theta)$, and $(\rho + p_r + 2p_\theta)$, represented, respectively, by Curves 1–6, vs x in the neighborhood of the throat. All curves are plotted with $\mathcal{C} = 1, \mathcal{D} = 1$, for which the throat is at $x_m = 0.5$, and the outer horizon is at $x_H^+ = 1$.

On the other hand, outside of the black hole horizon $(x > x_H^+)$, we always have $a(x) > 0$, and the corresponding effective energy density and pressures are given by

$$\rho(x) = \frac{\mathcal{C}^6(\mathcal{D}\mathcal{C}^6 - 640x^7 + 704\mathcal{D}x^6)x}{2^{13}(x^6+\hat{\mathcal{C}}^6)^{8/3}},$$
$$p_r(x) = -\frac{\mathcal{C}^6[64\mathcal{D}x^6 + \mathcal{C}^6(2x-\mathcal{D})]x}{2^{13}(x^6+\hat{\mathcal{C}}^6)^{8/3}},$$
$$p_\theta(x) = \frac{\mathcal{C}^6[64\mathcal{D}x^6 + \mathcal{C}^6(2x-\mathcal{D})]x}{2^{13}(x^6+\hat{\mathcal{C}}^6)^{8/3}}. \tag{3.41}$$

In particular, at the black hole horizon $(x_H^+ = \mathcal{D})$, we have

$$\rho = -p_r = p_\theta = \frac{8\mathcal{D}^2\mathcal{C}^6}{(64\mathcal{D}^6+\mathcal{C}^6)^{5/3}}, \tag{3.42}$$

so all the three energy conditions, WEC, SEC, and DEC, are satisfied at the black hole horizon. The surface gravity now is given by,

$$\kappa_{\rm BH} \equiv \frac{1}{2}a'(x=\mathcal{D}) = \frac{2\mathcal{D}^3}{(64\mathcal{D}^6+\mathcal{C}^6)^{2/3}}, \tag{3.43}$$

which is always positive, as now we have $\mathcal{D} > 0$.

At the spatial infinity $x \to \infty$, we find

$$\rho \approx -\frac{5\mathcal{C}^6}{64x^8} + \frac{11\mathcal{D}\mathcal{C}^6}{128x^9} + \mathcal{O}(\epsilon^{10}),$$
$$\rho + p_r \approx -\frac{5\mathcal{C}^6}{64x^8} + \frac{5\mathcal{D}\mathcal{C}^6}{64x^9} + \mathcal{O}(\epsilon^{10}),$$
$$\rho + p_\theta \approx -\frac{5\mathcal{C}^6}{64x^8} + \frac{3\mathcal{D}\mathcal{C}^6}{32x^9} + \mathcal{O}(\epsilon^{10}),$$
$$\rho + p_r + 2p_\theta \approx -\frac{5\mathcal{C}^6}{64x^8} + \frac{3\mathcal{D}\mathcal{C}^6}{32x^9} + \mathcal{O}(\epsilon^{10}), \tag{3.44}$$

from which we can see that none of the three energy conditions is satisfied. In addition, we also have

$$a(x) = \begin{cases} \frac{1}{4}\left(1 - \frac{2\mathcal{D}}{b}\right) + \mathcal{O}(\epsilon^2), & x \to \infty, \\ -\frac{4\mathcal{D}x^3}{\mathcal{C}^4} + \frac{4x^4}{\mathcal{C}^4} + \mathcal{O}(x^6), & x \to 0, \end{cases}$$
$$b(x) \simeq \begin{cases} 2x, & x \to \infty, \\ \frac{\mathcal{C}^2}{2x} + \frac{32x^5}{3\mathcal{C}^4} + \mathcal{O}(x^6), & x \to 0. \end{cases} \tag{3.45}$$

Therefore, the mass of the black hole is given by

$$M_{\rm BH} = \mathcal{D}. \tag{3.46}$$

To study the quantum gravitational effects further, in Fig. 10 we plot R and $\Delta\mathcal{K}$ in the region that covers the throat and the horizon, from which it can be seen that the deviation from GR quickly becomes vanishingly small around the horizon. In addition, as $x \to \infty$, we find that

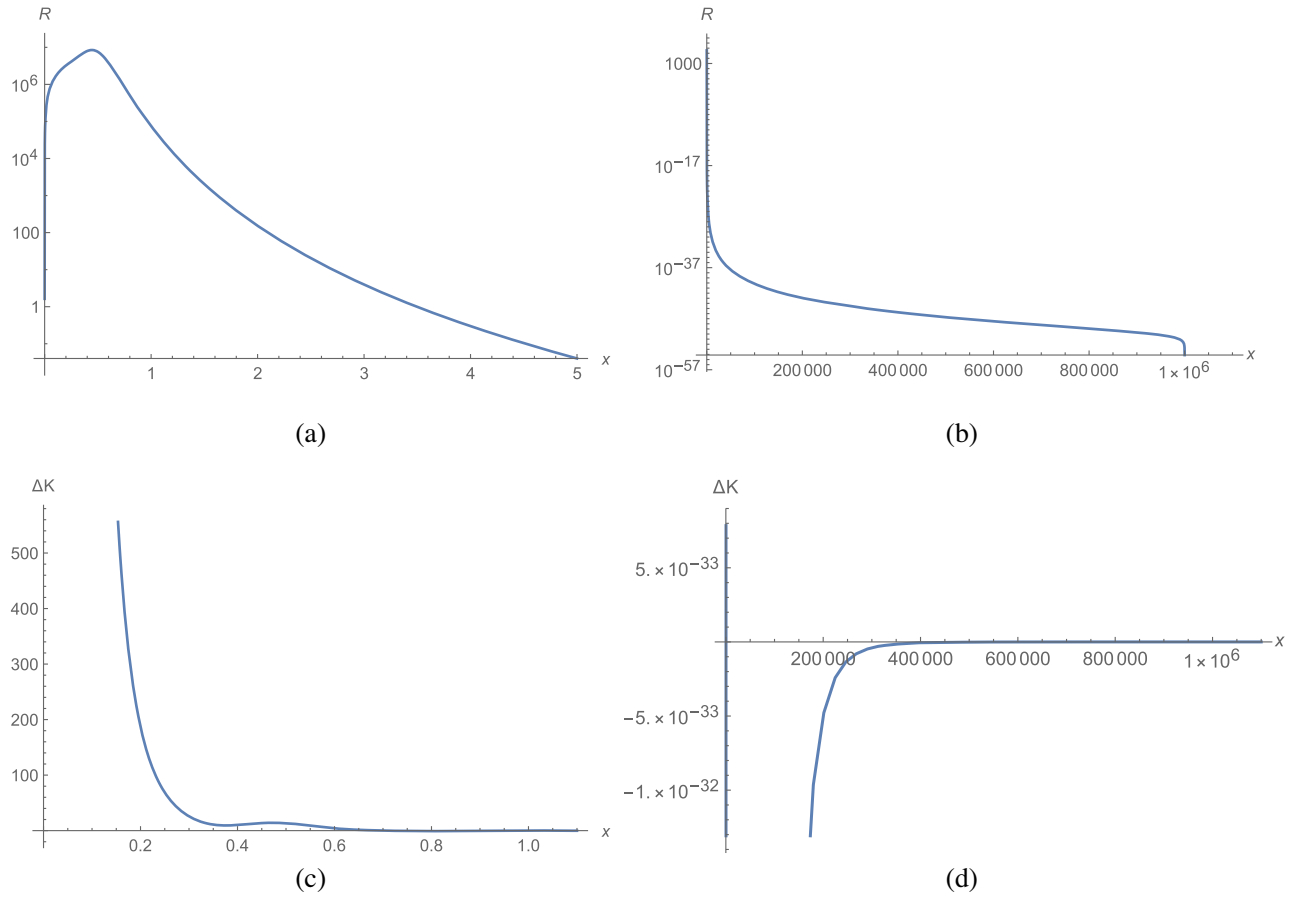

FIG. 10. Case $\Delta > 0, \mathcal{D} > 0, x_0 = 0, \mathcal{C} \neq 0$: The physical quantities R and $\Delta\mathcal{K}$. Here we choose $\mathcal{C} = 1$, $\mathcal{D} = 10^6$, so that $M_{\rm BH} = 10^6 M_{\rm Pl}, x_H^+ = \mathcal{D} = 10^6, x_m = \hat{\mathcal{C}} = 1/2$.

$$R \simeq -\frac{20\mathcal{C}^6}{b^8} + \mathcal{O}(\epsilon^9),$$
$$\Delta\mathcal{K} \simeq \frac{32\mathcal{C}^6}{3M_{\rm BH}b^5} + \mathcal{O}(\epsilon^6), \tag{3.47}$$

from which we can see that quantum corrections are decaying rapidly when $x \to \infty$.

When $x \to 0 (b \to \infty)$, we have

$$R \simeq \frac{8\mathcal{D}}{\mathcal{C}^2 b} + \mathcal{O}(b^{-2}),$$
$$\mathcal{K} \simeq \frac{240\mathcal{D}^2}{\mathcal{C}^4 b^2} + \mathcal{O}(b^{-3}), \tag{3.48}$$

which decays much less slowly than that in the Schwarzschild case, $\mathcal{K}^{GR} \to b^{-6}$.[3] It is even slower than that of the loop quantum black hole solution found by Ashtekar, Olmedo and Singh [21,22], in which $R \to b^{-2}$ and $\mathcal{K} \to b^{-4}$ [32].

(Case III.3.2) $\mathcal{D} < \hat{\mathcal{C}}$: In this case the throat locates always outside the black hole horizon, so in the region $x > x_H^+$ we always have $a(x) > 0$, and the corresponding effective energy density and pressures are given by Eq. (3.41). In particular, at the throat $(x = \hat{\mathcal{C}})$, we have

$$\rho = \frac{6\mathcal{D} - 5\hat{\mathcal{C}}}{2^{8/3}\hat{\mathcal{C}}^3}, \qquad p_r = -p_\theta = -\frac{1}{2^{8/3}\hat{\mathcal{C}}^2}, \tag{3.49}$$

from which we find that the WEC, SEC, and DEC are satisfied in the domain,

$$0 < \mathcal{C}/2 < \mathcal{D}. \tag{3.50}$$

Combining Eq. (3.50) with $\mathcal{D} < \hat{\mathcal{C}}$, we find that in this case, all the energy conditions are violated at the throat.

In addition, as $x \to 0$ (or $b(x) \to \infty$), we still have Eq. (3.40), from which we find that the WEC, SEC, and DEC are satisfied only at $x = 0$. At the spatial infinity $x \to \infty$, we still have Eq. (3.44), from which we can see

[3]In [47] a different conclusion was derived, as the authors implicitly assumed that $x_0\mathcal{C} \neq 0$. Therefore, our conclusion in this case does not essentially contradict to the one obtained in [47].

that none of the three energy conditions is satisfied. In addition, we also have Eq. (3.45), thus the mass of the black hole is given by Eq. (3.46).

For the quantum gravitational effects, we still have Eqs. (3.47) and (3.48). In Fig. 11 we plot R and $\Delta\mathcal{K}$ in the region that covers the throat and the horizon, from which it can be seen that the deviation from GR is still large around the horizon even for solar mass black holes, due to the fact that $\mathcal{C}$ is very large in this case and thus makes $\Delta\mathcal{K}$ large around horizon which can be seen from Eq. (3.47).

4. $\mathcal{C}=0$, $x_0 \neq 0$

If we assume that $\lambda_1 \neq 0$, from Eq. (2.6) we can see that this corresponds to the limit $C \to 0$. However, to keep $\mathcal{D} > 0$ and finite, we must require $DC \to$ finite and positive. Thus, we have

$$a(x) = \frac{(x^2-\Delta)X}{(X+\mathcal{D})Y^2}, \qquad b(x) = Y. \tag{3.51}$$

Clearly, $a(x) = 0$ leads to two real roots,

$$x_H^{\pm} = \pm\sqrt{\Delta}, \tag{3.52}$$

while $b(x)$ is a monotonically increasing function with $b(x=-\infty) = 0$ [cf. Fig. 1(c)]. Therefore, in contrast to the above cases, now the spacetime is not asymptotically flat as $x \to -\infty$, but rather it represents the center of the spacetime, at which a spacetime curvature singularity appears, as to be shown below. Therefore, in the current case the spacetime represents a black hole with two horizons located at $x = \pm\sqrt{\Delta}$. This is quite similar to the charged Reissner-Nordström (RN) solution.

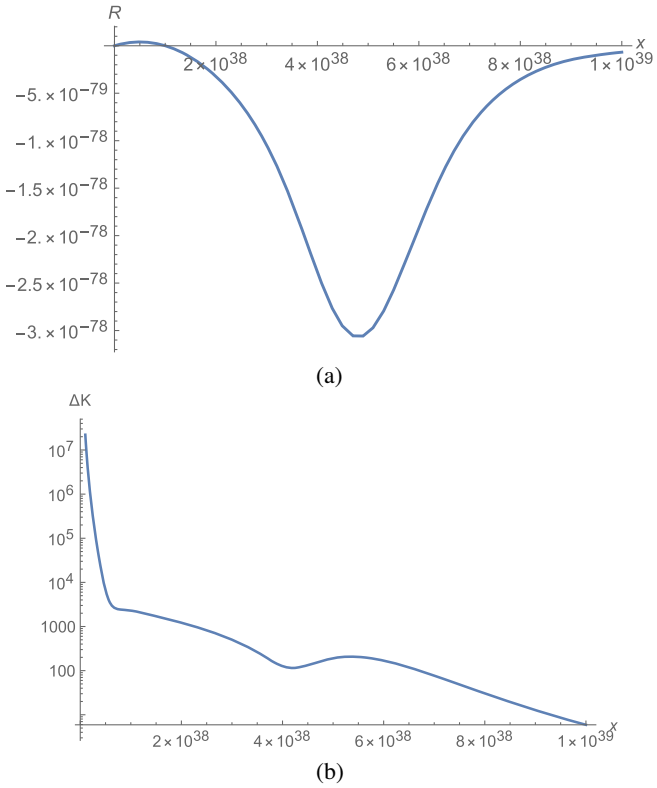

FIG. 11. Case $\Delta > 0, \mathcal{D} > 0, x_0 = 0, x_m > x_H^+$,: The quantities R and $\Delta\mathcal{K}$ vs x. Here we choose $\mathcal{C} = 10^{39}, \mathcal{D} = 10^{38}$, for which the outer horizon is located at $x_H^+ = 10^{38}$, and the throat is at $x_m = 5 \times 10^{38}$, while the black hole mass is $M_{\rm BH} = 10^{38} M_{\rm Pl}$.

In the trapped region, $x_H^- < x < x_H^+$, the effective energy density and pressures are given by

$$\begin{aligned}
\rho(x) =& \frac{x_0^2 Y^3}{X^2 (Y^6)^{8/3}}([1024x^{10} - 512\mathcal{D}x^9 + 2560x^8x_0^2 - 1024\mathcal{D}x^7x_0^2 + 2240x^6x_0^4 - 672\mathcal{D}x^5x_0^4 + 800x^4x_0^6 \\
& - 160\mathcal{D}x^3x_0^6 + 100x^2x_0^8 - 10\mathcal{D}xx_0^8 + 2x_0^{10}]X + 1024x^{11} - 512\mathcal{D}x^{10} + 3072x^9x_0^2 - 1280\mathcal{D}x^8x_0^2 \\
& + 3392x^7x_0^4 - 1120\mathcal{D}x^6x_0^4 + 1664x^5x_0^6 - 400\mathcal{D}x^4x_0^6 + 340x^3x_0^8 - 50\mathcal{D}x^2x_0^8 + 20xx_0^{10} - \mathcal{D}x_0^{10}), \\
p_r(x) =& -\frac{\mathcal{D}x_0^2 Y}{X^2 (Y^6)^{2/3}}, \\
p_\theta(x) =& \frac{x_0^2 Y^2}{2X^3 (Y^6)^{8/3}}([4096x^{12} - 4096\mathcal{D}x^{11} + 13312x^{10}x_0^2 - 10752\mathcal{D}x^9x_0^2 + 16384x^8x_0^4 - 10240\mathcal{D}x^7x_0^4 \\
& + 9408x^6x_0^6 - 4256\mathcal{D}x^5x_0^6 + 2480x^4x_0^8 - 720\mathcal{D}x^3x_0^8 + 244x^2x_0^{10} - 34\mathcal{D}xx_0^{10} + 4x_0^{12}]X + 4096x^{13} \\
& - 4096\mathcal{D}x^{12} + 15360x^{11}x_0^2 - 12800\mathcal{D}x^{10}x_0^2 + 22528x^9x_0^4 - 15104\mathcal{D}x^8x_0^4 + 16192x^7x_0^6 - 8288\mathcal{D}x^6x_0^6 \\
& + 5808x^5x_0^8 - 2080\mathcal{D}x^4x_0^8 + 924x^3x_0^{10} - 194\mathcal{D}x^2x_0^{10} + 44xx_0^{12} - 3\mathcal{D}x_0^{12}).
\end{aligned} \tag{3.53}$$

On the other hand, in the region $x < x_H^-$ or $x > x_H^+$, the effective energy density and pressures are given by

$$\rho(x) = \frac{\mathcal{D}x_0^2 Y}{X^2 (Y^6)^{2/3}},$$

$$\begin{aligned} p_r(x) = &-\frac{x_0^2 Y^3}{X^2 (Y^6)^{8/3}} ([1024x^{10} - 512\mathcal{D}x^9 + 2560x^8 x_0^2 - 1024\mathcal{D}x^7 x_0^2 + 2240x^6 x_0^4 - 672\mathcal{D}x^5 x_0^4 + 800x^4 x_0^6 \\ &- 160\mathcal{D}x^3 x_0^6 + 100x^2 x_0^8 - 10\mathcal{D}x x_0^8 + 2x_0^{10}]X + 1024x^{11} - 512\mathcal{D}x^{10} + 3072x^9 x_0^2 - 1280\mathcal{D}x^8 x_0^2 \\ &+ 3392x^7 x_0^4 - 1120\mathcal{D}x^6 x_0^4 + 1664x^5 x_0^6 - 400\mathcal{D}x^4 x_0^6 + 340x^3 x_0^8 - 50\mathcal{D}x^2 x_0^8 + 20x x_0^{10} - \mathcal{D}x_0^{10}), \\ p_\theta(x) = &\frac{x_0^2 Y^2}{2X^3 (Y^6)^{8/3}} ([4096x^{12} - 4096\mathcal{D}x^{11} + 13312x^{10} x_0^2 - 10752\mathcal{D}x^9 x_0^2 + 16384x^8 x_0^4 - 10240\mathcal{D}x^7 x_0^4 \\ &+ 9408x^6 x_0^6 - 4256\mathcal{D}x^5 x_0^6 + 2480x^4 x_0^8 - 720\mathcal{D}x^3 x_0^8 + 244x^2 x_0^{10} - 34\mathcal{D}x x_0^{10} + 4x_0^{12}]X + 4096x^{13} \\ &- 4096\mathcal{D}x^{12} + 15360x^{11} x_0^2 - 12800\mathcal{D}x^{10} x_0^2 + 22528x^9 x_0^4 - 15104\mathcal{D}x^8 x_0^4 + 16192x^7 x_0^6 - 8288\mathcal{D}x^6 x_0^6 \\ &+ 5808x^5 x_0^8 - 2080\mathcal{D}x^4 x_0^8 + 924x^3 x_0^{10} - 194\mathcal{D}x^2 x_0^{10} + 44x x_0^{12} - 3\mathcal{D}x_0^{12}). \end{aligned} \tag{3.54}$$

In Fig. 12 we plot the physical quantities $\rho, \rho \pm p_r$, $\rho \pm p_\theta$, and $\rho + p_r + 2 \pm p_\theta$ in the neighborhood of the two horizons, from which we can see that all these quantities become unbounded as $x \to -\infty$ (or $b(x) \to 0$).

In particular, at the horizon $(x = \sqrt{\Delta})$, we have

$$\rho = -p_r = \frac{(\sqrt{\Delta} + \mathcal{D})x_0^2}{\mathcal{D}Z^2},$$
$$p_\theta = \frac{x_0^4}{2\mathcal{D}^2 Z^2}, \tag{3.55}$$

so all the three energy conditions, WEC, SEC, and DEC, are satisfied in the domain

$$|x_0| < \mathcal{D}, \qquad (x_0 \neq 0). \tag{3.56}$$

The surface gravity at this horizon is given by,

$$\begin{aligned} \kappa_{\rm BH} &\equiv \frac{1}{2} a'(x = \sqrt{\Delta}) \\ &= \frac{Y^2}{2Z^5} ([32\mathcal{D}^6 - x_0^6 + 18\mathcal{D}^2 x_0^4 - 48\mathcal{D}^4 x_0^2]\sqrt{\Delta} \\ &\quad + 32\mathcal{D}^7 - 6\mathcal{D}x_0^6 + 38\mathcal{D}^3 x_0^4 - 64\mathcal{D}^5 x_0^2), \end{aligned} \tag{3.57}$$

which is always positive, provided that the conditions (3.56) hold.

On the other hand, at the horizon $x = -\sqrt{\Delta}$, we have

$$\begin{aligned} \rho = -p_r &= \frac{Y}{\mathcal{D}x_0^8} (16\mathcal{D}^4(\mathcal{D} + \sqrt{\Delta}) + x_0^4(5\mathcal{D} + \sqrt{\Delta}) \\ &\quad - 4\mathcal{D}^2 x_0^2(5\mathcal{D} + 3\sqrt{\Delta})), \\ p_\theta &= \frac{x_0^4}{2\mathcal{D}^2 Y^2}, \end{aligned} \tag{3.58}$$

so all the three energy conditions, WEC, SEC, and DEC, are satisfied in the domain given by Eq. (3.56). The surface gravity at this horizon is given by,

$$\begin{aligned} \kappa_{\rm BH} &\equiv \frac{1}{2} a'(x = -\sqrt{\Delta}) \\ &= -\frac{Y^2}{2Z^5} ([32\mathcal{D}^6 - x_0^6 + 18\mathcal{D}^2 x_0^4 - 48\mathcal{D}^4 x_0^2]\sqrt{\Delta} \\ &\quad - 32\mathcal{D}^7 + 6\mathcal{D}x_0^6 - 38\mathcal{D}^3 x_0^4 + 64\mathcal{D}^5 x_0^2), \end{aligned} \tag{3.59}$$

which is always negative when the conditions (3.56) hold.

As $x \to \pm\infty$, we find that

$$\begin{aligned} \rho(x) &= \begin{cases} \frac{\mathcal{D}x_0^2}{8x^5} + \mathcal{O}(\epsilon^6), & x \to \infty, \\ -\frac{8\mathcal{D}x}{x_0^4} + \mathcal{O}(\epsilon), & x \to -\infty, \end{cases} \\ p_r(x) &= \begin{cases} -\frac{x_0^2}{4x^4} + \frac{\mathcal{D}x_0^2}{8x^5} + \mathcal{O}(\epsilon^6), & x \to \infty, \\ -\frac{16x^2}{x_0^4} - \frac{8\mathcal{D}x}{x_0^4} - \frac{4}{x_0^2} + \mathcal{O}(\epsilon), & x \to -\infty, \end{cases} \\ p_\theta(x) &= \begin{cases} \frac{x_0^2}{4x^4} - \frac{\mathcal{D}x_0^2}{4x^5}, & x \to \infty, \\ \frac{16x^2}{x_0^4} + \frac{8\mathcal{D}x}{x_0^4} + \frac{4}{x_0^2} + \mathcal{O}(\epsilon), & x \to -\infty, \end{cases} \end{aligned} \tag{3.60}$$

from which we can show that none of the three energy conditions, WEC, SEC, and DEC, is satisfied at spatial infinity $x = \infty$ as well as at the center $b(x = -\infty) = 0$. In addition, we also have

$$\begin{aligned} a(x) &= \begin{cases} \frac{1}{4}\left(1 - \frac{2\mathcal{D}}{b}\right) + \mathcal{O}(\epsilon^2), & x \to \infty, \\ \frac{4x^4}{x_0^4} + \frac{4\mathcal{D}x^3}{x_0^4} + \frac{6x^2}{x_0^2} + \frac{4\mathcal{D}x}{x_0^2} \\ \quad + \frac{7}{4} + \frac{\mathcal{D}}{4x} + \mathcal{O}(\epsilon^2), & x \to -\infty, \end{cases} \\ b(x) &\simeq \begin{cases} 2x, & x \to \infty, \\ -\frac{x_0^2}{2x} + \frac{x_0^4}{8x^3} + \mathcal{O}(\epsilon^4), & x \to -\infty. \end{cases} \end{aligned} \tag{3.61}$$

Thus, the mass of the black hole is given by

$$M_{\rm BH} = \mathcal{D}. \tag{3.62}$$

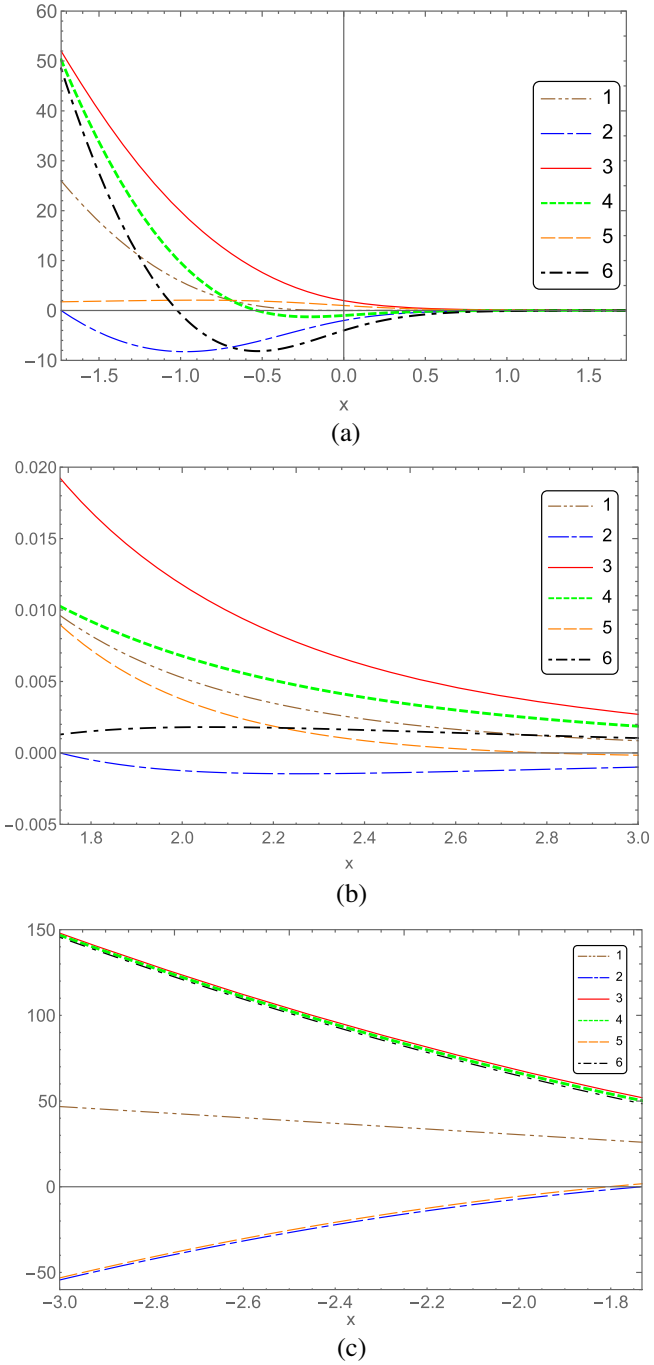

FIG. 12. Case $\Delta > 0, \mathcal{D} > 0, x_0 \neq 0, \mathcal{C} = 0$: The physical quantities, ρ, $(\rho + p_r)$, $(\rho - p_r)$, $(\rho + p_\theta)$, $(\rho - p_\theta)$, and $(\rho + p_r + 2p_\theta)$, represented, respectively, by Curves 1–6, vs x: (a) between the white and black horizons, $x_H^- \leq x \leq x_H^+$; (b) outside the black horizon, $x \geq x_H^+ = \sqrt{3}$; (c): outside the white horizon, $x \leq x_H^- = -\sqrt{3}$. All curves are plotted with $x_0 = 1, \mathcal{D} = 2$, for which the two horizons are located respectively at $x_H^\pm = \pm\sqrt{\Delta} = \pm\sqrt{3}$.

However, at $x = -\infty$ we have $b(-\infty) = 0$, and the physical quantities, ρ, p_r and p_θ, all become unbounded, so a spacetime curvature singularity appears at $x = -\infty$, and the solution has a RN-like structure, i.e., two horizons, one is inner and the other is outer, located, respectively, at $x = \pm\sqrt{\Delta}$. The spacetime singularity located at $b(-\infty) = 0$ is timelike.

On the other hand, in Fig. 13 we plot R and $\Delta\mathcal{K}$ in the region that covers the throat and the horizons, from which it can be seen that the deviation from GR quickly becomes vanishing small around the outer horizon, but around the inner horizon, R deviates from GR significantly. In fact, as $x \to \pm\infty$, we find that

$$R \simeq \begin{cases} -\frac{x_0^2}{4x^4} + \frac{\mathcal{D}x_0^2}{2x^5} + \mathcal{O}(\epsilon^6), & x \to \infty, \\ -\frac{16x^2}{x_0^4} - \frac{16\mathcal{D}x}{x_0^4} - \frac{4}{x_0^2} + \mathcal{O}(\epsilon), & x \to -\infty, \end{cases} \tag{3.63}$$

and

$$\mathcal{K} \simeq \begin{cases} \frac{3\mathcal{D}^2}{4x^6} + \mathcal{O}(\epsilon^7), & x \to \infty, \\ \frac{2816x^4}{x_0^8} + \frac{3072\mathcal{D}x^3}{x_0^8} + \frac{64x^2(15\mathcal{D}^2+22x_0^2)}{x_0^8} & \\ + \frac{640\mathcal{D}x}{x_0^6} + \frac{16(11x_0^2-8\mathcal{D}^2)}{x_0^6} + \mathcal{O}(\epsilon), & x \to -\infty, \end{cases} \tag{3.64}$$

from which we can see that, as $x \to -\infty$, both of the Ricci and Kretschmann scalars become unbounded, and a spacetime singularity appears at $b(x = -\infty) = 0$.

It is interesting to note that $\Delta\mathcal{K}$ is bounded and approaches a nonzero constant -1, as $x \to -\infty$. In fact, we have

$$\Delta\mathcal{K} \simeq \begin{cases} -\frac{4x_0^2}{3M_{\rm BH}x} + \mathcal{O}(\epsilon^2), & x \to \infty, \\ -1 + \frac{11x_0^4}{12M_{\rm BH}^2x^2} + \mathcal{O}(\epsilon^3), & x \to -\infty, \end{cases} \tag{3.65}$$

where in writing the above expressions we had set $\mathcal{K}^{GR} = 48M_{\rm BH}/b^6$ over the whole region $x \in (-\infty, \infty)$. Thus, near the singular point $b(x = -\infty) = 0$, the Kretschmann scalar of the quantum black hole diverges much more slowly than that of the Schwarzschild black hole. This can be seen from Eqs. (3.61) and (3.64), from which we find that $\mathcal{K} \propto b^{-4}$ as $x \to -\infty$.

5. $x_0 = \mathcal{C} = 0$

Since $\lambda_1\lambda_2 \neq 0$, from Eq. (2.6) we can see that this corresponds to the limits $C \to 0$ and $\sqrt{n} \to \infty$. However, to keep $\mathcal{D} > 0$, at these limits, we must require $DC/\sqrt{n} \to$ finite and positive. Then, we find that $\Delta = \mathcal{D}^2$, and from Eq. (2.9) we find $X = |x|$, and

$$Y = x + |x| = \begin{cases} 2x, & x \geq 0, \\ 0, & x < 0. \end{cases} \tag{3.66}$$

Therefore, the spacetime must be restricted to the region $x \geq 0$, in which we have

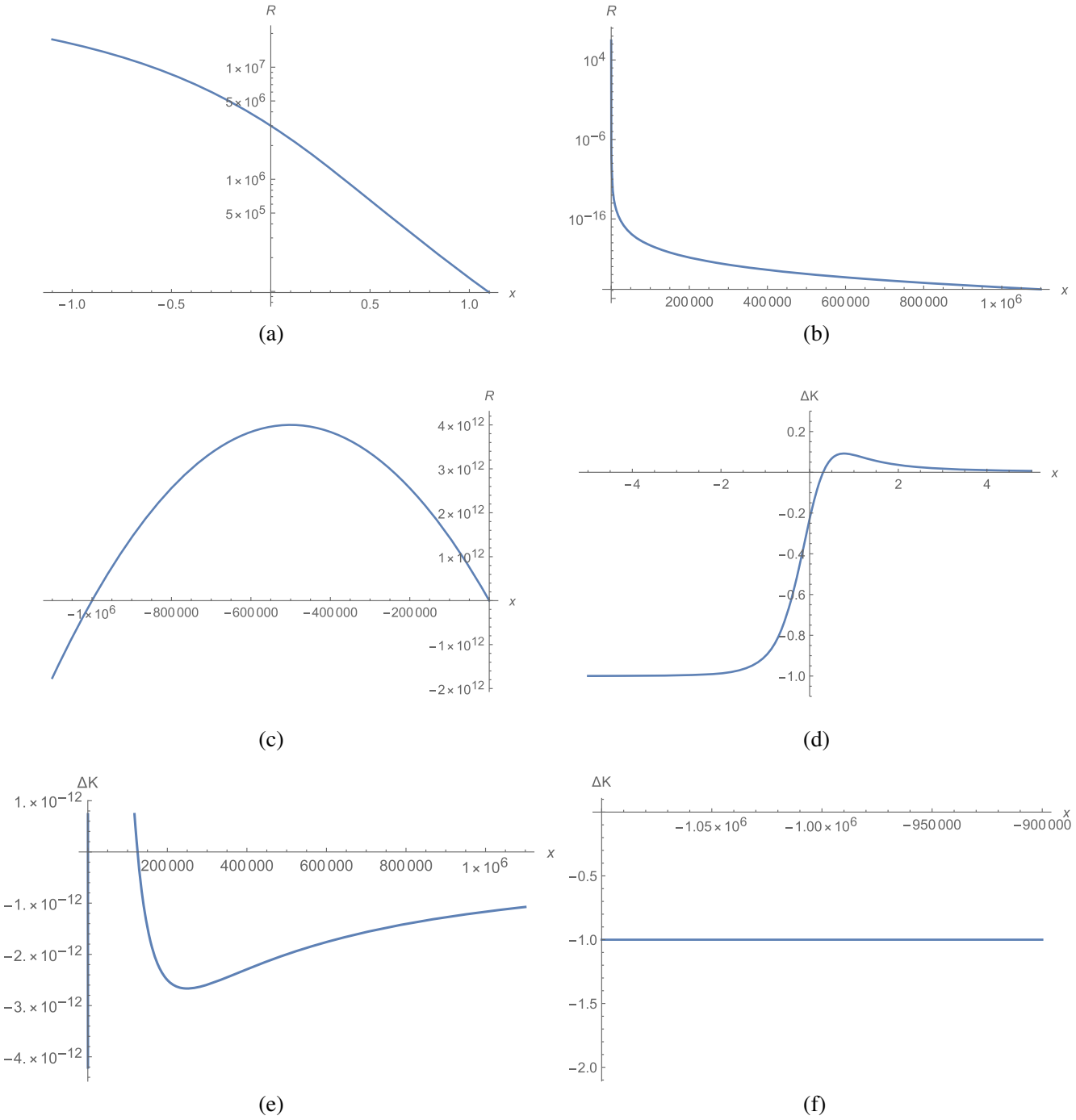

FIG. 13. Case $\Delta > 0, \mathcal{D} > 0, x_0 \neq 0, \mathcal{C} = 0$: The physical quantities R and $\Delta\mathcal{K}$ vs x. Here we choose $x_0 = 1$, $\mathcal{D} = 10^6$, so that $M_{\rm BH} = 10^6 M_{\rm Pl}$, and the horizons are located at $x = \pm\mathcal{D} = \pm 10^6$.

$$a(x) = \frac{x - \mathcal{D}}{4x} = \frac{1}{4}\left(1 - \frac{2\mathcal{D}}{b}\right),$$
$$b(x) = (x + \sqrt{x^2}) = 2x, \tag{3.67}$$

and

$$\rho(x) = p_r = p_\theta(x) = 0. \tag{3.68}$$

In fact, this is precisely the Schwarzschild solution, and will take its standard form, by setting $r = 2x$ and rescaling t,

$$ds^2 = \left(1 - \frac{2m}{r}\right)dt^2 + \left(1 - \frac{2m}{r}\right)^{-1} dr^2 + r^2 d\Omega^2, \tag{3.69}$$

where $m \equiv \mathcal{D}$. This case can be also considered as the limit of $\lambda_{1,2} \to 0$, for which the GR limit is obtained. Therefore,

the results are consistent with the effective theory of quantum black holes, as the singularities are always avoided exactly because of the replacement (1.9). When $\lambda_{1,2} \to 0$, the classical limits are recovered.

B. $\mathcal{D} < 0$

In this case, similar to the last one, let us consider $x_0\mathcal{C} \neq 0$ and $x_0\mathcal{C} = 0$, separately.

1. $x_0\mathcal{C} \neq 0$

Then, since $\Delta = \mathcal{D}^2 - x_0^2 > 0$, we must have

$$\mathcal{D} < -|x_0|. \tag{3.70}$$

Thus, from Eq. (2.8) we find that

$$a(x) = \frac{(X + |\mathcal{D}|)XY^2}{Z^2}, \qquad b(x) = \frac{Z}{Y}, \tag{3.71}$$

where X, Y, and Z are given by Eq. (2.9). From the above expressions, it can be shown that there are two asymptotically flat regions, corresponding to $x \to \pm\infty$, respectively. They are still connected by a throat located at x_m given by Eq. (3.3) [cf. Fig. 1(a)]. But since $a(x) \neq 0$ for any given x, horizons, either WHs or BHs, do not exist.

At the throat, the effective energy density ρ and pressures p_r and p_θ are still given by Eq. (3.30). Then, it can be easily shown that none of the three energy conditions can be satisfied in the current case, because condition Eq. (3.31) is always violated for $\mathcal{D} < 0$.

At the spatial infinities $x \to \pm\infty$, we find that the expression of ρ, p_r, p_θ are still given by Eq. (3.18), from which we can see that *none of the three energy conditions is satisfied either*. The asymptotic expressions of $a(x)$ and $b(x)$ are still given by Eq. (3.19), and the total masses measured at $x \to \pm\infty$ are

$$M_+ = \mathcal{D}, \qquad M_- = \frac{\mathcal{D}\mathcal{C}^2}{x_0^2}, \tag{3.72}$$

but since we now have $\mathcal{D} < 0$, they are all negative. Note that from now on, we use $M_\pm$ to denote the total masses of the spacetimes measured at $x = \pm\infty$, when no horizons (either BHs or WHs) exist, while reserve $M_{BH/WH}$ to denote the black (white) hole masses.

It can be shown that in the present case the deviation from GR decays rapidly when away from the throat from both directions of it only for some particular choice of the free parameters. In particular, as $x \to \pm\infty$, we find that the asymptotic expressions of $R(x)$ and $\Delta\mathcal{K}(x)$ are still given by Eq. (3.27) and Eq. (3.28), with $M_{\rm BH}(M_{WH})$ being replaced by $M_+(M_-)$. Therefore, we still have $|\Delta\mathcal{K}_+/\Delta\mathcal{K}_-| = 1 + \mathcal{O}(\epsilon^2)$, as $|x| \to \infty$. That is, whether $M_- \gg M_+$ or not, $|\Delta\mathcal{K}_+|$ will always have the same asymptotic magnitude as $|\Delta\mathcal{K}_-|$, and both of them approach their GR limits as $\mathcal{O}(1/|x|)$.

2. $x_0 = 0$, $\mathcal{C} \neq 0$

In this case $a(x)$ and $b(x)$ are still given by Eq. (3.34), but since $\mathcal{D} < 0$, $a(x) = 0$ is possible only when

$$x_H = 0, \tag{3.73}$$

where $b(x = 0) = \infty$. Therefore, in the current case there is no black/white hole horizon either, while the minimum of $b(x)$ now is still located at $x_m \equiv \hat{\mathcal{C}}$ [cf. Fig. 1(b)]. On the other hand, in this case the effective energy density and pressures are still given by Eq. (3.41), which are all become zero as $x \to 0$.

At the throat ($x = \hat{\mathcal{C}}$), ρ, p_r, p_θ are given by Eq. (3.49), but since now we have $\mathcal{D} < 0$, none of the three energy conditions is satisfied at the throat.

At the spatial infinity $x \to \infty$, on the other hand, we have the same expressions as given by Eq. (3.44), from which we can see that none of the three energy conditions is satisfied. The asymptotic behavior of $a(x)$ and $b(x)$ are still given by Eq. (3.45). Therefore, the total mass at $x \to \infty$ is given by

$$M_+ = \mathcal{D} < 0. \tag{3.74}$$

On the other hand, to study the quantum gravitational effects further, we consider the physical quantities R and $\Delta\mathcal{K}$ and find that the deviation from GR also quickly becomes vanishingly small as $x \to \infty$ for some particular choice of the free parameters. In particular, as $x \to \infty$, we find that the asymptotic expressions of $R(x)$ and $\Delta\mathcal{K}(x)$ are still given by Eq. (3.47), with $M_{\rm BH}$ being replaced by M_+.

3. $x_0 \neq 0$, $\mathcal{C} = 0$

From Eq. (2.8) we find that

$$a(x) = \frac{(X + |\mathcal{D}|)X}{Y^2}, \qquad b(x) = Y, \tag{3.75}$$

where X, Y, and Z are given by Eq. (2.9). Clearly, $a(x) = 0$ has no real roots, thus no horizons exist, while $b(x)$ is still a monotonically increasing function with $b(x = -\infty) = 0$ [cf. Fig. 1(c)].

On the other hand, in this case the effective energy density and pressures are still given by Eq. (3.54). In particular, at the spatial infinities $x \to \pm\infty$, they stall take the forms of Eq. (3.60), from which we find none of the three energy conditions, WEC, SEC, and DEC, is satisfied. In addition, the asymptotic behaviors of $a(x)$ and $b(x)$ are given by Eq. (3.61). Therefore, the total mass at $x = \infty$ is still given by Eq. (3.62), which is always negative.

However, at $x = -\infty$ we have $b(-\infty) = 0$, and the physical quantities, ρ, p_r and p_θ, all become unbounded, so a spacetime curvature singularity appears at $x = -\infty$.

In addition, from R and $\Delta\mathcal{K}$ we find that the deviation from GR quickly becomes vanishingly small as $x \to +\infty$, but as $x \to -\infty$, R deviates from GR significantly, as a spacetime curvature singularity now appears at $x = -\infty$, at which we have $b(x = -\infty) = 0$.

4. $x_0 = \mathcal{C} = 0$

In this case, the solution is precisely the Schwarzschild solution with negative mass, and will take its standard form, by setting $r = 2x$ and rescaling t,

$$ds^2 = \left(1 - \frac{2m}{r}\right)dt^2 + \left(1 - \frac{2m}{r}\right)^{-1} dr^2 + r^2 d\Omega^2, \tag{3.76}$$

where $m \equiv \mathcal{D} < 0$.

This completes the analysis of the solutions in the case $\Delta > 0$. In Table II, we summarize the main properties of these solutions.

IV. SPACETIMES WITH $\Delta = 0$

From Eq. (2.10) we find that this case corresponds to

$$|\lambda_2| = \frac{3}{2}|CD|, \quad \text{or} \quad |\mathcal{D}| = |x_0|. \tag{4.1}$$

Then, from Eqs. (2.8) and (2.9) we obtain

$$a(x) = \frac{x^2 X Y^2}{(X + \mathcal{D})Z^2}, \qquad b(x) = \frac{Z}{Y}, \tag{4.2}$$

where

$$X \equiv \sqrt{x^2 + \mathcal{D}^2}, \qquad Y \equiv x + X,$$
$$Z \equiv (Y^6 + \mathcal{C}^6)^{1/3}. \tag{4.3}$$

To study these solutions further, in the following let us consider the three possibilities, $\mathcal{D} > 0$, $\mathcal{D} = 0$ and $\mathcal{D} < 0$, separately.

A. $\mathcal{D} > 0$

In this subcase, there are still two possibilities, $\mathcal{C} \neq 0$ and $\mathcal{C} = 0$.

1. $\mathcal{C} \neq 0$

In this case, since we also have $\mathcal{D} > 0$, we find that

$$b(x) = \begin{cases} \infty, & x = \infty, \\ 2^{1/3}\mathcal{C}, & x = x_m, \\ \infty, & x = -\infty, \end{cases} \tag{4.4}$$

where $x_m \equiv (\mathcal{C}^2 - \mathcal{D}^2)/(2\mathcal{C})$ [cf. Fig. 1(a)].

On the other hand, $a(x) = 0$ leads to $x_H^{\pm} = 0$, which is a double root. This is similar to the charged RN solution in the extreme case $|e| = m$. At the horizon, we have

$$b(0) = \frac{(\mathcal{C}^6 + \mathcal{D}^6)^{1/3}}{|\mathcal{D}|}, \tag{4.5}$$

and

$$\rho = -p_r = 2p_\theta = \frac{\mathcal{D}^2}{(\mathcal{D}^6 + \mathcal{C}^6)^{2/3}}, \tag{4.6}$$

from which we find that all the WEC, SEC, and DEC are satisfied. In addition, the surface gravity at the horizon is,

$$\kappa_{\rm BH} \equiv \frac{1}{2}a'(x = 0) = 0, \tag{4.7}$$

as in the extremal case of the RN solution.

At the throat, the effective energy density ρ and pressures p_r and p_θ are given by

$$\rho = \frac{-5\mathcal{D}^2 + 12\mathcal{D}\mathcal{C} - 5\mathcal{C}^2}{2^{2/3}\mathcal{C}^2(\mathcal{D}^2 + \mathcal{C}^2)}, \qquad p_r = -\frac{1}{2^{2/3}\mathcal{C}^2},$$
$$p_\theta = \frac{(\mathcal{D}^2 + \mathcal{C}^2)^3 - 4\mathcal{D}^3\mathcal{C}^3}{2^{2/3}(\mathcal{D}^2 + \mathcal{C}^2)^3}, \tag{4.8}$$

from which we find that WEC, SEC, and DEC are satisfied only when

$$\mathcal{D} = \mathcal{C}. \tag{4.9}$$

Then, from the expression $x_m = (\mathcal{C}^2 - \mathcal{D}^2)/(2\mathcal{C})$, we can see when $\mathcal{D} = \mathcal{C}$ we also have $x_m = 0$, i.e., the black hole horizon now coincides with the throat.

In Fig. 14 we plot out the quantities $\rho, \rho \pm p_r, \rho \pm p_\theta$ and $\rho + p_r + 2p_\theta$ vs x in the neighborhood of the throat for $\mathcal{C} = 1.5, \mathcal{D} = 2$. With these choices, the throat is located at $x_m \approx -0.437$, and the horizon is at $x_H^{\pm} = 0$. From these curves we can see clearly that the three energy conditions, WEC, SEC, and DEC, are satisfied only at the horizon.

At the spatial infinities $x \to \pm\infty$, we find that

$$\rho(x) = \begin{cases} \frac{\mathcal{D}^3}{8x^5} + \mathcal{O}(\epsilon^6), & x \to \infty, \\ -\frac{\mathcal{D}^7}{8x^5\mathcal{C}^4} + \mathcal{O}(\epsilon^6), & x \to -\infty, \end{cases}$$
$$p_r(x) = \begin{cases} -\frac{\mathcal{D}^2}{4x^4} + \frac{\mathcal{D}^3}{8x^5} + \mathcal{O}(\epsilon^6), & x \to \infty, \\ -\frac{\mathcal{D}^6}{4x^4\mathcal{C}^4} - \frac{\mathcal{D}^7}{8x^5\mathcal{C}^4} + \mathcal{O}(\epsilon^6), & x \to -\infty, \end{cases}$$
$$p_\theta(x) = \begin{cases} \frac{\mathcal{D}^2}{4x^4} - \frac{\mathcal{D}^3}{4x^5} + \mathcal{O}(\epsilon^6), & x \to \infty, \\ \frac{\mathcal{D}^6}{4x^4\mathcal{C}^4} + \frac{\mathcal{D}^7}{4x^5\mathcal{C}^4} + \mathcal{O}(\epsilon^6), & x \to -\infty, \end{cases} \tag{4.10}$$

and

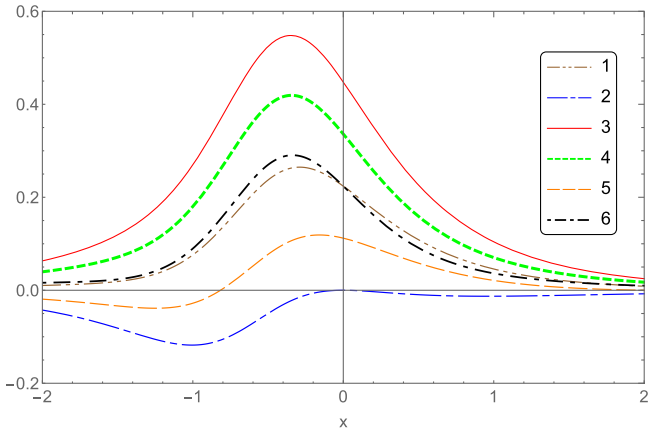

FIG. 14. Case $\Delta = 0, \mathcal{D} > 0, \mathcal{C} \neq 0$: The physical quantities, ρ, $(\rho + p_r)$, $(\rho - p_r)$, $(\rho + p_\theta)$, $(\rho - p_\theta)$, and $(\rho + p_r + 2p_\theta)$, represented, respectively, by Curves 1–6, vs x in the neighborhood of the throat. All graphs are plotted with $\mathcal{C} = 1.5, \mathcal{D} = 2$, for which the throat is at $x_m \approx -0.437$, and horizons are at $x_H^{\pm} = 0$.

$$a(x) = \begin{cases} \frac{1}{4}\left(1 - \frac{2\mathcal{D}}{b}\right) + \mathcal{O}(\epsilon^2), & x \to \infty, \\ \frac{\mathcal{D}^4}{4\mathcal{C}^4}\left(1 - \frac{(2\mathcal{C}^2/\mathcal{D})}{b}\right) + \mathcal{O}(\epsilon^2), & x \to -\infty, \end{cases}$$
$$b(x) \simeq \begin{cases} 2x + \mathcal{O}(\epsilon), & x \to \infty, \\ -2(\mathcal{C}^2/\mathcal{D}^2)x + \mathcal{O}(\epsilon), & x \to -\infty, \end{cases} \tag{4.11}$$

where $\epsilon \equiv 1/x$. Therefore, the masses of the black and white holes are given, respectively, by

$$M_{\rm BH} = \mathcal{D}, \qquad M_{WH} = \frac{\mathcal{C}^2}{\mathcal{D}}. \tag{4.12}$$

On the other hand, from Eq. (4.10) we find that in the limit $x \to \infty$ we have

$$\begin{aligned} \rho &\approx \frac{\mathcal{D}^3}{8x^5} + \mathcal{O}(\epsilon^6), \\ \rho + p_r &\approx -\frac{\mathcal{D}^2}{4x^4} + \frac{\mathcal{D}^3}{4x^5} + \mathcal{O}(\epsilon^6), \\ \rho + p_\theta &\approx \frac{\mathcal{D}^2}{4x^4} - \frac{\mathcal{D}^3}{8x^5} + \mathcal{O}(\epsilon^6), \\ \rho + p_r + 2p_\theta &\approx \frac{\mathcal{D}^2}{4x^4} - \frac{\mathcal{D}^3}{4x^5} + \mathcal{O}(\epsilon^6), \end{aligned} \tag{4.13}$$

while in the limit $x \to -\infty$, we have

$$\begin{aligned} \rho &\approx -\frac{\mathcal{D}^7}{8x^5\mathcal{C}^4} + \mathcal{O}(\epsilon^6), \\ \rho + p_r &\approx -\frac{\mathcal{D}^6}{4x^4\mathcal{C}^4} - \frac{\mathcal{D}^7}{4x^5\mathcal{C}^4} + \mathcal{O}(\epsilon^6), \\ \rho + p_\theta &\approx \frac{\mathcal{D}^6}{4x^4\mathcal{C}^4} + \frac{\mathcal{D}^7}{8x^5\mathcal{C}^4} + \mathcal{O}(\epsilon^6), \\ \rho + p_r + 2p_\theta &\approx \frac{\mathcal{D}^6}{4x^4\mathcal{C}^4} + \frac{\mathcal{D}^7}{4x^5\mathcal{C}^4} + \mathcal{O}(\epsilon^6). \end{aligned} \tag{4.14}$$

Therefore, *none of the three energy conditions is satisfied at both* $x = -\infty$ *and* $x = \infty$.

In Fig. 15, we plot R and $\Delta\mathcal{K}$ for solar mass black/white holes in the region that covers the throat, with $\mathcal{C} = \mathcal{D} = x_0 = 10^6$, for which the horizon and the throat are all located at $x_H^{\pm} = x_m = 0$. In this case, it can be seen that the deviations from GR decay rapidly when away from the throat from both directions, and the quantum gravitational effects are mainly concentrated in the neighborhood of it.

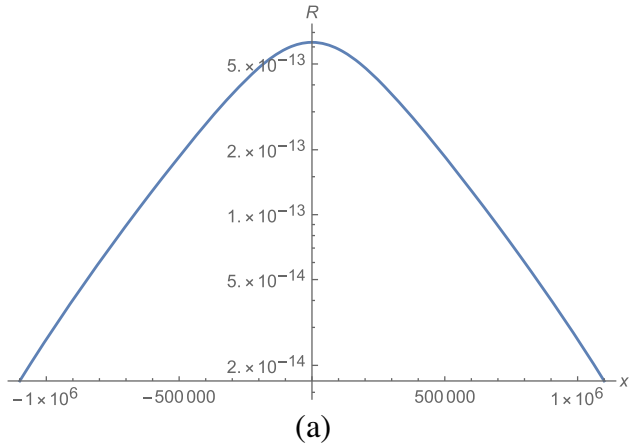

(a)

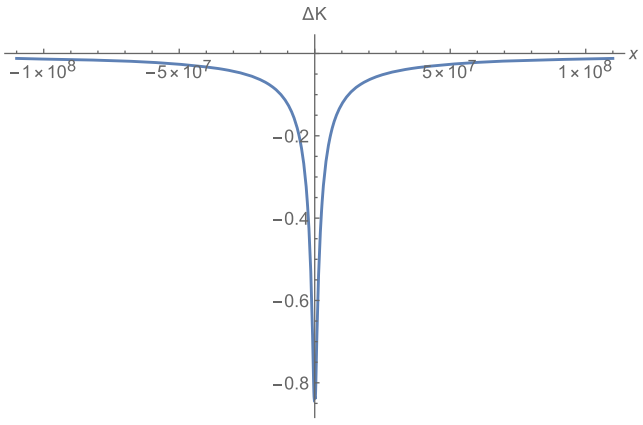

(b)

FIG. 15. *Case* $\Delta = 0, \mathcal{D} > 0, \mathcal{C} \neq 0$: R and $\Delta\mathcal{K}$ vs x. Here we choose $\mathcal{C} = x_0 = 10^6$, for which the horizon and the throat are all located at $x_H^{\pm} = x_m = 0$.

In addition, as $x \to \pm\infty$, we find that

$$R \simeq \begin{cases} -\frac{\mathcal{D}^2}{4x^4} + \frac{\mathcal{D}^3}{2x^5} + \mathcal{O}(\epsilon^6), & x \to \infty, \\ -\frac{\mathcal{D}^6}{4x^4\mathcal{C}^4} - \frac{\mathcal{D}^7}{2x^5\mathcal{C}^4} + \mathcal{O}(\epsilon^6), & x \to -\infty, \end{cases} \tag{4.15}$$

and

$$\Delta\mathcal{K} \simeq \begin{cases} -\frac{4M_{\rm BH}}{3x} + \mathcal{O}(\epsilon^2), & x \to \infty, \\ +\frac{4\mathcal{C}^2}{3M_{WH}x} + \mathcal{O}(\epsilon^2), & x \to -\infty, \end{cases} \tag{4.16}$$

where $M_{\rm BH}$ and M_{WH} are given by Eq. (4.12).

2. $\mathcal{C} = 0$

In this case, we have

$$a(x) = \frac{x^2 X}{(X+\mathcal{D})Y^2}, \qquad b(x) = Y. \tag{4.17}$$

Then, $a(x) = 0$ leads to $x = 0$, which is a double root, as mentioned above. The geometric radius $b(x)$ is a monotonically increasing function with $b(x = -\infty) = 0$ [cf. Fig. 1(c)].

In Fig. 16 we plot the physical quantities $\rho, \rho \pm p_r, \rho \pm p_\theta$ and $\rho + p_r + 2 \pm p_\theta$ in the neighborhood of the horizon $x_H = 0$, at which, we have

$$\rho = -p_r = 2p_\theta = \frac{1}{\mathcal{D}^2}, \tag{4.18}$$

so all the three energy conditions, WEC, SEC, and DEC, are satisfied. In addition, the surface gravity at this horizon also vanishes.

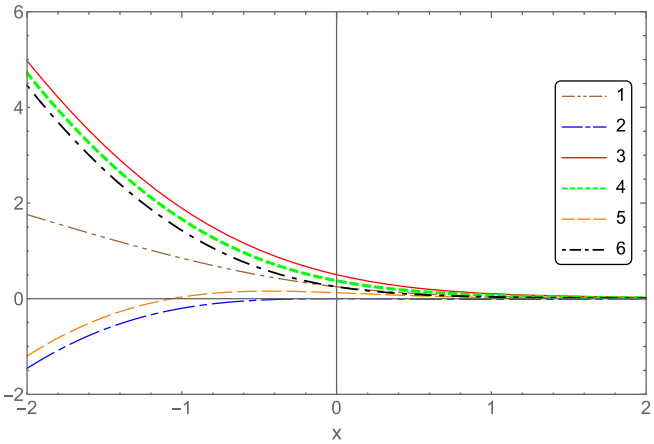

FIG. 16. Case $\Delta = 0, \mathcal{D} > 0, \mathcal{C} = 0$: The physical quantities, ρ, $(\rho + p_r)$, $(\rho - p_r)$, $(\rho + p_\theta)$, $(\rho - p_\theta)$, and $(\rho + p_r + 2p_\theta)$, represented, respectively, by Curves 1–6, vs x in the neighborhood of the horizon $x_H^{\pm} = 0$. All graphs are plotted with $\mathcal{D} = 2$.

At the spatial infinities $x \to \pm\infty$, we find that

$$\begin{aligned} \rho(x) &= \begin{cases} \frac{\mathcal{D}^3}{8x^5} + \mathcal{O}(\epsilon^6), & x \to \infty, \\ -\frac{8x}{\mathcal{D}^3} + \mathcal{O}(\epsilon), & x \to -\infty, \end{cases} \\ p_r(x) &= \begin{cases} -\frac{\mathcal{D}^2}{4x^4} + \frac{\mathcal{D}^3}{8x^5} + (\epsilon^6), & x \to \infty, \\ -\frac{16x^2}{\mathcal{D}^4} - \frac{8r}{\mathcal{D}^3} - \frac{4}{\mathcal{D}^2} + \mathcal{O}(\epsilon), & x \to -\infty, \end{cases} \\ p_\theta(x) &= \begin{cases} \frac{\mathcal{D}^2}{4x^4} - \frac{\mathcal{D}^3}{4x^5} + \mathcal{O}(\epsilon^6), & x \to \infty, \\ \frac{16x^2}{\mathcal{D}^4} + \frac{8x}{\mathcal{D}^3} + \frac{4}{\mathcal{D}^2} + \mathcal{O}(\epsilon), & x \to -\infty, \end{cases} \end{aligned} \tag{4.19}$$

from which we can see that none of the three energy conditions, WEC, SEC, and DEC, is satisfied at the spatial infinities. In addition, we also have

$$\begin{aligned} a(x) &= \begin{cases} \frac{1}{4}\left(1 - \frac{2\mathcal{D}}{b}\right) + \mathcal{O}(\epsilon^2), & x \to \infty, \\ \frac{4x^4}{\mathcal{D}^4} + \frac{4x^3}{\mathcal{D}^3} + \frac{6x^2}{\mathcal{D}^2} + \frac{4x}{\mathcal{D}} & \\ \quad + \frac{7}{4} + \frac{\mathcal{D}}{4x} + \mathcal{O}(\epsilon^2), & x \to -\infty, \end{cases} \\ b(x) &\simeq \begin{cases} 2x + \mathcal{O}(\epsilon), & x \to \infty, \\ -\frac{\mathcal{D}^2}{2x} + \frac{\mathcal{D}^4}{8x^3} + \mathcal{O}(\epsilon^4), & x \to -\infty. \end{cases} \end{aligned} \tag{4.20}$$

Therefore, the mass of the black hole is given by

$$M_{\rm BH} = \mathcal{D}. \tag{4.21}$$

However, at $x = -\infty$ we have $b(-\infty) = 0$, and the physical quantities, ρ, p_r, and p_θ, all become unbounded, so a spacetime curvature singularity appears at $x = -\infty$.

To study the quantum gravitational effects further, in Fig. 17 we plot R and $\Delta\mathcal{K}$, from which it can be seen that the deviation from GR quickly becomes vanishingly small as $x \to \infty$. However, as $x \to -\infty$, R diverges, as now the spacetime is singular at $b(x = -\infty) = 0$. In fact, as $x \to \pm\infty$, we find that

$$R \simeq \begin{cases} -\frac{\mathcal{D}^2}{4x^4} + \frac{\mathcal{D}^3}{2x^5} + \mathcal{O}(\epsilon^6), & x \to \infty, \\ -\frac{16x^2}{\mathcal{D}^4} - \frac{16x}{\mathcal{D}^3} - \frac{4}{\mathcal{D}^2} + \mathcal{O}(\epsilon), & x \to -\infty, \end{cases} \tag{4.22}$$

$$\mathcal{K} \simeq \begin{cases} \frac{3\mathcal{D}^2}{4x^6} - \frac{\mathcal{D}^3}{x^7} + \mathcal{O}(\epsilon^8), & x \to \infty, \\ \frac{2816x^4}{\mathcal{D}^8} + \frac{3072x^3}{\mathcal{D}^7} + \frac{2368x^2}{\mathcal{D}^6} & \\ \quad + \frac{640x}{\mathcal{D}^5} + \frac{48}{\mathcal{D}^4} + \mathcal{O}(\epsilon), & x \to -\infty, \end{cases} \tag{4.23}$$

and

$$\Delta\mathcal{K} \simeq \begin{cases} -\frac{4M_{\rm BH}}{3x} + \mathcal{O}(\epsilon^2), & x \to \infty, \\ -1 + \frac{11\mathcal{D}^4}{12M_{\rm BH}^2x^2} + \mathcal{O}(\epsilon^3), & x \to -\infty. \end{cases} \tag{4.24}$$

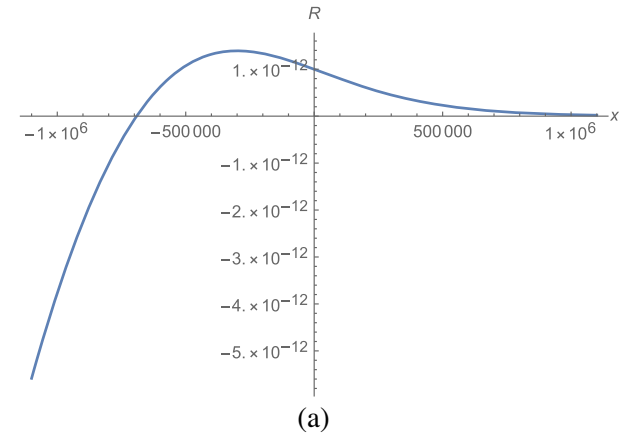

(a)

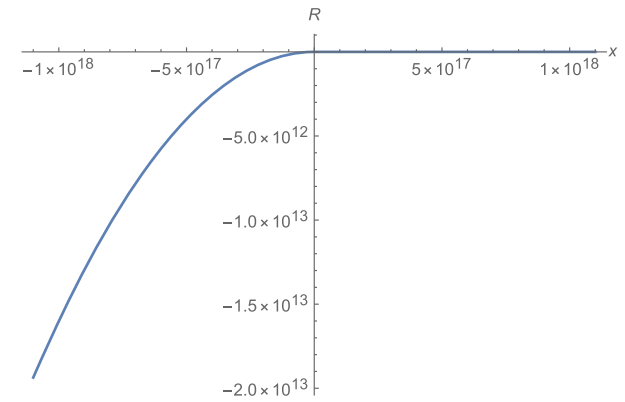

(b)

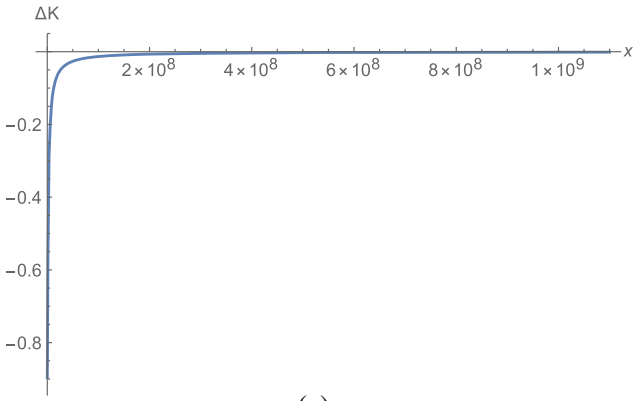

(c)

FIG. 17. Case $\Delta = 0, \mathcal{D} > 0, \mathcal{C} = 0$: R and $\Delta\mathcal{K}$ vs x. Here we choose $x_0 = 10^6$, $\mathcal{D} = 10^6$, so that $M_{\rm BH} = 10^6 M_{\rm Pl}$. Note that the horizon is located at $x_H^{\pm} = 0$, and the spacetime is singular at $b(x = -\infty) = 0$.

B. $\mathcal{D} = 0$

In this case, since $|\mathcal{D}| = |x_0|$, we also have $x_0 = 0$. Then, from Eq. (2.6), this corresponds to the limit $n \to \infty$. Again, to study the solutions further, we consider the two cases $\mathcal{C} \neq 0$ and $\mathcal{C} = 0$, separately.

1. $\mathcal{C} \neq 0$

From Eq. (2.9) we find $X = |x|$, and

$$Y = x + |x| = \begin{cases} 2x, & x \geq 0, \\ 0, & x < 0. \end{cases} \tag{4.25}$$

Thus, from Eq. (2.8) we find $a(x) = 0$ and $b(x) = \infty$ for $x \leq 0$, that is, the metric becomes singular for $x \leq 0$. However, since $b(0) = \infty$, it is clear that now $x = 0$ already represents the spatial infinity. Therefore, in this case we only need to consider the region $x \in (0, \infty)$ [cf. Fig. 1(b)]. In this case we have

$$a(x) = \frac{x^2 Y^2}{Z^2}, \qquad b(x) = \frac{Z}{Y}. \tag{4.26}$$

Clearly, $a(x) = 0$ leads to a double root, $x_H^{\pm} = 0$, while the minimum of $b(x)$ now is located at $x_m \equiv \hat{\mathcal{C}} = \mathcal{C}/2$, so we have

$$b(x) = \begin{cases} \infty, & x = 0, \\ 2^{4/3}\hat{\mathcal{C}}, & x = \hat{\mathcal{C}}, \\ \infty, & x = \infty. \end{cases} \tag{4.27}$$

The spacetime becomes antitrapped at $x = 0$. Since $b(x = 0) = \infty$, this antitrapped point now also corresponds to the spatial infinity at the other side of the throat, located at $x_m = \hat{\mathcal{C}}$.

On the other hand, the effective energy density and pressures are now given by

$$\begin{aligned} \rho(x) &= -\frac{5120 x^8 \mathcal{C}^6}{(64x^6 + \mathcal{C}^6)^{8/3}}, \\ p_r(x) &= -\frac{16 x^2 \mathcal{C}^{12}}{(64x^6 + \mathcal{C}^6)^{8/3}}, \\ p_\theta(x) &= \frac{16 x^2 \mathcal{C}^{12}}{(64x^6 + \mathcal{C}^6)^{8/3}}, \end{aligned} \tag{4.28}$$

which all become zero as $x \to 0$. They are also vanishing as $x \to \infty$.

At the throat $(x = \hat{\mathcal{C}})$, we have

$$\rho = -\frac{5}{2^{8/3}\hat{\mathcal{C}}^2}, \qquad p_r = -p_\theta = -\frac{1}{2^{8/3}\hat{\mathcal{C}}^2}, \tag{4.29}$$

so we find that none of the WEC, SEC, and DEC is satisfied.

At the spatial infinity $x \to \infty$, on the other hand, we find

$$\begin{aligned}\rho &\approx -\frac{5\mathcal{C}^6}{64x^8} + \mathcal{O}(\epsilon^9),\\ \rho + p_r &\approx -\frac{5\mathcal{C}^6}{64x^8} + \mathcal{O}(\epsilon^9),\\ \rho + p_\theta &\approx -\frac{5\mathcal{C}^6}{64x^8} + \mathcal{O}(\epsilon^9),\\ \rho + p_r + 2p_\theta &\approx -\frac{5\mathcal{C}^6}{64x^8} + \mathcal{O}(\epsilon^9),\end{aligned} \tag{4.30}$$

while as $x \to 0$ (or $b(x) \to \infty$), we find that

$$\begin{aligned}\rho &\approx -\frac{5120x^8}{\mathcal{C}^{10}} + \mathcal{O}(x^{11}),\\ \rho + p_r &\approx -\frac{16x^2}{\mathcal{C}^4} - \frac{7168x^8}{3\mathcal{C}^{10}} + \mathcal{O}(x^{11}),\\ \rho + p_\theta &\approx \frac{16x^2}{\mathcal{C}^4} - \frac{23552x^8}{3\mathcal{C}^{10}} + \mathcal{O}(x^{11}),\\ \rho + p_r + 2p_\theta &\approx \frac{16x^2}{\mathcal{C}^4} - \frac{23552x^8}{3\mathcal{C}^{10}} + \mathcal{O}(x^{11}),\end{aligned} \tag{4.31}$$

from which we can see that none of the three energy conditions is satisfied.

In addition, we also have

$$\begin{aligned}a(x) &= \begin{cases} \frac{1}{4}\left(1 - \frac{2\mathcal{C}^6}{3b^6}\right) + \mathcal{O}(\epsilon^7), & x \to \infty,\\ \frac{4x^4}{\mathcal{C}^4} + \mathcal{O}(x^6), & x \to 0,\end{cases}\\ b(x) &\simeq \begin{cases} 2x + \mathcal{O}(\epsilon), & x \to \infty,\\ \frac{\mathcal{C}^2}{2x} + \frac{32x^5}{3\mathcal{C}^4} + \mathcal{O}(x^6). & x \to 0.\end{cases}\end{aligned} \tag{4.32}$$

Thus, the space-time is asymptotically flat as $x \to \infty$, with a black/hole mass given by

$$M_{BH/WH} = 0. \tag{4.33}$$

On the other hand, to study the quantum gravitational effects, in Fig. 18 we plot R and $\mathcal{K}$ in the region that covers the throat, and in the asymptotical regions $x \to 0$ and $x \to \infty$, from which it can be seen that the deviation from GR is mainly in the region near the throat, and quickly becomes vanishingly small as $x \to \infty$ or $x \to 0$.

The spacetime is also asymptotically flat as $x \to 0 (b(0) = \infty)$. In fact, we find

$$\begin{aligned}R &\simeq \begin{cases} -\frac{5\mathcal{C}^6}{64x^8} + \mathcal{O}(\epsilon^9), & x \to \infty,\\ -\frac{16x^2}{\mathcal{C}^4} + \mathcal{O}(x^4), & x \to 0,\end{cases}\\ \mathcal{K} &\simeq \begin{cases} \frac{127\mathcal{C}^{12}}{4096x^{16}} + O(\epsilon^{19}), & x \to \infty,\\ \frac{2816x^4}{\mathcal{C}^8} + O(x^6), & x \to 0.\end{cases}\end{aligned} \tag{4.34}$$

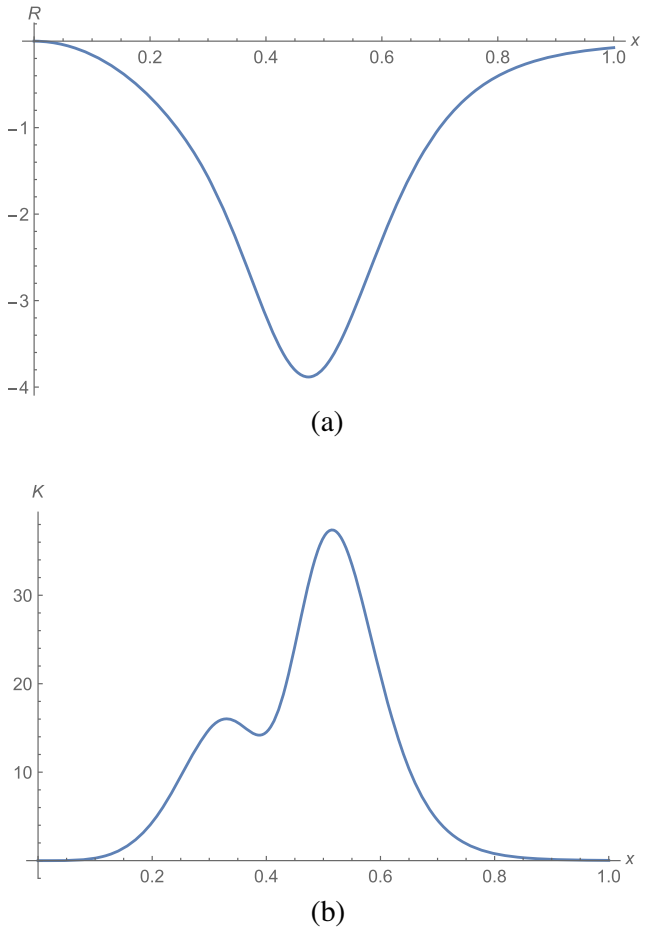

FIG. 18. Case $\Delta = 0, \mathcal{D} = 0, \mathcal{C} \neq 0$: R and $\mathcal{K}$ vs x. Here we choose $\mathcal{C} = 1$. Note that now the throat is at $x = \hat{\mathcal{C}} = 1/2$.

2. $\mathcal{C} = 0$

From Eq. (2.9) we find

$$Y = x + |x| = \begin{cases} 2x, & x \geq 0,\\ 0, & x < 0.\end{cases} \tag{4.35}$$

Therefore, the spacetime must be restricted to the region $x \geq 0$, in which we have

$$a(x) = \frac{1}{4}, \qquad b(x) = (x + \sqrt{x^2}) = 2x, \tag{4.36}$$

and

$$\rho(x) = p_r = p_\theta(x) = 0. \tag{4.37}$$

In fact, this is precisely the Minkowski solution, and will take its standard form, by setting $r = 2x$ and rescaling t.

C. $\mathcal{D} < 0$

Similar to the last subcase, now we also need to consider the cases $\mathcal{C} \neq 0$ and $\mathcal{C} = 0$ separately.

1. $\mathcal{C} \neq 0$

When $\mathcal{D} < 0$, we find that

$$b(x) = \begin{cases} \infty, & x = \infty, \\ 2^{1/3}\mathcal{C}, & x = x_m, \\ \infty, & x = -\infty, \end{cases} \tag{4.38}$$

where $x_m \equiv (\mathcal{C}^2 - \mathcal{D}^2)/(2\mathcal{C})$ [cf. Fig. 1(a)]. On the other hand, $a(x) = 0$ has no real roots, thus in the current case no black/white hole horizons exist.

But, as shown by Eq. (4.38), a throat still exists at $x = x_m$, at which the effective energy density ρ and pressures p_r and p_θ are still given by Eq. (4.8), from which we find that none of the three energy conditions is satisfied at this point.

At the spatial infinities $x \to \pm\infty$, we find that the effective energy density ρ and pressures p_r and p_θ are still given by Eqs. (4.10), (4.13), and(4.14), from which we can see that *none of the three energy conditions is satisfied at both* $x = -\infty$ *and* $x = \infty$. In addition, the asymptotic expression of $a(x)$ and $b(x)$ are still given by Eq. (4.11). Therefore, the total mass at $x \to \infty$ is given by

$$M_+ = \mathcal{D} < 0, \tag{4.39}$$

while the total mass at $x \to -\infty$ is given by

$$M_- = \frac{\mathcal{C}^2}{\mathcal{D}} < 0. \tag{4.40}$$

It can be shown that in the present case the quantum gravitational effects are also concentrated in the region near the throat, and are vanishing rapidly when away from it in each side of the throat.

2. $\mathcal{C} = 0$

In this case, we have

$$a(x) = \frac{(X + |\mathcal{D}|)X}{Y^2}, \qquad b(x) = Y. \tag{4.41}$$

Thus, $a(x) = 0$ has no real roots, and $b(x)$ becomes a monotonically increasing function with $b(-\infty) = 0$ and $b(\infty) = \infty$ [cf. Fig. 1(c)]. Therefore, in this case a throat does not exist.

At the spatial infinities $x \to \pm\infty$, we find that the effective energy density ρ and pressures p_r and p_θ are still given by Eq. (4.19), from which we find that none of the three energy conditions, WEC, SEC and DEC, is satisfied at the spatial infinity. In addition, the asymptotic expressions of $a(x)$ and $b(x)$ are still given by Eq. (4.20). Therefore, the total mass at $x \to \infty$ is given by

$$M_+ = \mathcal{D} < 0. \tag{4.42}$$

However, at $x = -\infty$ we have $b(-\infty) = 0$, and the physical quantities, ρ, p_r and p_θ, all become unbounded, so a spacetime curvature singularity appears at $x = -\infty$. Since no horizon exists, such a singularity is also naked.

This completes our analysis for the case $\Delta = 0$, and the main properties of these solutions are summarized in Table III.

V. SPACETIMES WITH $\Delta < 0$

In this case we have

$$a(x) = \frac{(x^2 + |\Delta|)XY^2}{(X + \mathcal{D})Z^2}, \qquad b(x) = \frac{Z}{Y}, \tag{5.1}$$

where X, Y, Z are given by Eq. (2.9), while Δ is given by Eq. (2.10), from which we find $\Delta < 0$ implies

$$|\mathcal{D}| < |x_0|. \tag{5.2}$$

Then, we find that

$$b(x) = \begin{cases} \infty, & x = \infty, \\ 2^{1/3}\mathcal{C}, & x = x_m, \\ \infty, & x = -\infty, \end{cases} \tag{5.3}$$

where $x_m \equiv (\mathcal{C}^2 - x_0^2)/(2\mathcal{C})$ [cf. Fig. 1(a)].

To study the solutions further, as what we did in the last case, let us consider the solutions with $\mathcal{D} > 0, \mathcal{D} = 0$, and $\mathcal{D} < 0$, separately.

A. $\mathcal{D} > 0$

Then, we find $a(x)$ is nonzero for any $x \in (-\infty, \infty)$, and in particular we have

$$a(x) = \begin{cases} \frac{1}{4}, & x = \infty, \\ \frac{x_0^4}{4\mathcal{C}^2}, & x = -\infty. \end{cases} \tag{5.4}$$

Thus, in the current case horizons do not exist. But, a throat does exist, as shown by Eq. (5.3). At the throat, the effective energy density ρ and pressures p_r and p_θ are still given by Eq. (3.30), from which we find that WEC, SEC, and DEC are still satisfied, provided that

$$|x_0| \leq \sqrt{\mathcal{C}(2\mathcal{D} - \mathcal{C})}, \qquad 0 < \mathcal{C} \leq 2\mathcal{D}. \tag{5.5}$$

In addition, we also have the constraint $|\mathcal{D}| < |x_0|$, as now we are considering the case $\Delta < 0$.

At the spatial infinities $x \to \pm\infty$, we find that the effective energy density ρ and pressures p_r and p_θ can be also written in the forms of Eq. (3.18), from which we

can see that *none of the three energy conditions is satisfied at both* $x = -\infty$ *and* $x = \infty$.

The asymptotic expressions of $a(x)$ and $b(x)$ are still given by Eq. (3.19). Therefore, the total mass at $x \to \infty$ is given by

$$M_+ = \mathcal{D}, \tag{5.6}$$

while the total mass at $x \to -\infty$ is given by

$$M_- = \frac{\mathcal{D}\mathcal{C}^2}{x_0^2}. \tag{5.7}$$

It can be shown that the quantum gravitational effects are concentrated in the region near the throat, and are rapidly vanishing as away from the throat in each side of it only by proper choice of the free parameters involved in the solutions, as in the corresponding case $\Delta > 0, \mathcal{D} > 0$ and $x_0\mathcal{C} \neq 0$.

Although no horizons exist in the present case, the corresponding solution is very interesting on its own rights: *it represents a wormhole spacetime, in which all the three energy conditions, WEC, SEC, and DEC, are satisfied in the neighborhood of the throat, provided that Eq. (5.5) holds, while none of them is satisfied at the asymptotically flat regions (spatial infinities)* $x \to \pm\infty$.

It should be also noted that the above analysis does not cover the limit cases $x_0 \to 0$ and $\mathcal{C} \to 0$. However, since now $|\mathcal{D}| < |x_0|$, the cases $x_0 = 0, \mathcal{C} \neq 0$ and $x_0 = \mathcal{C} = 0$ do not exist. So, only the limiting case, $\mathcal{C} = 0$, $x_0 \neq 0$, exists.

(i) $\mathcal{C} = 0, x_0 \neq 0$: In this case, we have

$$a(x) = \frac{(x^2 + |\Delta|)X}{(X + \mathcal{D})Y^2}, \qquad b(x) = Y. \tag{5.8}$$

Clearly, $a(x) = 0$ does not have real solutions, while $b(x)$ is a monotonically increasing function with $b(x = -\infty) = 0$, as shown in Fig. 1(c).

At the spatial infinities $x \to \pm\infty$, we find that the effective energy density ρ and pressures p_r and p_θ are still given by Eq. (3.60), from which we can see that *none of the three energy conditions is satisfied at both* $x = -\infty$ *and* $x = \infty$.

The asymptotic expression of $a(x)$ and $b(x)$ are still given by Eq. (3.61). Therefore, the total mass at $x \to \infty$ is given by

$$M_+ = \mathcal{D}. \tag{5.9}$$

However, at $x = -\infty$ we have $b(-\infty) = 0$, and the physical quantities, ρ, p_r, and p_θ, all become unbounded, so a spacetime curvature singularity appears at $x = -\infty$.

B. $\mathcal{D} = 0$

From Eq. (2.8) we find that

$$a(x) = \frac{X^2Y^2}{Z^2}, \qquad b(x) = \frac{Z}{Y}, \tag{5.10}$$

where X, Y, and Z are given by Eq. (2.9). From the above expressions, it can be shown that there are two asymptotically flat regions, corresponding to $x \to \pm\infty$, respectively. They are still connected by a throat located at x_m given by Eq. (3.3) [cf. Fig. 1(a)]. But since $a(x) \neq 0$ for any given $x \in (-\infty, \infty)$, as it can be seen from the above expression, horizons, either WHs or BHs, do not exist.

At the throat, the effective energy density ρ and pressures p_r and p_θ are given by

$$\rho = -\frac{5}{2^{8/3}\hat{\mathcal{C}}^2}, \qquad p_r = -p_\theta = -\frac{1}{2^{8/3}\hat{\mathcal{C}}^2}, \tag{5.11}$$

so none of the WEC, SEC, and DEC is satisfied.

At the spatial infinities $x \to \pm\infty$, we find that the effective energy density ρ and pressures p_r and p_θ take the forms,

$$\begin{aligned}
\rho(x) &= \begin{cases} -\frac{5\mathcal{C}^6}{64x^8} + \mathcal{O}(\epsilon^9), & x \to \infty, \\ -\frac{5x_0^{16}}{64x^8\mathcal{C}^{10}} + \mathcal{O}(\epsilon^9), & x \to -\infty, \end{cases} \\
p_r(x) &= \begin{cases} -\frac{x_0^2}{4x^4} + \mathcal{O}(\epsilon^6), & x \to \infty, \\ -\frac{x_0^6}{4x^4\mathcal{C}^4} + \mathcal{O}(\epsilon^6), & x \to -\infty, \end{cases} \\
p_\theta(x) &= \begin{cases} \frac{x_0^2}{4x^4} + \mathcal{O}(\epsilon^6), & x \to \infty, \\ \frac{x_0^6}{4x^4\mathcal{C}^4} + \mathcal{O}(\epsilon^6), & x \to -\infty, \end{cases}
\end{aligned} \tag{5.12}$$

from which we can see that *none of the three energy conditions is satisfied at both* $x = -\infty$ *and* $x = \infty$.

In addition, we also have

$$\begin{aligned}
a(x) &= \begin{cases} \frac{1}{4}\left(1 + \frac{2x_0^2}{b^2}\right) + \mathcal{O}(\epsilon^3), & x \to \infty, \\ \frac{x_0^4}{4\mathcal{C}^4}\left(1 + \frac{2\mathcal{C}^4}{x_0^2 b^2}\right) + \mathcal{O}(\epsilon^2), & x \to -\infty, \end{cases} \\
b(x) &\simeq \begin{cases} 2x + \mathcal{O}(\epsilon), & x \to \infty, \\ -\frac{2x\mathcal{C}^2}{x_0^2} + \mathcal{O}(\epsilon). & x \to -\infty, \end{cases}
\end{aligned} \tag{5.13}$$

from which we can see that the space-time is asymptotically flat as $x \to \pm\infty$.

Similar to the last subcase, the quantum gravitational effects are concentrated in the region near the throat, and are rapidly vanishing as away from the throat in each side of it for the proper choice of the free parameters, as in the corresponding case $\Delta > 0, \mathcal{D} = 0$ and $x_0\mathcal{C} \neq 0$.

In addition, the above analysis is valid only for $x_0\mathcal{C} \neq 0$. Otherwise, we have the following limiting case.

(i) $x_0 \neq 0, \mathcal{C} = 0$: Then, we have

$$a(x) = \frac{X^2}{Y^2}, \qquad b(x) = Y. \tag{5.14}$$

Since $a(x) \neq 0$ for any given real value of x, as it can be seen from the above expression, horizons, either WHs or BHs, do not exist, but $b(x)$ is still a monotonically increasing function with $b(x = -\infty) = 0$, as shown in Fig. 1(c).

At the spatial infinities $x \to \pm\infty$, we find that the effective energy density ρ and pressures p_r and p_θ are given by

$$\rho(x) = \begin{cases} 0, & x \to \infty, \\ 0, & x \to -\infty, \end{cases}$$
$$p_r(x) = \begin{cases} -\frac{x_0^2}{4x^4} + \mathcal{O}(\epsilon^6), & x \to \infty, \\ -\frac{16x^2}{x_0^4} - \frac{4}{x_0^2} + \frac{x_0^2}{4x^4} + \mathcal{O}(\epsilon^6), & x \to -\infty, \end{cases}$$
$$p_\theta(x) = \begin{cases} \frac{x_0^2}{4x^4} + \mathcal{O}(\epsilon^6), & x \to \infty, \\ \frac{16x^2}{x_0^4} + \frac{4}{x_0^2} - \frac{x_0^2}{4x^4} + \mathcal{O}(\epsilon^6), & x \to -\infty, \end{cases} \tag{5.15}$$

from which we can see that *none of the three energy conditions is satisfied to the leading order of* $(1/x)$ *at both* $x = -\infty$ *and* $x = \infty$.

In addition, we also have

$$a(x) = \begin{cases} \frac{1}{4}\left(1 + \frac{2x_0^2}{b^2}\right) + \mathcal{O}(\epsilon^3), & x \to \infty, \\ \frac{4x^4}{x_0^4} + \frac{6x^2}{x_0^2} + \frac{7}{4} + \mathcal{O}(\epsilon^2), & x \to -\infty, \end{cases}$$
$$b(x) \simeq \begin{cases} 2x + \mathcal{O}(\epsilon), & x \to \infty, \\ -\frac{x_0^2}{2x} + \mathcal{O}(\epsilon^3), & x \to -\infty, \end{cases} \tag{5.16}$$

from which we can see that the space-time is asymptotically flat as $x \to +\infty$, but a spacetime curvature singularity appears at $x = -\infty$, where $b(x = -\infty) = 0$, as it can be seen from the above expressions.

C. $\mathcal{D} < 0$

From Eq. (2.8) we find that

$$a(x) = \frac{(X + |\mathcal{D}|)XY^2}{Z^2}, \qquad b(x) = \frac{Z}{Y}, \tag{5.17}$$

where X, Y and Z are given by Eq. (2.9). From the above expressions, it can be shown that there are two asymptotically flat regions, corresponding to $x \to \pm\infty$, respectively. They are still connected by a throat located at x_m given by Eq. (3.3) [cf. Fig. 1(a)]. But since $a(x) \neq 0$ for any given x, horizons, either WHs or BHs, do not exist.

At the throat, the effective energy density ρ and pressures p_r and p_θ are given by Eq. (3.30). Then, it can be easily shown that none of the three energy conditions, WEC, SEC, and DEC, can be satisfied in the current case.

Similarly, the quantum gravitational effects are concentrated in the region near the throat for only when the free parameters are properly chosen, and are rapidly vanishing as away from the throat in each side of it.

At the spatial infinities $x \to \pm\infty$, we find that the expression of ρ, p_r, p_θ are still given by Eq. (3.18), from which we can see that *none of the three energy conditions is satisfied to the leading order of* $(1/x)$.

The asymptotic expressions of $a(x)$ and $b(x)$ are given by Eq. (3.19), and the total mass at $x \to \pm\infty$ is still given by Eq. (3.20), but since we now have $\mathcal{D} < 0$, the total mass becomes negative.

Similar to the last case, the above analysis holds only for $x_0\mathcal{C} \neq 0$. When $x_0\mathcal{C} = 0$, we find that only the possibility, $x_0 \neq 0$, $\mathcal{C} = 0$, is allowed.

(i) $x_0 \neq 0, \mathcal{C} = 0$: From Eq. (2.8) we find that

$$a(x) = \frac{(X + |\mathcal{D}|)X}{Y^2}, \qquad b(x) = Y, \tag{5.18}$$

where X, Y and Z are given by Eq. (2.9). Clearly, $a(x) = 0$ has no real roots, thus no horizons exist. On the other hand, $b(x)$ is still a monotonically increasing function with $b(x = -\infty) = 0$, as shown in Fig. 1(c).

At the spatial infinities $x \to \pm\infty$, we find that the effective energy density and pressures are still given by Eq. (3.60), from which we find that none of the three energy conditions, WEC, SEC, and DEC, is satisfied at the spatial infinities. In addition, the asymptotic behaviors of $a(x)$ and $b(x)$ are still given by Eq. (3.61). Therefore, the total mass at $x = \infty$ is still given by Eq. (3.47), which is always negative.

However, at $x = -\infty$ we have $b(-\infty) = 0$, and the physical quantities, ρ, p_r, and p_θ, all become unbounded, so a spacetime curvature singularity appears at $x = -\infty$.

This completes our analysis for the solutions with $\Delta < 0$, and the main properties of these solutions are summarized in Table III.

VI. CONCLUSIONS

In this paper, we have studied in detail the main properties of spherically symmetric black/white hole solutions, found recently by Bodendorfer, Mele, and Münch [47], inspired by the effective loop quantum gravity, and paid particular attention to their local and global properties, as well as to the energy conditions of the effective energy-momentum tensor of the spacetimes. Although this effective energy-momentum tensor is purely due to the quantum

geometric effects, and is not related to any real matter fields, it does provide important information on how the spacetime singularity is avoided, and the deviations of the spacetimes from the classical one (the Schwarzschild solution). In particular, spacetime singularities inevitably occur in general relativity, as longer as matter fields satisfy some energy conditions, as follows directly from the Hawking-Penrose singularity theorems [50]. In addition, due to the Birkhoff theorem, the spacetime is uniquely described by the Schwarzschild black hole solution in general relativity. Therefore, the presence of this effective energy-momentum tensor also characterizes the deviations of the quantum solutions from the classical one.

The most general metric for static spherically symmetric spacetimes, without loss of the generality, can be always cast in the form,

$$ds^2 = -a(x)dt^2 + \frac{dx^2}{a(x)} + b^2(x)(d^2\theta + \sin^2\theta d^2\phi),$$

subjected to the following additional gauge transformations (gauge residuals),

$$t = \alpha\tilde{t} + t_0, \qquad x = \xi(\tilde{x}), \tag{6.1}$$

where α and t_0 are constant, and $\xi(\tilde{x})$ is an arbitrary function of $\tilde{x}$. Therefore, in general the phase space are four-dimensional, spanned by (a, b, p_a, p_b), but with one constraint, the Hamiltonian constraint, $H_{\rm eff} = 0$. So, the phase space is actually three-dimensional, and the trajectories of the system are uniquely determined once the three "initial" conditions are given. However, due to the polymerization (1.9), two new parameters are introduced, so the phase space is enlarged to five-dimensional, due to the polymerization quantizations. Nevertheless, the trajectories of the system are also gauge-invariant under the transformations (6.1), which reduce the dimensions of the phase space from five to three again. Therefore, *the phase space in this model is generically three-dimensional*.

The above general arguments can be seen clearly from the particular solutions considered in this paper, and the three physically independent free parameters now can be chosen as $(\mathcal{C}, \mathcal{D}, x_0)$, defined explicitly by Eq. (2.6),

$$\mathcal{D} \equiv \frac{3CD}{2\sqrt{n}}, \qquad \mathcal{C} \equiv (16C^2\lambda_1^2)^{1/6}, \qquad x_0 \equiv \frac{\lambda_2}{\sqrt{n}}, \tag{6.2}$$

out of the five parameters, $\lambda_1, \lambda_2, n, C$, and D, introduced in [47]. Thus, in comparison with the relativistic case, the polymerizations introduce two more free parameters, and only when they vanish, i.e., $\lambda_1 = \lambda_2 = 0$ (or $\mathcal{C} = x_0 = 0$), can the solutions reduce to the Schwarzschild one with its mass $M_{\rm BH} = \mathcal{D}$, and a spacetime curvature singularity located at the center $(b = 0)$ appears. If any of them vanishes, the corresponding moment conjugate, P_1 or P_2, can become unbounded at some points (or in some regions) of the spacetime. As a result, spacetime curvature singularities will appear. From Tables II–IV it can be seen that in the current model the condition for such singularities to appear is indeed $\lambda_1 = 0$ (or $\mathcal{C} = 0$), the cases corresponding to Fig. 1(c).

The asymptotical properties of the spacetimes also depend on the choices of the two parameters $\mathcal{C}$ and x_0. In particular, when $\mathcal{C}x_0 \neq 0$, we have $x \in (-\infty, \infty)$, and a minimal point (throat) of $b(x)$ always exists, with $b(\pm\infty) = \infty$ [cf. Fig. 1(a)]. When $\mathcal{C} \neq 0$ but $x_0 = 0$, the range of x is restricted to $x \in (0, \infty)$ with $b(0) = \infty$ and $b(\infty) = \infty$. In this case, a minimum of $b(x)$ also exists [cf. Fig. 1(b)]. When $\mathcal{C} = 0$ and $x_0 \neq 0$, the range of x is also $x \in (-\infty, \infty)$, but now $b(x)$ is a monotonically increasing function of x with $b(-\infty) = 0$ and $b(\infty) = \infty$ [cf. Fig. 1(c)].

In [47,48,53], the authors considered the case

$$\Delta \equiv \mathcal{D}^2 - x_0^2 > 0, \qquad \mathcal{D} > 0, \qquad \mathcal{C}x_0 \neq 0, \tag{6.3}$$

for which the black and white hole horizons always exist, located at

$$x_H^{\pm} = \pm\sqrt{\Delta},$$

respectively, as shown in Sec. III A [See also Table II]. The corresponding spacetime has two asymptotically flat regions $x \to \pm\infty$, which are connected by a throat located at

$$x_m = \frac{1}{2\mathcal{C}}(\mathcal{C}^2 - x_0^2),$$

as can be seen from Eq. (3.3) and Fig. 1(a)]. It is remarkable to note that in this case the surface gravity at the black hole horizon $x = x_H^+$ is always positive, while at the white hole horizon $x = x_H^-$, it is always negative, as the latter represents an antitrapped surface. In the asymptotical region $x \to +\infty$, the ADM mass reads

$$M_{\rm BH} = \mathcal{D}, \tag{6.4}$$

while in the asymptotical region $x \to -\infty$, it reads

$$M_{WH} = \frac{\mathcal{D}\mathcal{C}^2}{x_0^2}, \tag{6.5}$$

as given explicitly in Eq. (3.20), which are all positive, too. All the above properties are mainly due to the fact that the Komar energy density [51] $(\rho + \sum_i p_i)$ remains positive over a large region of the spacetime, despite that all the three energy conditions are violated in most part of the spacetime, including the regions near the throat and horizons, as well as in the two asymptotically flat regions.

In addition, the quantum gravitational effects are mainly concentrated in the neighborhood of the throat. However, in the current model, such effects can be still large at the two horizons even for solar mass black/white hole spacetimes, depending on the choice of the free parameters. They become negligible near the black/white hole horizons only for some particular choices of these free parameters [cf. Eq. (3.26)].

Moreover, the ratio $M_{\rm BH}/M_{WH}$ can take in principle any value, $M_{\rm BH}/M_{WH} \in (0,\infty)$, as the three parameters $\mathcal{C},\mathcal{D},x_0$ now are all arbitrary [subjected only to the constraint $\mathcal{C} \geq 0$ as can be seen from Eq. (6.2)] [48].

It should be also noted that the region defined by Eq. (6.3) is quite small in the whole three-dimensional phase space, spanned by $(\mathcal{C},\mathcal{D},x_0)$, where

$$\mathcal{D}, x_0 \in (-\infty,\infty), \qquad \mathcal{C} \in [0,\infty), \tag{6.6}$$

although the cases with $\mathcal{D}=0$, or $\mathcal{C}=0$, or $x_0=0$ can be obtained only by taking certain proper limits of the five free parameters, λ_1,λ_2,n,C, and D, as explained explicitly in the content.

With all the above in mind, we have explored the whole three-dimensional phase space of the three free parameters $(\mathcal{C},\mathcal{D},x_0)$, and found that the solutions have very rich physics. In particular, the existence of the black/white horizons crucially depends on the values of Δ. When $\Delta>0$, they always exist and are located at $x_H^{\pm}=\pm\sqrt{\Delta}$, respectively. The spacetime in the region $x_H^- < x < x_H^+$ becomes trapped. When $\Delta=0$, they also exist, but now become degenerate, $x_H^{\pm}=0$, that is, $a(x)=0$ now has a double root, the trapped region $(a(x)<0)$ disappears, and the surface gravity at the horizon is always zero now, quite similar to the extreme case of the charged RN solution with $|e|=m$. When $\Delta<0$, the equation $a(x)=0$ has no real roots, and, as a result, in this case no horizons exist at all, neither a trapped region.

Thus, depending on the choices of the three free parameters, $\mathcal{C},\mathcal{D},x_0$, there are various cases that all have different (local and global) properties. In Secs. III–V, we have studied the cases $\Delta>0$, $\Delta=0$, and $\Delta<0$, separately, and in each of which all the three possible choices of $\mathcal{C}$ and x_0, as illustrated in Fig. 1, raise and have been studied in detail. Their main properties are summarized in the three tables, Tables II–IV. From these tables, the following interested cases are worthwhile of particularly mentioning:

(i) $\Delta>0,\mathcal{D}>0,\mathcal{C}x_0\neq 0$: As mentioned above, in this case the solutions were first studied in [47,48,53], and in the present paper we have studied them in detail, and found the remarkable features stated above. In particular, we have shown explicitly that the quantum geometric efforts are mainly concentrated in the region near the throat (transition surface). However, in the current model such effects can be still large at the black/white hole horizons even for solar mass black/white holes. They become negligible only in a restricted region of the 3D phase space, defined by Eq. (3.26).

(ii) $\Delta=0,\mathcal{D}>0,\mathcal{C}x_0\neq 0$: In this case, the black/white horizons coincide and all are located at $x_H^{\pm}=0$, so the surface gravity at the horizon is zero, quite similar to the extreme case $|e|=m$ of the RN solution in general relativity. But, it is fundamentally different from the RN solution, as now there are no spacetime curvature singularities, and the spacetime becomes asymptotically flat in both of the regions $x\to\pm\infty$.

In addition, all the three energy conditions are satisfied at the horizon, but at the throat $x=x_m$, they are satisfied only when $\mathcal{D}=\mathcal{C}$, for which the throat coincides with the horizon, i.e., $x_m=x_H^{\pm}=0$.

Similar to the last case (in fact, in all the cases, including $\Delta>0$ and $\Delta<0$), none of the three energy conditions is satisfied at the spatial infinities $b(\pm\infty)=\infty$, although the quantum gravitational effects are also mainly concentrated at the throat, as shown in Fig. 15. In this case, the black/white hole masses are also given by Eqs. (6.4) and (6.5) but now with $|x_0|=\mathcal{D}$.

(iii) $\Delta<0,\mathcal{D}>0,\mathcal{C}x_0\neq 0$: In this case, the function $a(x)$ is always positive, and no horizons exist, although a throat does exist, as shown in Fig. 1(a), at which all the three energy conditions are satisfied, as long as the conditions (5.5) hold. By properly choosing the free parameters, the quantum geometric effects can be made to be mainly concentrated at the throat, and the spacetime is asymptotically flat at both of the two limits, $x\to\pm\infty$, with the ADM masses, given, respectively, by Eqs. (6.4) and (6.5), which can be all positive. However, since no horizons exist, the spacetimes now represent wormholes without any spacetime curvature singularities. Again, this is not in conflict to the Hawking-Penrose singularity theorems [50], as none of the three energy conditions holds at the asymptotically flat regions, $x=\pm\infty$.

The main properties of other interesting cases can be found in Tables II–IV.

It should be noted that, although in this paper we have studied only the solutions found recently in [47], we expect that quantum black hole solutions share similar properties. In particular, due to the quantum geometric effects, an effective energy-momentum tensor inevitably appears, which generically violates the weak/strong energy conditions at the throat, so the spacetime is opened up by such repulsive forces. As a result, the throat will connect two asymptotically flat regions. For spherical spacetimes [42], such effects are uniquely characterized by the two quantum parameters λ_1 and λ_2. The classical limit is obtained by setting $\lambda_1=\lambda_2=0$. Therefore, the singularities inside the

classical black holes are resolved by the polymerization [41], given by Eq. (1.9), provided that

$$\lambda_1\lambda_2 \neq 0. \tag{6.7}$$

If any of these two parameters vanishes, a spacetime curvature singularity can appear, as it is shown explicitly by the current model.

Therefore, spherically quantum black holes should generically also contain three free parameters, which uniquely determine the location of the throat and the two masses, measured by observers located in the two asymptotically flat regions. Here we use "black holes" to emphasize the fact that in such resultant spacetimes white/black hole horizons are not necessarily always present, and spacetimes with wormhole structures (without horizons) can be equally possible, unless the two free parameters λ_1 and λ_2 are fixed by some physical considerations [21,22,42]. It is also equally true that the two (Komar) masses are independent and can be assigned arbitrary values, unless additional physics is taken into account [21,22,47,48]. To understand these issues further, one way is to consider the formation of such spacetimes from gravitational collapse of realistic matter fields [54–61].

Finally, we would like to mention that to get a universal curvature upper bound in these polymer black holes, we need to impose specific relations between black and white hole masses [47], which amounts to impose further constraint in the parameter space. In this paper, we did not impose this condition in order to study properties in the whole parameter space. To overcome this problem, recently BMM proposed another set of canonical variables in which one of the canonical momentum is precisely the square root of the Kretschmann scalar [48]. In this new model, a universal curvature upper bound can be obtained without any further constraint on the relation between black and white hole masses.

ACKNOWLEDGMENTS

We would like to thank Profs. Pisin Chen and Parampreet Singh for their valuable comments and suggestions, which lead to various modifications. W-C. G. is supported by Baylor University through the Baylor Physics graduate program. This work is also partially supported by the National Natural Science Foundation of China with the Grants No. 11665016, No. 11675145, No. 11975116, and No. 11975203, and Jiangxi Science Foundation for Distinguished Young Scientists under the Grant No. 20192BCB23007.

APPENDIX: THE GENERAL EXPRESSIONS OF THE ENERGY DENSITY AND PRESSURES

Inserting the solutions given by Eq. (2.8) into Eq. (2.15), we find that

$$\begin{aligned}\rho(x) = \frac{Y^3}{X^2Z^8}[&(10\mathcal{D}x_0^{10}x + 160\mathcal{D}x_0^8x^3 - 20x_0^6\mathcal{C}^6 + 672\mathcal{D}x_0^6x^5 + 1024\mathcal{D}x_0^4x^7 - 260x_0^4\mathcal{C}^6x^2\\ &+ 110\mathcal{D}x_0^4\mathcal{C}^6x + 512\mathcal{D}x_0^2x^9 - 560x_0^2\mathcal{C}^6x^4 + 440\mathcal{D}x_0^2\mathcal{C}^6x^3 - 320\mathcal{C}^6x^6 + 352\mathcal{D}\mathcal{C}^6x^5)X\\ &+ \mathcal{D}\mathcal{C}^{12} + \mathcal{D}x_0^{12} + 50\mathcal{D}x_0^{10}x^2 + 400\mathcal{D}x_0^8x^4 + 22\mathcal{D}x_0^6\mathcal{C}^6 + 1120\mathcal{D}x_0^6x^6 - 100x_0^6\mathcal{C}^6x\\ &+ 1280\mathcal{D}x_0^4x^8 - 500x_0^4\mathcal{C}^6x^3 + 286\mathcal{D}x_0^4\mathcal{C}^6x^2 + 512\mathcal{D}x_0^2x^{10} - 720x_0^2\mathcal{C}^6x^5 + 616\mathcal{D}x_0^2\mathcal{C}^6x^4\\ &- 320\mathcal{C}^6x^7 + 352\mathcal{D}\mathcal{C}^6x^6],\end{aligned} \tag{A1}$$

$$\begin{aligned}p_r(x) = -\frac{Y^3}{X^2Z^8}[&(2x_0^{12} + 100x_0^{10}x^2 - 10\mathcal{D}x_0^{10}x + 800x_0^8x^4 - 160\mathcal{D}x_0^8x^3 + 2240x_0^6x^6\\ &- 672\mathcal{D}x_0^6x^5 + 2560x_0^4x^8 - 1024\mathcal{D}x_0^4x^7 + 10\mathcal{D}x_0^4\mathcal{C}^6x + 1024x_0^2x^{10} - 512\mathcal{D}x_0^2x^9\\ &+ 40\mathcal{D}x_0^2\mathcal{C}^6x^3 + 2\mathcal{C}^{12} + 32\mathcal{D}\mathcal{C}^6x^5)X - \mathcal{D}\mathcal{C}^{12} - \mathcal{D}x_0^{12} + 20x_0^{12}x + 340x_0^{10}x^3\\ &- 50\mathcal{D}x_0^{10}x^2 + 1664x_0^8x^5 - 400\mathcal{D}x_0^8x^4 + 2\mathcal{D}x_0^6\mathcal{C}^6 + 3392x_0^6x^7 - 1120\mathcal{D}x_0^6x^6\\ &+ 3072x_0^4x^9 - 1280\mathcal{D}x_0^4x^8 + 26\mathcal{D}x_0^4\mathcal{C}^6x^2 + 1024x_0^2x^{11} - 512\mathcal{D}x_0^2x^{10} + 56\mathcal{D}x_0^2\mathcal{C}^6x^4\\ &+ 32\mathcal{D}\mathcal{C}^6x^6],\end{aligned} \tag{A2}$$

and

$$
\begin{aligned}
p_\theta(x) = \frac{Y^2}{2X^3Z^8}[&(4x_0^{14} + 244x_0^{12}x^2 - 34\mathcal{D}x_0^{12}x + 2480x_0^{10}x^4 - 720\mathcal{D}x_0^{10}x^3 + 9408x_0^8x^6 \\
&- 4256\mathcal{D}x_0^8x^5 + 16384x_0^6x^8 - 10240\mathcal{D}x_0^6x^7 + 12\mathcal{D}x_0^6\mathcal{C}^6x + 13312x_0^4x^{10} - 10752\mathcal{D}x_0^4x^9 \\
&+ 88\mathcal{D}x_0^4\mathcal{C}^6x^3 + 4x_0^2\mathcal{C}^{12} + 4096x_0^2x^{12} - 4096\mathcal{D}x_0^2x^{11} + 192\mathcal{D}x_0^2\mathcal{C}^6x^5 + 128\mathcal{D}\mathcal{C}^6x^7 \\
&+ 4\mathcal{C}^{12}x^2 - 2\mathcal{D}\mathcal{C}^{12}x)X - 3\mathcal{D}x_0^{14} + 44x_0^{14}x + 924x_0^{12}x^3 - 194\mathcal{D}x_0^{12}x^2 + 5808x_0^{10}x^5 \\
&- 2080\mathcal{D}x_0^{10}x^4 + 2\mathcal{D}x_0^8\mathcal{C}^6 + 16192x_0^8x^7 - 8288\mathcal{D}x_0^8x^6 + 22528x_0^6x^9 - 15104\mathcal{D}x_0^6x^8 \\
&+ 40\mathcal{D}x_0^6\mathcal{C}^6x^2 + 15360x_0^4x^{11} - 12800\mathcal{D}x_0^4x^{10} + 168\mathcal{D}x_0^4\mathcal{C}^6x^4 - 3\mathcal{D}x_0^2\mathcal{C}^{12} + 4096x_0^2x^{13} \\
&- 4096\mathcal{D}x_0^2x^{12} + 256\mathcal{D}x_0^2\mathcal{C}^6x^6 + 4x_0^2\mathcal{C}^{12}x + 128\mathcal{D}\mathcal{C}^6x^8 + 4\mathcal{C}^{12}x^3 - 2\mathcal{D}\mathcal{C}^{12}x^2]. \qquad \text{(A3)}
\end{aligned}
$$

[1] P. Singh, Are loop quantum cosmos never singular? Classical Quantum Gravity **26**, 125005 (2009).
[2] A. Ashtekar and P. Singh, Loop quantum cosmology: A status report, Classical Quantum Gravity **28**, 213001 (2011).
[3] A. Ashtekar and M. Bojowald, Quantum geometry and the Schwarzschild singularity, Classical Quantum Gravity **23**, 391 (2006).
[4] L. Modesto, Loop quantum black hole, Classical Quantum Gravity **23**, 5587 (2006).
[5] M. Campiglia, R. Gambini, and J. Pullin, Loop quantization of spherically symmetric midi-superspaces: The interior problem, AIP Conf. Proc. **977**, 52 (2008).
[6] C. G. Boehmer and K. Vandersloot, Loop quantum dynamics of the Schwarzschild interior, Phys. Rev. D **76**, 104030 (2007).
[7] D. W. Chiou, Phenomenological dynamics of loop quantum cosmology in Kantowski-Sachs spacetime, Phys. Rev. D **78**, 044019 (2008).
[8] R. Gambini and J. Pullin, Black Holes in Loop Quantum Gravity: The Complete Space-Time, Phys. Rev. Lett. **101**, 161301 (2008).
[9] L. Modesto, Semiclassical loop quantum black hole, Int. J. Theor. Phys. **49**, 1649 (2010).
[10] D. W. Chiou, Phenomenological loop quantum geometry of the Schwarzschild black hole, Phys. Rev. D **78**, 064040 (2008).
[11] J. Brannlund, S. Kloster, and A. DeBenedictis, The evolution of lambda black holes in the mini-superspace approximation of loop quantum gravity, Phys. Rev. D **79**, 084023 (2009).
[12] R. Gambini and J. Pullin, An introduction to spherically symmetric loop quantum gravity black holes, AIP Conf. Proc. **1647**, 19 (2015).
[13] A. Joe and P. Singh, Kantowski-Sachs spacetime in loop quantum cosmology: Bounds on expansion and shear scalars and the viability of quantization prescriptions, Classical Quantum Gravity **32**, 015009 (2015).
[14] A. Corichi and P. Singh, Loop quantization of the Schwarzschild interior revisited, Classical Quantum Gravity **33**, 055006 (2016).
[15] N. Dadhich, A. Joe, and P. Singh, Emergence of the product of constant curvature spaces in loop quantum cosmology, Classical Quantum Gravity **32**, 185006 (2015).
[16] J. Cortez, W. Cuervo, H. A. Morales-Tcotl, and J. C. Ruelas, Effective loop quantum geometry of Schwarzschild interior, Phys. Rev. D **95**, 064041 (2017).
[17] J. Olmedo, S. Saini, and P. Singh, From black holes to white holes: A quantum gravitational, symmetric bounce, Classical Quantum Gravity **34**, 225011 (2017).
[18] A. Perez, Black holes in loop quantum gravity, Rep. Prog. Phys. **80**, 126901 (2017).
[19] A. Barrau, K. Martineau, and F. Moulin, A status report on the phenomenology of black holes in loop quantum gravity: Evaporation, tunneling to white holes, dark matter and gravitational waves, Universe **4**, 102 (2018).
[20] E. Bianchi, M. Christodoulou, F. D'Ambrosio, H. M Haggard, and C. Rovelli, White holes as remnants: A surprising scenario for the end of a black hole, Classical Quantum Gravity **35**, 225003 (2018).
[21] A. Ashtekar, J. Olmedo, and P. Singh, Quantum Transfiguration of Kruskal Black Holes, Phys. Rev. Lett. **121**, 241301 (2018).
[22] A. Ashtekar, J. Olmedo, and P. Singh, Quantum extension of the Kruskal spacetime, Phys. Rev. D **98**, 126003 (2018).
[23] C. Rovelli, Black hole evolution traced out with loop quantum gravity, Physics **11**, 127 (2018).
[24] E. Alesci, S. Bahrami, and D. Pranzetti, Quantum gravity predictions for black hole interior geometry, Phys. Lett. B **797**, 134908 (2019).
[25] M. Assanioussi, A. Dapor, and K. Liegener, Perspectives on the dynamics in a loop quantum gravity effective description of black hole interiors, Phys. Rev. D **101**, 026002 (2020).
[26] N. Bodendorfer, F. M. Mele, and J. Munch, (b,v)-type variables for black to white hole transitions in effective loop quantum gravity, arXiv:1911.12646.
[27] R. Carballo-Rubio, F. Di Filippo, S. Liberati, and M. Visser, Opening the Pandora's box at the core of black holes, Classical Quantum Gravity **37**, 145005 (2020).

[28] F. Moulin, A. Barrau, and K. Martineau, An overview of quasinormal modes in modified and extended gravity, Universe **5**, 202 (2019).
[29] D. Arruga, J. Ben Achour, and K. Noui, Deformed general relativity and quantum black holes interior, Universe **6**, 39 (2020).
[30] C. Liu, T. Zhu, Q. Wu, K. Jusufi, M. Jamil, M. Azreg-Anou, and A. Wang, Shadow and quasinormal modes of a rotating loop quantum black hole, Phys. Rev. D **101**, 084001 (2020).
[31] I.Agullo, V. Cardoso, A. del Rio, M. Maggiore, and J. Pullin, Gravitational-wave signatures of quantum gravity, arXiv:2007.13761.
[32] A. Ashtekar and J. Olmedo, Properties of a recent quantum extension of the Kruskal geometry, Int. J. Mod. Phys. D **29**, 2050076 (2020).
[33] C. Zhang, Y.-G. Ma, S.-P. Song, and X.-D. Zhang, Loop quantum Schwarzschild interior and black hole remnant, Phys. Rev. D **102**, 041502 (2020).
[34] R. Gambini, J. Olmedo, and J. Pullin, Spherically symmetric loop quantum gravity: Analysis of improved dynamics, Classical Quantum Gravity **37**, 205012 (2020).
[35] J. G. Kelly, R. Santacruz, and E. Wilson-Ewing, Effective loop quantum gravity framework for vacuum spherically symmetric space-times, arXiv:2006.09302.
[36] M. Bojowald, S. Brahma, and D. h. Yeom, Effective line elements and black-hole models in canonical loop quantum gravity, Phys. Rev. D **98**, 046015 (2018).
[37] C. Rovelli and F. Vidotto, Small black/white hole stability and dark matter, Universe **4**, 127 (2018).
[38] C. Rovelli and P. Martin-Dussaud, Interior metric and ray-tracing map in the firework black-to-white hole transition, Classical Quantum Gravity **35**, 147002 (2018).
[39] P. Martin-Dussaud and C. Rovelli, Evaporating black-to-white hole, Classical Quantum Gravity **36**, 245002 (2019).
[40] K. A. Meissner, Black-hole entropy in loop quantum gravity, Classical Quantum Gravity **21**, 5245 (2004).
[41] T. Thiemann, *Modern Canonical Quantum General Relativity* (Cambridge University Press, Cambridge, England, 2008).
[42] A. Ashtekar, Black hole evaporation: A perspective from loop quantum gravity, Universe **6**, 21 (2020).
[43] M. Bouhmadi-Lopez, S. Brahma, C. Y. Chen, P. Chen, and D. h. Yeom, Asymptotic non-flatness of an effective black hole model based on loop quantum gravity, Phys. Dark Universe **30**, 100701 (2020).
[44] M. Bojowald, Comment (2) on "Quantum Transfiguration of Kruskal Black Holes", arXiv:1906.04650.
[45] M. Bojowald, A no-go result for covariance in models of loop quantum gravity, Phys. Rev. D **102**, 046006 (2020).
[46] H. Goldstein, C. Poole, and J. Safko, in *Classical Mechanics*, 3rd ed. (Addison Wesley, New York, 2002), pp. 368–424.
[47] N. Bodendorfer, F. M. Mele, and J. Münch, Effective quantum extended spacetime of polymer Schwarzschild black hole, Classical Quantum Gravity **36**, 195015 (2019).
[48] N. Bodendorfer, F. M. Mele, and J. Münch, Mass and horizon Dirac observables in effective models of quantum black-to-white hole transition, arXiv:1912.00774.
[49] A. Ashtekar, T. Pawlowski, P. Singh, and K. Vandersloot, Loop quantum cosmology of $k = 1$ FRW models, Phys. Rev. D **75**, 024035 (2007).
[50] S. W. Hawking and G. F. R. Ellis, *The Large Scale Structure of Spacetime* (Cambridge University Press, Cambridge, England, 1973).
[51] A. Komar, Covariant conservation laws in general relativity, Phys. Rev. **113**, 934 (1959).
[52] G. D. Birkhoff, *Relativity and Modern Physics* (Harvard University Press, Cambridge, Massachusetts, 1923).
[53] M. Bouhmadi-Lopez, S. Brahma, C.-Y. Chen, P. Chen, and D.-h. Yeom, A consistent model of non-singular Schwarzschild black hole in loop quantum gravity and its quasinormal modes, J. Cosmol. Astropart. Phys. 07 (2020) 066.
[54] M. Bojowald, R. Goswami, R. Maartens, and P. Singh, Black Hole Mass Threshold from Nonsingular Quantum Gravitational Collapse, Phys. Rev. Lett. **95**, 091302 (2005).
[55] L. Modesto, Gravitational collapse in loop quantum gravity, Int. J. Theor. Phys. **47**, 357 (2008).
[56] Y. Zhang, Y. Zhu, L. Modesto, and C. Bambi, Can static regular black holes form from gravitational collapse? Eur. Phys. J. C **75**, 96 (2015).
[57] Y. Liu, D. Malafarina, L. Modesto, and C. Bambi, Singularity avoidance in quantum-inspired inhomogeneous dust collapse, Phys. Rev. D **90**, 044040 (2014).
[58] J. Ben Achour, S. Brahma, and J.-P. Uzan, Bouncing compact objects. Part I. Quantum extension of the Oppenheimer-Snyder collapse, J. Cosmol. Astropart. Phys. 03 (2020) 041.
[59] J. Ben Achour, S. Brahma, and J.-P. Uzan, Bouncing compact objects II: Effective theory of a pulsating Planck star, arXiv:2001.06153.
[60] J. Ben Achour, S. Brahma, S. Mukohyama, and J.-P. Uzan, Towards consistent black-to-white hole bounces from matter collapse, J. Cosmol. Astropart. Phys. 09 (2020) 020.
[61] J. G. Kelly, R. Santacruz, and E. Wilson-Ewing, Black hole collapse and bounce in effective loop quantum gravity, arXiv:2006.09325.